



Volume 9, Issue 1-2, December 2023

Dhaka University of Engineering & Technology, Gazipur, Bangladesh

# Chief Patron Prof. Dr. M. Habibur Rahman Honorable Vice Chancellor

#### Patron

#### Prof. Dr. Mohammad Abdur Rashid

Honorable Pro-Vice Chancellor

### **DUET Journal Management Committee**

01.	Prof. Dr. Md. Nazrul Islam	Chairman
02.	Director (Research & Extension)	Member-Secretary
03.	Prof. Dr. Abu Talib Md. Kaosar Jamil Dept. of Physics	Member
04.	Prof. Dr. Mohammod Abul Kashem Dept. of Computer Science & Engineering	Member
05.	Prof. Dr. Md. Arefin Kowser Dept. of Mechanical Engineering	Member
06.	Prof. Dr. Md. Abdus Shahid Dept. of Textile Engineering	Member
07.	Prof. Dr. Fazlul Hasan Siddiqui Dept. of Computer Science & Engineering	Member
08.	Prof. Dr. Md. Arifur Rahman Dept. of Electrical & Electronic Engineering	Member
09.	Engr. Solaiman Ahmed Computer Programmer, ICT Cell	Member

### **Table of Contents**

Sl. No.		Page
01.	Local Condensation and Evaporation Heat Transfer Coefficient Measurements of Binary Mixture Refrigerant R454B Inside a Plate Heat Exchanger  Md. Mahbubur Rahman, Afnan Hasan, Djiby Bal, Keishi Kariya and Akio Miyara	1
02.	Traffic Congestion in Megacity Dhaka: Case Studies from Seoul and Copenhagen Analyzing the Potential Measures <i>Md. Arifuzzaman</i>	11
03.	A Simulation Study of Daylighting Performance for Different Window Configurations in an Architectural Design Studio to Enhance Lighting Quality at DUET, Gazipur Farhana Ahsan	22
04.	Development and Quality Assessment of Composite Biscuits Fortified with Potato and Corn Flour Raju Ahmmed, Fatema Ahmed Toma, Kanis Fatema Tuna, Md. Shofiul Azam	34
05.	Study of Erosion and Accretion of Jamuna River Using GIS and Remote Sensing Technology M. Abdeen, K. Rayhan, S. Hasan, N. Zishan, and S. Anwar	41

### Local Condensation and Evaporation Heat Transfer Coefficient Measurements of Binary Mixture Refrigerant R454B Inside a Plate Heat Exchanger

Md. Mahbubur Rahman<sup>1,2,\*</sup>, Afnan Hasan<sup>1,3</sup>, Djiby Bal<sup>1</sup>, Keishi Kariya<sup>4</sup> and Akio Miyara<sup>4,5</sup>

<sup>1</sup>Graduate School of Science and Engineering, Saga University, Saga 840-8502, Japan

<sup>2</sup>Department of Mechanical Engineering, Khulna University of Engineering & Technology, Khulna 9203, Bangladesh

<sup>3</sup>Department of Mechanical Engineering, Chittagong University of Engineering & Technology, Chattogram 4349, Bangladesh

<sup>4</sup>Department of Mechanical Engineering, Saga University, Saga 840-8502, Japan

<sup>5</sup>International Institute for Carbon-Neutral Energy Research, Kyushu University, Fukuoka 819-0395, Japan

#### **ABSTRACT**

This paper explores the evaluation of the local heat transfer coefficient of a binary mixture refrigerant R454B experimentally in a vertical brazed plate heat exchanger during both condensation and evaporation. The experiments were carried out at different mass fluxes of 10 kg/m²s and 50 kg/m²s in a specially designed test section. This test section incorporates eight stainless steel plates: two chevron plates processed at 60° for the refrigerant flow channel, two flat plates for heat transfer, and four plates dedicated to water flow channels on both sides of the refrigerant channel. The refrigerant and water flow in a counter pattern, with the refrigerant centrally flowing between the two water channels on the outer sides. To measure wall surface temperatures near the refrigerant and water sides, 20 thermocouples were strategically placed within the test section. The local heat transfer coefficients were calculated using wall temperatures from the refrigerant side, refrigerant saturation temperature, and local heat flux under downward flow condition during condensation and upward flow condition during evaporation experiments. The experimental measurement results showed that local heat transfer coefficients decreases with increase of wetness during condensation and local heat transfer coefficient increases with the increase of vapor quality during evaporation with different values in horizontal direction inside the plate heat exchanger.

Keywords: Plate heat exchanger, heat transfer, evaporation, condensation and mixture refrigerant

#### 1. INTRODUCTION

Plate Heat Exchangers (PHEs) find extensive use across various industrial sectors such as dairy, processing, paper production, refrigeration, heating, ventilation, and air conditioning. Their superiority over other heat exchanger types stems from several factors. PHEs excel in saving energy and space due to their higher ratio of heat transfer area to volume. They're lightweight, feature flexible designs, and boast high thermal efficiencies. Their adaptable design provides a significant edge when modifying the heat transfer area; adding or removing plates can be done seamlessly without disrupting pipe connections.

The European Union has set in motion a plan to gradually eliminate refrigerants with higher Global Warming Potential (GWP), especially in portable air conditioners and household refrigerators/freezers, following regulations in EU No. 517/2014. This has led to increased interest in alternative refrigerants that boast low GWP and zero Ozone Depletion Potential (ODP). However, these low GWP refrigerants often come with elevated costs and greater energy consumption. To address this challenge, exploring blended refrigerants that meet acceptable criteria has emerged as a potential solution. Researchers are actively seeking alternatives that exhibit both low GWP and comparable heat transfer properties. While prior studies extensively investigated the heat transfer characteristics of various refrigerants in plate heat exchangers during condensation and evaporation, most focused on overall heat transfer traits [1]-[14], with only a of local heat transfer within plate heat exchangers. Sarraf et al.[19] utilized Infrared Thermography (IR) to ascertain local heat transfer coefficients in a prototype brazed plate heat exchanger (BPHE) during the complete condensation of R601. Through infrared thermography, they identified the global and local thermo-hydraulic features of the PHE, including vapor quality, heat flux density, and heat transfer coefficient. Their investigation also delved into the influence of mass flux on these properties. Wang and Kabelac [20] conducted experimental research on the quasi-local heat transfer characteristics of R1234ze(E) and R134a within a microstructured plate heat exchanger. Their study focused on analyzing the impact of refrigerant mass flux and saturation temperature on condensation heat transfer. Additionally, they drew conclusions regarding transitions observed in vapor quality, demonstrating shifts from laminar flow to turbulent flow and illustrating film condensation phenomena. Longo et al. [22] similarly explored the local heat transfer coefficients of R32 and R410A within a BPHE. Their study centered on identifying a transition concerning mass flux, moving from gravity-controlled condensation to forced convection condensation. The local heat transfer coefficient fluctuates not just along the flow direction but also across the width due to gas-liquid distribution [23]-[25]. Variations in refrigerant distribution at the inlet and outlet lead to maldistribution, affecting local condensation heat transfer within a plate heat exchanger [22]. The presence of different boiling mechanisms in the liquid-preferred and vapor-preferred paths induces alterations in local evaporation heat transfer within plate heat exchanger [18].

limited number [15]-[22] exploring the specific intricacies

<sup>\*</sup> Corresponding author's email: mahbub rahman@me.kuet.ac.bd

Since the research work about local heat transfer coefficient is scarce, to gain deeper insights into heat transfer behaviors, detailed knowledge about local heat transfer becomes imperative. However, measurements of local wall temperatures and heat fluxes are difficult because of the complicated structure. A specially designed test section has been constructed for the measurement of heat transfer coefficient of a zeotropic mixture refrigerant R454B in the present study. The physiochemical properties of the refrigerant are shown in Table 1.

Table 1 Physiochemical properties of R454B

Refrigerant	R454B		
Composition mass percentage	R32 68.9%		
	R1234yf 31.1%		
Temperature glide ( °C)	1.5		
ASHRAE Safety class	A2L		
GWP	467		
ODP	0		
Molar weight (kg/kmol)	62.6		
Normal boiling point (°C)	-50.73		
Critical pressure (kPa)	5041		
Critical temperature ( °C)	77.0		
Liquid density(kg/m <sup>3</sup> )	1001		
Temperature glide ( °C)	1.5		
Liquid thermal conductivity	105.4		
$(mW/m\cdot K)$			
Vaporisation enthalpy (kJ/kg)	227.51		

The findings in the present study will help to better understand the local heat transfer phenomena inside the plate heat exchanger.

#### 2. EXPERIMENTAL SETUP AND PROCEDURES

#### 2.1 Refrigerant loop

The experimental setup in the present study consists of five

different loops and a data acquisition system for the investigation of local heat transfer of the mixture refrigerant R454B in a vertical brazed plate heat exchanger [26]. They have a refrigerant loop shown in Figure 1, three water loops for preheater, test section and condenser and a cold-water brine loop for the subcooler. The refrigerant loop is the primary loop of the experimental setup. For attaining various experimental conditions, it is needed to control the flow and temperature in the other four loops.

The refrigerant loop comprises a setup of a magnetic pump, a refrigerant mass flow meter, a preheater, a test section "the plate heat exchanger", a condenser, a subcooler, three mixing chambers and three sight glasses. A magnetic pump circulates the refrigerant in the whole loop. A mass flow meter is positioned between the pump and the preheater to control the flow rate of the refrigerant. The preheater transfers heat from the water to the refrigerant to reach a specific vapor quality at the inlet of the test section. The vapor of a certain quality then entered the test section and the refrigerant R454B condensed (in condensation experiment) or evaporated (in boiling experiment) there. The vapor-liquid two-phase refrigerant from the outlet of the test section is finally condensed in the condenser. Then the refrigerant is subcooled by controlling the flow rate of a low-temperature water brine mixture in the subcooler. The system pressure of the refrigerant loop can be controlled by adjusting the temperature in the condenser. The purpose of the filter was to remove any solid particles that may have been present in the loop. The refrigerant coming from the exit of the test section was maintained in a subcooled condition to prevent cavitation at the pump inlet [27].

#### 2.2 Test section

Eight stainless steel plates (material SUS303) were brazed together to form the specifically designed test section that

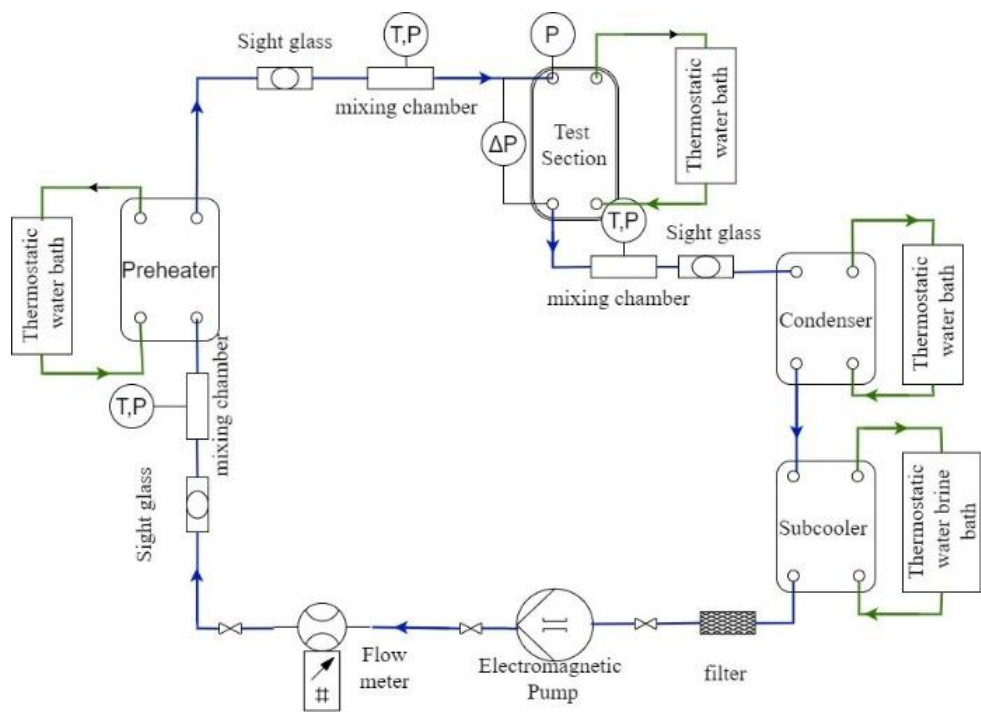


Figure 1: Refrigerant flow loop of experimental setup[27]

was utilized in this study. Among two of them were processed chevron plates of angle  $60^{\circ}$ .

The flow of the refrigerant occurs in the channel created by the space between these two chevron plates. Two flat plates were set for heat transfer measurements next to the chevron-shaped plates. The other four plates were dedicated to forming two water flow channels. Figure 2a represents a detailed view of thermocouple measurement points and the flow of water and refrigerants in the cross-section of the test plate. The red and blue regions, shown in Figure 2b, indicate, respectively, the refrigerant and cooling water channels. Table 2shows the geometrical characteristics of the test section with the geometrical attributes shown in Figure 3.

#### 2.3 Experimental procedures

Prior to conducting each experiment, the setup's system pressure is first maintained at a predetermined level through adjusting the condenser's temperature. The hot water loop for the preheater's temperature and flow rate are then modified to achieve the required vapor quality of R454B at the test section's inlet. Changing the temperature and flow rate of the water loop for the test section allows for adjustment of the heat transfer rate between the counter flow channels in the test section. Any modification to the system variables causes a change in the flow's temperature and pressure. A statistically steady state condition can be reached in between 20 and 100 minutes. The data acquisition device is subsequently turned on, and in the following 40 seconds, it scans each data channel ten times.

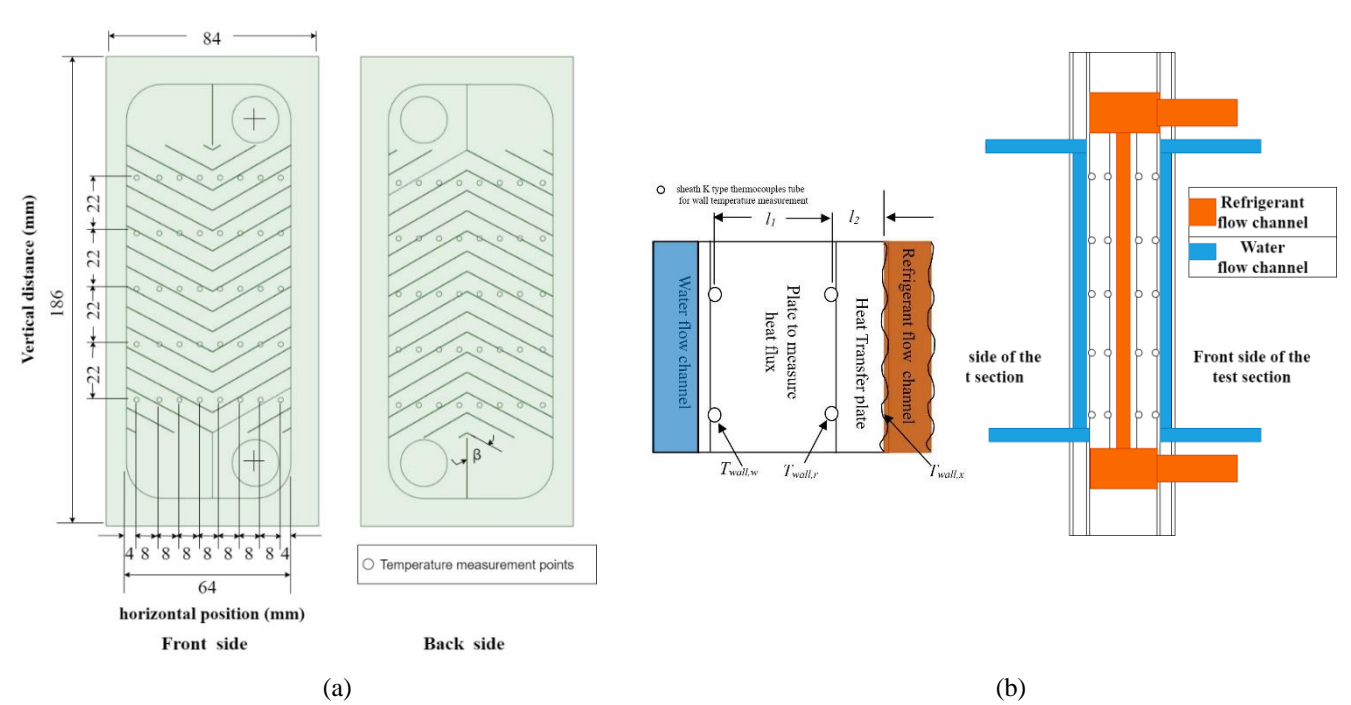


Figure 2: Details of (a) measurement positions and (b) flow directions [27]

Table 2:Geometrical characteristics of the test section [28]

Parameters	Value
Fluid Flow plate length, L (mm)	117.5
Plate width, W (mm)	64
Plate thickness (mm)	5
Area of the plate (m <sup>2</sup> )	0.0075
Corrugation type	Chevron
Chevron angle, $\beta(^0)$	60
Corrugation pitch, P(mm)	5.6
Corrugation depth, b(mm)	1.5
Number of plates	8
Number of channels on the refrigerant side	1
Number of channels on the water side	2
Thermal conductivity of the plate (W/m·K)	16.7

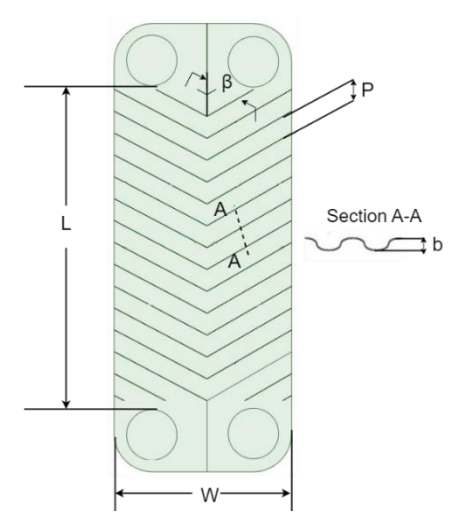


Figure 3: Geometrical attributes of the chevron plate

#### 3. DATA REDUCTION

#### 3.1 Local heat transfer coefficient

By assuming the steady state one dimensional heat conduction, the local heat flux  $q_x$  can be estimated from wall temperatures near refrigerant side  $(T_{wall,r})$  and water side  $(T_{wall,w})$  and thermal conductivity  $(\lambda_p)$  of the

plate shown in Eq. (1)
$$q_x = \lambda_p \left( \frac{T_{wall,r} - T_{wall,w}}{l_1} \right)$$
 (1)

 $l_1$  is the distance between thermocouples. The wall surface temperature of refrigerant side  $T_{wall,x}$  can be calculated assuming linear temperature distribution as Eq.(2)

$$T_{wall,x} = T_{wall,r} \pm \left(\frac{q_x l_2}{\lambda}\right)$$
 (2)  
'+' sign is for condensation and '-' sign is for evaporation.

l<sub>2</sub> is the distance between thermocouple and wall surface. The local heat transfer coefficient (LHTC) $\alpha_x$  is determined from the difference between wall surface temperature and saturation temperature shown in Eq. (3)

$$\alpha_x = \frac{q_x}{T_{sat} \sim T_{wall,x}}$$

$$T_{sat} \text{ is the saturation temperature of the working fluid side.}$$
(3)

#### 3.2 Vapor quality

The local specific enthalpy  $(h_i)$  on the test plate is derived using the following procedure.

$$h = f(T, P) \tag{4}$$

The amount of heat exchange in the preheater  $(Q_{w,pre})$  is calculated by Eq. (5):

$$Q_{w,pre} = m_w \left( h_{w,pre,out} - h_{w,pre,in} \right) \tag{5}$$

where  $\vec{m}_w$  is mass flow rate of water and  $h_{w,pre,in}$  and  $h_{w,pre,in}$ are the specific enthalpies of the preheater outlet and inlet of the water respectively.

The specific enthalpy at test section inlet  $(h_{t,in})$  is obtained from the amount of heat exchange  $(Q_{w,pre})$  for the preheater, mass flow rate  $(\dot{m_r})$  of the refrigerant and heat loss  $(Q_{loss})$  from the outlet of the preheater to the inlet of the test section.

$$h_{t,in} = h_{r,pre,in} + \frac{Q_{w,pre}}{\dot{m}_r} - \frac{Q_{loss}}{\dot{m}_r}$$
 (6)

The heat loss  $Q_{loss}$  is calculated from the steady state heat conduction equation of the multilayer cylinder.

The local specific enthalpy is calculated as follows.

$$h_i = h_{\rm t,in} \pm \frac{Q_i}{\dot{m}}$$

$$h_{i+1} = h_i \pm \frac{Q_{i+1}}{\dot{m}} \tag{7}$$

'+' sign is for evaporation and '-' sign is for condensation. the heat flow between two neighboring thermocouples obtained from the local heat flux  $q_x$  and the heat transfer area A<sub>i</sub>.

$$Q_i = q_x A_i \tag{8}$$

 $Q_i = q_x A_i$  (8) The local vapor quality  $(x_i)$  is determined from specific

$$x_i = \frac{h_i - h_l}{h_v - h_l} \tag{9}$$

 $h_l$  and  $h_v$  are the specific enthalpies of saturated liquid and saturation vapor respectively.

Since mixture refrigerant R454B is azeotropic binary mixture of R32 and R1234yf with 68.9% and 31.1 % by mass respectively, the local refrigerant saturation temperatures are calculated by the mixture component mass balance.

$$\dot{m}_b w_b = \dot{m}_V w_V + \dot{m}_l w_l \tag{10}$$

 $\dot{m}_b, \ \dot{m}_l, \ \dot{m}_V$  represent the total mass flow rate, liquid phase mass flow rate and the vapor phase mass flow rate respectively.

As thermodynamic vapor quality is also defined as

$$x = \frac{\dot{m}_V}{\dot{m}_b} \tag{11}$$

From Eq. (10) and Eq. (11) the following relationship can

$$w_L = \frac{w_b}{1 + x\left(\frac{w_V}{w_L} - 1\right)} \tag{12}$$

 $w_b$ ,  $w_L$  and  $w_V$  are the bulk mass fraction, liquid phase mass fraction and vapor phase mass fraction of the binary mixture, respectively.

The bulk concentration of the binary temperature under operational conditions can be determined by the use of gas chromatography.

The saturation temperature T<sub>sat</sub> is calculated by REFPROP 10 [29] with the following relation as shown Eq. (13).

$$T_{sat} = f(w_l, P) \tag{13}$$

The corresponding enthalpy for liquid and vapor phase is also evaluated from REFPROP 10.0 [29] by the function of the concentration and the pressures at the measurement point.

$$h_l = f(w_l, P) \tag{14}$$

$$h_{v} = f(w_{v}, P) \tag{15}$$

#### 3.3 Experimental uncertainty

The values of the experimental uncertainty are reported [23][28] for the heat transfer coefficient and the vapor quality within  $\pm 12\%$  and  $\pm 4.5\%$  respectively.

#### 4. EXPERIMENTAL RESULTS AND DISCUSSIONS

The condensation and evaporation experiments in a brazed plate heat exchanger were conducted to determine the heat transfer coefficients (both local and average) for the mixed refrigerant R454B. The heat transfer coefficients at various measurement points along the horizontal distance were examined for both the front and back sides of the plates, which served as the refrigerant flow channel in the test section. The results illustrate the variation of local heat transfer coefficients with vapor quality under

different flow and thermal conditions. Additionally, the average heat transfer coefficients of the mixture refrigerant R454B were experimentally obtained and compared with those of R1234yf in the same test facility.

# 4.1 Local condensation and evaporation heat transfer coefficient measurement for mixture refrigerant R454B

The experiments for the condensation and evaporation heat transfer (HT) of R454B mixture refrigerant inside the plate heat exchanger were carried out in two different mass fluxes of  $10~kg/m^2s$  and  $50~kg/m^2s$ . Table 3 represents the thermal conditions for condensation heat transfer experiment.

Table 3.Test condition for condensation HT experiment

	Mass	$T_{sat}$	Vapor	Heat Flux,
Refrigerant	Flux, G	[°C]	Quality	$q [kW/m^2]$
	[kg/m <sup>2</sup> s]		[-]	
R454B	10	30	1.0-0.0	9.2-11.5
K434B	50	30	1.0-0.0	6.8-18.9

The thermal conditions for evaporation heat transfer have been shown in Table 4.

Table 4.Test condition for evaporation HT experiment

Refrigerant	Mass Flux, G [kg/m <sup>2</sup> s]	T <sub>sat</sub> [°C]	Vapor Quality [-]	Heat Flux, q [kW/m <sup>2</sup> ]
R454B	10	10	0.0-0.9	9.0-14.2
K434D	50	10	0.0-1.0	15.3-40.2

Figure 4 and Figure 5 illustrate the variation of the local heat transfer coefficient (LHTC) in the horizontal direction of the plate for different vapor qualities within

the test section, along with the horizontal average heat transfer coefficient during the condensation of R454B in a plate heat exchanger for mass fluxes 10 kg/m²s and 50 kg/m²s respectively at saturation temperature of 30 °C. Moreover, Figure 6 and Figure 7 showcase the change in the local heat transfer coefficient (LHTC) in the horizontal direction of the plate for various vapor qualities within the test section, along with the horizontal average heat transfer coefficient during the evaporation of R454B in a plate heat exchanger for mass fluxes 10kg/m²s and 50 kg/m²s respectively at saturation temperature of 10 °C. From Figure 4(a), (b), (c), (d) and (e) and Figure 5(a), (b), (c), (d) and (e), in the course of the condensation process

of the mixed refrigerant R454B in the plate heat exchanger, at mass fluxes of 10 kg/m<sup>2</sup>s and 50 kg/m<sup>2</sup>s, the local condensation heat transfer coefficient within the plate exhibits variability both in horizontal positions and vapor quality along the vertical distance of the Plate Heat Exchanger (PHE). The differences between the front side and back side heat transfer coefficient (HTC) are observed due to the geometrical pattern difference of the chevron plate heat exchanger [27]. The local condensation heat transfer coefficient reaches its maximum near the inlet port and minimum at the end faces on the left and right, attributed to refrigerant maldistribution, a phenomenon also evidenced by Longo et al [22]. The horizontal average condensation heat transfer coefficients for a mass flux of 10 kg/m<sup>2</sup>s are observed to decrease from about 2.7 to 1.5 kW/m<sup>2</sup>K with the increase of wetness i.e decrease of vapor quality from about 0.85 to 0.25 shown in Figure 4(f) due to the fact that lower vapor quality results in a thicker liquid film that reduces the heat transfer efficiency.

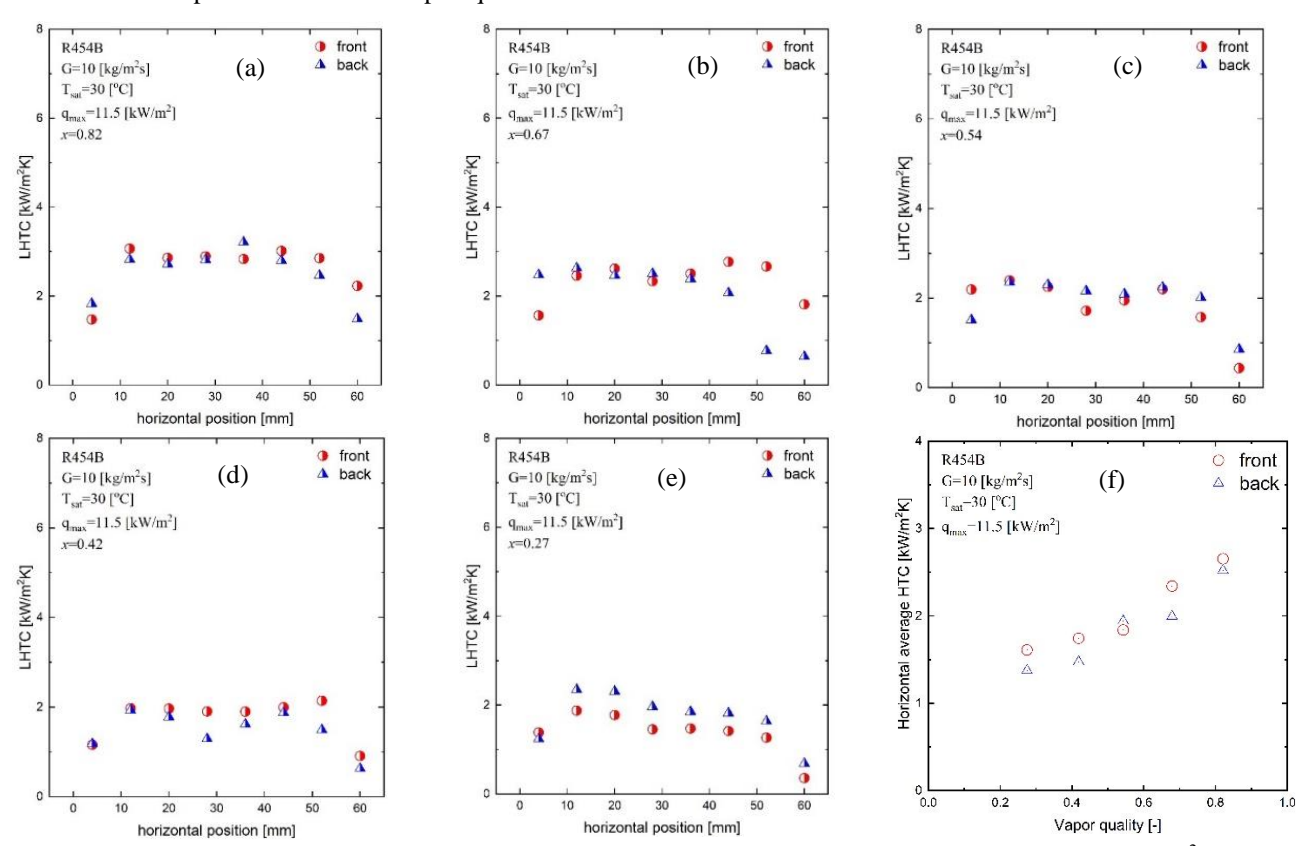


Figure 4: Condensation heat transfer coefficient of mixture refrigerant R454B for mass flux G=10 kg/m<sup>2</sup>s: (a)-(e) variation of local heat transfer coefficient with horizontal distance and (f) horizontal average heat transfer coefficient vs vapor quality.

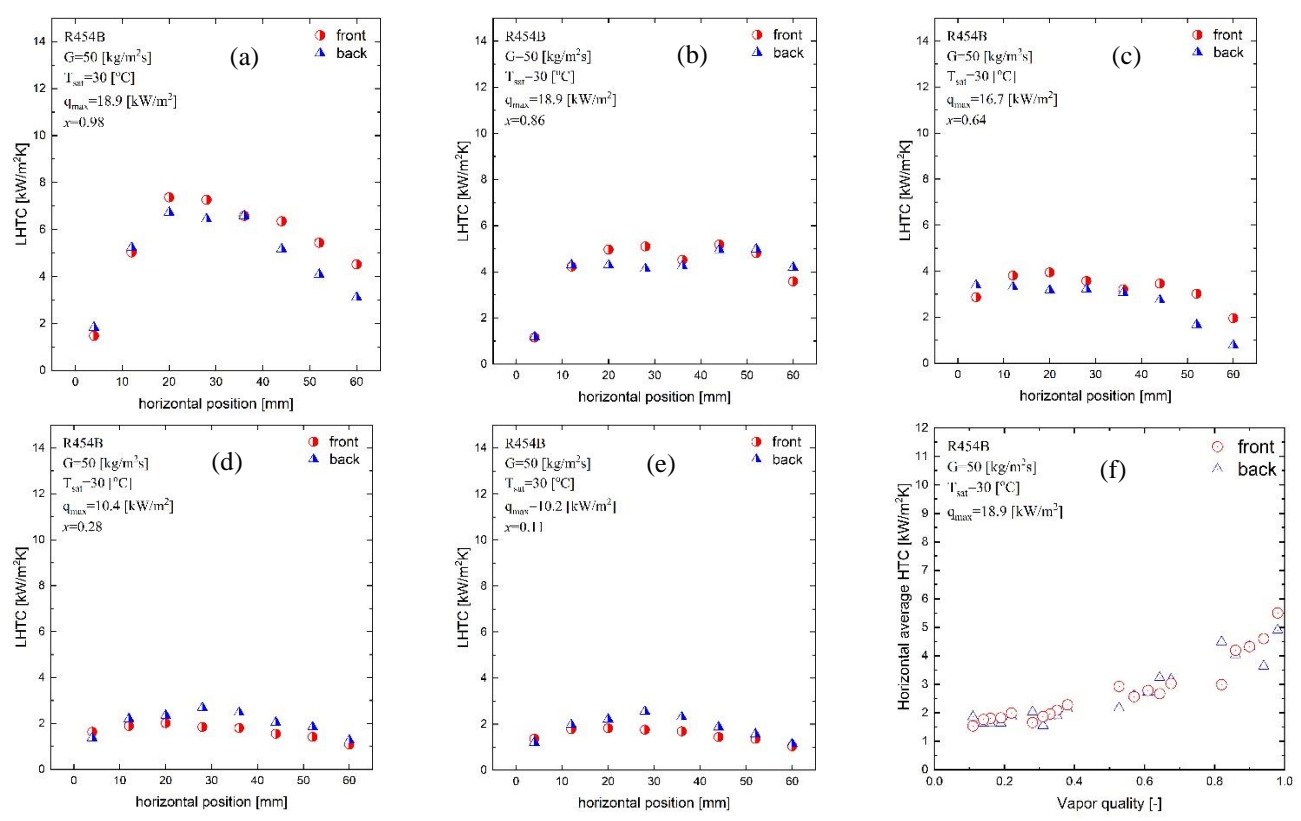


Figure 5: Condensation heat transfer coefficient of mixture refrigerant R454B for mass flux  $G=50 \text{ kg/m}^2\text{s}$ : (a) – (e) variation of local heat transfer coefficient with horizontal distance and (f) horizontal average heat transfer coefficient vs vapor quality

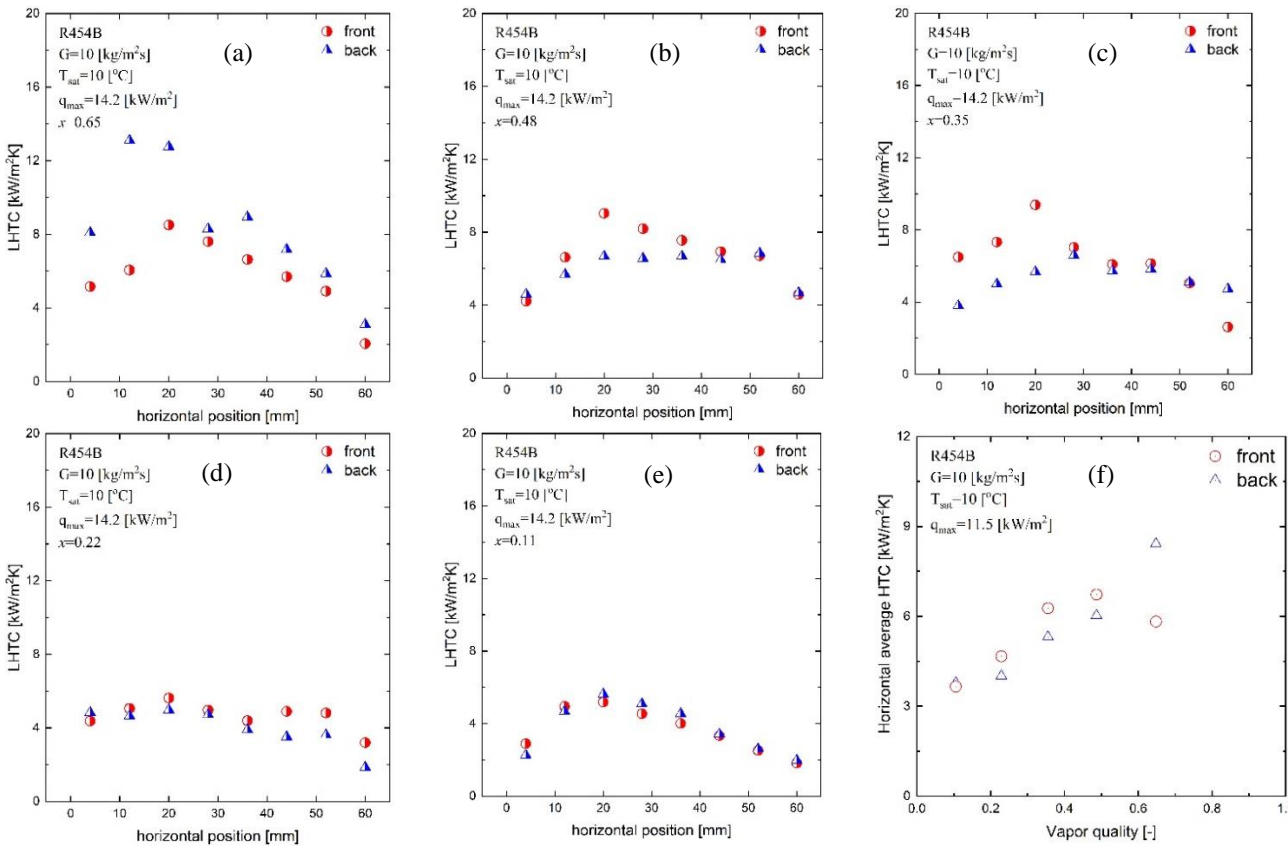


Figure 6: Evaporation heat transfer coefficient of mixture refrigerant R454B for mass flux  $G=10 \text{ kg/m}^2\text{s}$ : (a) – (e) variation of local heat transfer coefficient with horizontal distance and (f) horizontal average heat transfer coefficient vs vapor quality

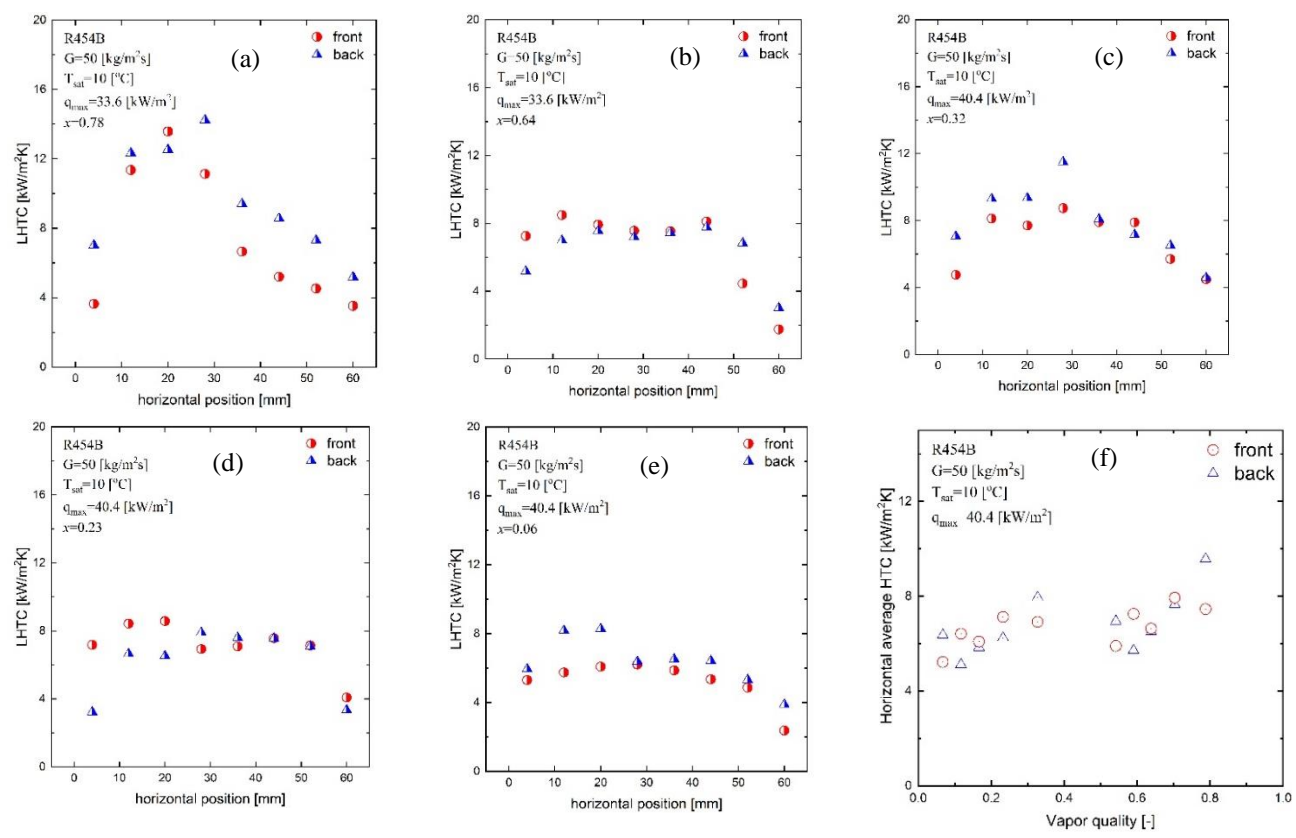


Figure 7: Evaporation heat transfer coefficient of mixture refrigerant R454B for mass flux  $G=50 \text{ kg/m}^2\text{s}$ : (a) – (e) variation of local heat transfer coefficient with horizontal distance and (f) horizontal average heat transfer coefficient vs vapor quality

From Figure 5(f), the horizontal average condensation HTC for a mass flux of  $50 \text{ kg/m}^2\text{s}$  was found to decrease from  $5.5 \text{ to } 1.5 \text{ KW/m}^2\text{K}$  with the decrease of vapor quality from 1.0 to 0.1. The elevated heat transfer coefficients observed at high vapor qualities (x>0.6) during the condensation experiment, particularly at a high mass flux of  $50 \text{ kg/m}^2\text{s}$  in Figure 5(f), can be largely attributed to the substantial reduction in condensate film thickness. This thinning of the condensate film leads to a notable increase in the heat transfer coefficient.

From Figure 6(a), (b), (c), (d) and (e) and Figure 7(a), (b), (c), (d) and (e), greater zigzag patterns are evident in the trends of local evaporation heat transfer coefficient data during the evaporation of the mixture refrigerant R454B in the plate heat exchanger at mass fluxes of 10 kg/m<sup>2</sup>s and 50 kg/m<sup>2</sup>s. This behavior is attributed to increased turbulence and the intricate flow dynamics within the Plate Heat Exchanger (PHE). The local heat transfer coefficient values are observed to be higher in the middle section of the test plate due to the dominance of the convection boiling regime, particularly in the vapor-preferred pathway, as supported by the findings of Lee et al [18]. The horizontal average evaporation heat transfer coefficient for a mass flux of 10 kg/m<sup>2</sup>s are observed to increase from about 3.2 to 8.5 kW/m<sup>2</sup>K with the increase of vapor quality from about 0.10 to 0.72 shown in Figure 6(f) due to the fact that higher vapor quality results in a higher vapor velocity augmenting convective heat transfer through increased turbulence.

From Figure 7(f), the horizontal average evaporation HTC for a mass flux of 50 kg/m²s was found to increase from about 4.5 to 8.8 KW/m²K with the increase of vapor quality from 0.05 to 0.8. The evaporation heat transfer coefficient exhibits a significantly higher value at high vapor qualities (x > 0.5) and a high mass flux of 50 kg/m²s in Figure 7(f). This pronounced increase can be attributed to the increased turbulence and intricate flow dynamics prevalent under those specific test conditions.

The front side and back side horizontal average condensation heat coefficient for both mass fluxes of 10 kg/m<sup>2</sup>s and 50 kg/m<sup>2</sup>s do not have significant differences showing negligible effect of geometrical attributes of front side and back side of the plate heat exchanger with the only significant variation in horizontal distance as the results illustrated in Figure 4 and Figure 5. Furthermore, due to turbulence and flow behavior, the difference between the front side horizontal average evaporation heat transfer coefficient and back side horizontal average evaporation heat transfer coefficient observed in Figure 6 and Figure 7 are pronounced specially at high mass flux of 50 kg/m<sup>2</sup>s in comparison to lower mass flux of 10 kg/m<sup>2</sup>s signifying the effect of geometrical pattern of the front side and back side of the test plate. However, the effect of mass transfer resistance of mixture refrigerant R454B on local and average heat transfer coefficient in brazed type chevron plate heat exchanger are needed to be investigated in detail for understanding the heat transfer behavior of mixture refrigerant during condensation and evaporation.

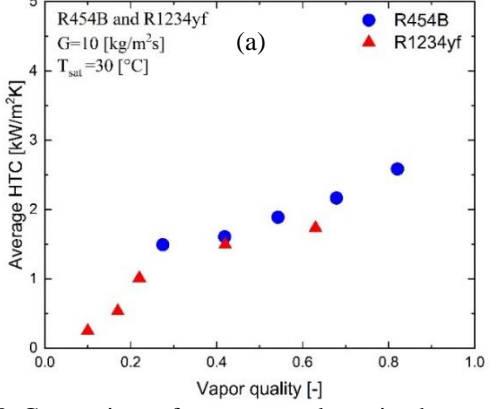
### 4.2 Comparison of heat transfer coefficient of R454B and R1234yf during condensation and evaporation

Figure 8 and Figure 9 show the comparison of experimentally measured average heat coefficients of R454B and R1234yf for mass flux of 10 kg/m<sup>2</sup>s and 50 kg/m<sup>2</sup>s during condensation and evaporation respectively. The average heat transfer coefficient is calculated by making average of previously obtained the front side horizontal average heat transfer coefficient and back side horizontal average heat transfer coefficient in the experiment. From Figure 8(a) and 8(b) it is observed that the average condensation heat transfer coefficient of both R454B and R1234yf decreases with increase of wetness (1-x) i.e. with decrease of vapor quality.

The low vapor quality in low mass flux results in thick condensate film that reduces the heat transfer coefficient in the test plate. The condensation heat transfer coefficient value for R454B is almost similar with R1234yf for vapor quality of x<0.4 at low mass flux of 10 kg/m²s and for vapor quality of x<0.5 at high mass flux of50 kg/m²s since the gravity controlled condensation dictates the condensation process, possibly showing negligible effect on heat transfer coefficient for both the R1234yf refrigerant and mixture refrigerant R454B (having constituents R1234yf) in this context. Moreover, the condensation heat transfer coefficient for R454B surpasses that of R1234yf at high vapor quality (x<0.7), especially

under larger mass flux conditions of 50 kg/m²s during forced convective condensation. This observation aligns with findings from another research group [30], which reported similar trends in their experimental study of condensation heat transfer in a microfin tube. The superior liquid thermal conductivity of R454B compared to R1234yf [29] can also contribute to the higher heat transfer coefficient exhibited by R454B relative to R1234yf. The average HTC of R454B increases from 1.5 to 5.0 kW/m²K and the average HTC of R1234yf increases from 0.8 to 3.1 kW/m²K when mass flux of 10 to 50 kg/m²s during the condensation heat transfer experiments around saturation temperature 30 °C.

From Figure 9(a) and 9(b) it is observed that the average evaporation heat transfer coefficient of both R454B and R1234yf increases with the increase of vapor quality. Since the heat transfer in the evaporation depends greatly on the flow pattern, increasing the mass flux creates more complex flow resulting the more zigzag trends in the heat transfer coefficients. Vertically across the plate, the heat transfer coefficients in the high vapor quality region are greater than those in the low vapor quality region. In evaporation process, in the higher vapor quality region, vapor specific volume increases, and the vapor velocity becomes faster at a given mass flux It is attributed that the velocity of vapor enhances the convection heat transfer since the turbulence level inside the plate heat exchanger increase. Moreover, the average HTC of R454B increases from 3.8 to 8.9 kW/m<sup>2</sup>K and the average HTC of R1234yf increases from 3.5 to 7.2 kW/m<sup>2</sup>K when mass flux of 10



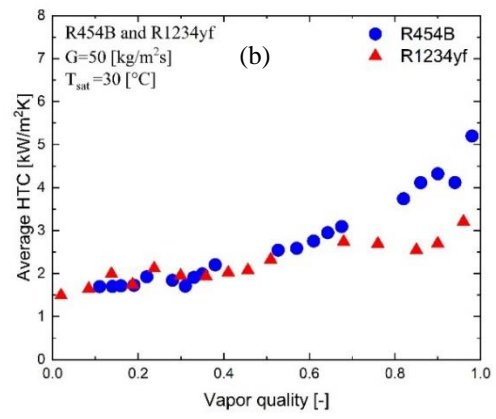
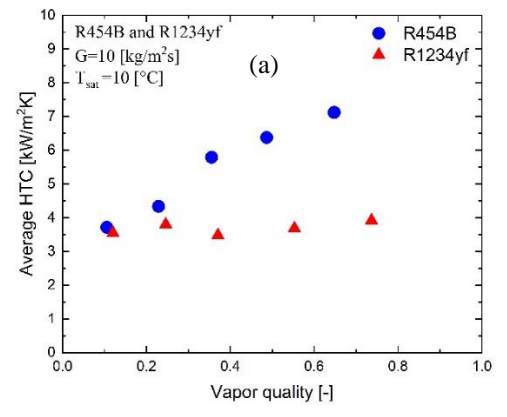


Figure 8: Comparison of average condensation heat transfer coefficients of R454B and R1234yf for mass flux (a)  $G = 10 \text{ kg/m}^2\text{s}$  and (b)  $G = 50 \text{ kg/m}^2\text{s}$ .



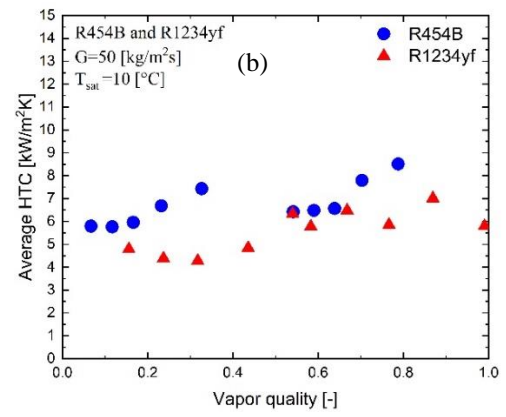


Figure 9: Comparison of average evaporation heat transfer coefficients of R454B and R1234yf for mass flux (a)  $G = 10 \text{ kg/m}^2\text{s}$  and (b)  $G=50 \text{ kg/m}^2\text{s}$ .

to 50 kg/m²s during the evaporation heat transfer experiments around saturation temperature 10 °C. The evaporation heat transfer coefficient of R454B is also observed higher than that of R1234yf similar to condensation heat transfer coefficient results.

The heat transfer coefficients (HTCs) of R454B demonstrate a moderate improvement in comparison to R1234yf, showing an enhancement in the range of 1.1 to 1.7 times. This modest increase in HTCs is particularly noteworthy considering the composition of R454B, which includes a significant proportion of R32, accounting for approximately 68.9%. The limited growth in HTCs can be attributed to factors such as the influence of mass transfer resistance and the presence of a temperature glide within the zeotropic mixture refrigerant. These intricacies in composition contribute to a relatively subdued improvement in heat transfer performance for R454B when compared to R1234yf.

#### 5. CONCLUSION

The local heat transfer coefficient of R454B (R32/R1234yf) were measured during condensation and evaporation in a vertical brazed plate heat exchanger. The experimental results for heat transfer can be summarized as follows:

- •The local heat transfer coefficient of R454B was found to vary both in flow direction in vertical cross section and width direction in horizontal distances of the plate. The maximum value was found near the inlet port because of inlet refrigerant distribution effect and also the tendency to flow the vapor preferred path.
- •The high heat transfer coefficients of R454B in the high vapor quality (x>0.6) at high mass flux of 50 kg/m²s in condensation experiment significantly attribute the condensate film thickness getting thinner results in an increase of heat transfer coefficient. The evaporation heat transfer coefficient of R454B in the high vapor quality (x>0.5) at high mass flux of 50 kg/m²s is much higher because of the more turbulence and complex flow at that test conditions.
- •The HTCs of R454B is moderately larger than R1234yf, increasing 1.1 to 1.7 times enhancement. HTC's growth is comparatively negligible, with R454B having a notable R32 composition of roughly 68.9% due to the deterioration of HTC caused by mass transfer resistance and the presence of a temperature glide of zeotropic mixture refrigerant.

#### **ACKNOWLEDGEMENTS**

The study was funded by New Energy and Industrial Technology Development Organization (NEDO), Japan. The author also would like to acknowledge Dr. ThihaTun, Mr. Kunpei Yoshida and Mr. Saide Diaw for their help and support in this work. We would like to acknowledge the presentation of the findings discussed in this paper at ISTP-33 (33<sup>rd</sup> International Symposium on Transport Phenomena) held in Kumamoto, Japan in September 24-27, 2023 where no formal proceedings were published.

#### **NOMENCLATURE**

#### **Abbreviations**

PHE	Plate Heat Exchanger
<i>BPHE</i>	Brazed Plate Heat Exchanger
GWP	Global Warming Potential
ODP	Ozone Depletion Potential
EU	European Union
HT	Heat Transfer
HTC	Heat Transfer Coefficient
LHTC	Local Heat Transfer Coefficient

#### **Symbols**

A: area	$[m^2]$
h: specific enthalpy	[J/kg]
Q: heat exchange amount	[kJ]
G: mass flux	$[kg/(m^2s]$
a: heat transfer coefficient	$[kW/(m^2 \cdot K]$
λ: thermal conductivity	$[kW/m \cdot K]$
x: vapor quality	[ ]
P: pressure	[MPa]
T: temperature	[°C]
q: heat flux	$[W/m^2]$
m: refrigerant mass flow rate	[kg/s]
W: mass fraction	[ ]
L: distance between thermocuples	[mm]

#### **Subscripts**

x: local point	l: liquid
w: water	v: vapor
r: refrigerant	p: plate

#### REFERENCES

- [1] D.H.Han, K.J. Lee and Y.H.Kim, "Experiments on the characteristics of evaporation of R410A in brazed plate heat exchangers with different geometric configurations". Applied Thermal Engineering 23 (10), 1209–1225.2003.
- [2] D.H. Han, K.J. Lee and Y.H. Kim, "The characteristics of condensation in brazed plate heat exchangers with different chevron angles". Journal of Korean Physics Sociecty, 43, 66–73, 2003.
- [3] Y.Y. Hsieh, and T.F. Lin , "Evaporation Heat Transfer and Pressure Drop of Refrigerant R-410A Flow in a Vertical Plate Heat Exchanger". Journal of Heat Transfer transactions of The ASME, 125, 852-857,2003.
- [4] A. Jokar, S.J.Eckels, M.H. Honsi, and T.P. Gielda, "Condensation heat transfer and pressure drop of brazed plate heat exchangers using refrigerant R-134a", Journal of Enhanced Heat Transfer, 11, 161–182.2004
- [5] W.S Kuo, Y.M. Lie, Y.Y.Hsieh, and T.F. Lin, "Condensation heat transfer and pressure drop of refrigerant R-410A flow in a vertical plate heat exchanger", International Journal of Heat and Mass Transfer48, 5205–5220,2005.
- [6] A. Jokar, M.H. Hosni and S.J. Eckels, "Dimensional analysis on the evaporation and condensation of refrigerant R-134a in minichannel plate heat exchangers", Applied Thermal Engineering ,26, 2287–2300, 2006.

- [7] J. Huang , T.J. Sheer and M. Bailey-McEwan "Heat transfer and pressure drop in plateheat exchanger refrigerant evaporators", International Journal of Refrigeration 35 325–335 .2012.
- [8] T.S. Khan, M.S. Khan, M.C. Chyu, and Z. H.Ayub, "Experimental investigation of evaporation heat transfer and pressure drop of ammonia in a 60° chevron plate heat exchanger", International Journal of Refrigeration 35 336–348, 2012.
- [9] T.S. Khan, M.S. Khan, M.C. Chyu, and Z. H.Ayub, "Evaporation heat transfer and pressure drop of ammonia in a mixed configuration chevron plate heat exchanger", International Journal of Refrigeration 41 92–102, 2014
- [10] B.H. Shon, S.W.Jeon, Y. Kim and Y.T. Kang, "Condensation and evaporation characteristics of low GWP refrigerants in plate heat exchangers", International Journal of Air-Conditioning and Refrigeration, 24(02), p.1630004.2016.
- [11] A. Desideri , J. Zhang , M. RyhlKærn , T. Ommen , J. Wronski , V. Lemort and F. Haglind, "An experimental analysis of flow boiling and pressure drop in a brazed plate heat exchanger for organic Rankine cycle power systems", International Journal of Heat and Mass Transfer113, 6–21 .96, 2017.
- [12] J. Zhang , A. Desideri , M. RyhlKærn , T. Ommen, J. Wronski and F. Haglind, "Flow boiling heat transfer and pressure drop characteristics of R134a, R1234yf and R1234ze in aplate heat exchanger for organic Rankine cycle units", International Journal of Heat and Mass Transfer 108 1787–1801,2017.
- $[13]\ M.\ Imran$  , M. Usman , Y. Yang and B.S. Park, "Flow boiling of R245fa in the brazed plate heat exchanger: thermal and hydraulic performance assessment", International Journal of Heat and Mass Transfer 110 657-670,2017 .
- [14] B.H Shon, C.W.Jung, O.J. Kwon, C.K. Choi and Y.T. Kang, "Characteristics on condensation heat transfer and pressure drop for a low GWP refrigerant in brazed plate heat exchanger", International Journal of Heat and Mass Transfer 122, 1272–1282,2018.
- [15] E.M Djordjedvic, S. Kabelac, and S.P. Šerbanovic, "Mean heat transfer coefficient and pressure drop during the evaporation of 1,1,1,2 tetrafluoroethane (R-134a) in a plate heat exchanger", Journal of the Serbian Chemical Society72 833–846,2007.
- [16] E.M Djordjedvic, S. Kabelac, and S.P. Šerbanovic, "Heat transfer coefficient and pressure drop during refrigerant R134a condensation in a plate heat exchanger", Chemical Papers. 62 78–85,2008.
- [17] E.M. Djordjedvi and S. Kabelac, "Flow boiling of R134a and ammonia in a plate heat exchanger", International Journal of Heat Mass Transfer 51 6235–6242,2008 .
- [18] D.C. Lee , D. Kim , S. Park , J. Lim and Y. Kim, "Evaporation heat transfer coefficient and pressure drop of R-1233zd(E) in a brazed plate heat exchanger", Applied Thermal Engineering 130,1147–1155, 2018 .
- [19] K. Sarraf, S. Launay, G. El Achkar and L. Tadrist, "Local vs global heat transfer and flow analysis of hydrocarbon complete condensation in plate heat

- exchanger based on infrared thermography", International Journal of Heat Mass Transfer 90 878–893,2015 .
- [20] R. Wang, and S. Kabelac, "Condensation quasi-local heat transfer and frictional pres-sure drop of R1234ze(E) and R134a in a micro-structured plate heat exchanger", Applied Thermal Engineering 197, 117404,2021.
- [21] K.Kariya, M.S. Mahmud, A. Kawazoe and A. Miyara, "Local heat transfer characteristics of the R1234ze (E) two phase flow inside a plate heat exchanger". International Refrigeration and Air Conditioning Conference, West Lafayette, IA, USA, 11–14 July 2016; pp. 1–8,2016.
- [22] G.A. Longo, S. Mancin, G. Righetti, and C. Zilio, "Local heat transfer coefficients of R32 and R410a condensation inside a brazed plate heat exchanger (BPHE)". International Journal of Heat Mass Transfer, 194, 123041,2022.
- [23] M.S. Mahmud, K. Kariya and A. Miyara "Local Condensation Heat Transfer Characteristics of Refrigerant R1234ze(E) Flow Inside a Plate Heat Exchanger", International Journal of Air-Conditioning and Refrigeration, Vol. 25, 1750004,2017.
- [24] K. Kariya, and A. Miyara, "Condensation and evaporation heat transfer characteristics of pure and binary-mixture HFO refrigerants inside a plate heat exchanger". IIR International Congress of Refrigeration, Montréal, QC, Canada, 24–30 August 2019; pp. 1644–1651,2019.
- [25] T. Tun, K. Kariya and A. Miyara, "Consideration on local heat transfer measurement of plate heat exchanger with the aid of simulation", EPI International Journal of Engineering 3,1–9,2020.
- [26] M.M Rahman, T. Tun, K. Kariya and A. Miyara, "Experimental Study of Condensation Local Heat Transfer Characteristics of R454B in a Plate Heat Exchanger" JSRAE Annual Conference, Okayama, Japan, 2022
- [27] M.M. Rahman, D. Bal, K. Kariya and A. Miyara "Experimental analysis of local condensation heat transfer characteristics of  $CF_3I$  inside a plate heat exchanger", Fluids 8, no. 5: 150,2023.
- [28] D. Bal, M.M. Rahman, K. Kariya and A. Miyara, "Experimental study of evaporation local heat transfer characteristics of  $CF_3I$  in plate heat exchanger". International Heat Transfer Conference (IHTC), Cape town, South Africa, 2023
- [29] E. Lemmon, M.L. Huber and M.O. McLinden, NIST Standard Reference Database 23: Reference Fluid Thermodynamic and Transport Properties REFPROP, Version 10.0; Standard Reference Data Program; National Institute of Standards and Technology: Gaithersburg, MD, USA, 2018.
- [30] A.K Mainil, H. Ubudiyah ,N. Sakamoto, K. Kariya and A. Miyara, "Experimental Study on Condensation Heat Transfer of R454B inside Small Diameter Microfin Tube". International Refrigeration and Airconditioing Conference, Paper 2411 Purdue, USA, 2022.

# Traffic Congestion in Megacity Dhaka: Case Studies from Seoul and Copenhagen Analyzing the Potential Measures

#### Md. Arifuzzaman

Department of Architecture, Dhaka University of Engineering & Technology, Gazipur-1707

E-mail: arifuzzaman@duet.ac.bd

#### **ABSTRACT**

Traffic congestion is a contemporary urban problem in many cities around the world. The capital megacity, Dhaka, in Bangladesh, also faces a tremendous traffic congestion problem as it hampers the city's efficient commute system, reduces the average transport speed on urban roads, and significantly destroys the productive working hours of the city people. The Bangladesh government has taken packages of strategic plans to reduce traffic congestion in Dhaka. This study analyses two case studies from Seoul in South Korea (Republic of Korea) and Copenhagen in Denmark to learn from their adopted measures to minimize traffic congestion on urban roads. Based on the analysis of the potential measures, this study suggests that promoting the public transportation system and its effective integration with the walking and non-motorized biking infrastructures may help reduce traffic congestion in Dhaka.

#### 1. INTRODUCTION

Traffic congestion on urban roads is a common aspect in many cities all over the world. Traffic congestion occurs when the sheer demand for transportation causes an outrageous physical presence of the transports on the streets, slowing down the average speeds of the vehicles and hampering the regular transportation flows [1]. Traffic congestion destroys a comfortable urban commute system and kills the urban dweller's productive time. Urban planners worldwide take different initiatives to control, reduce, or eliminate traffic congestion from the vibrant urban transportation streams. The context of Dhaka city in Bangladesh is not different from the urban impacts of traffic congestion, which brings much distress and destroys the productive hours of the urban inhabitants.

Dhaka is the capital city of Bangladesh, a South Asian developing country. Dhaka is a megacity with a population of 19.5 million in 2018 (megacities are cities with a population greater than 10 million). The United Nations projects that the city may have a population of more than 28 million by 2030 [2]. Dhaka contributes 36% to the country's Gross Domestic Product (GDP) and holds 31.8% of the country's total employment, which denotes the high importance of this megacity in the country's development [3]. This megacity's population density is 43,578 people per square kilometre, making it one of the world's densest cities [4]. The population increase rate of Dhaka city is 3.96% per year, which is contributed by both natural increase (1.47%) and regional migration to the city (2.49%) [3]. Due to the city's primacy in the prospective economic growth, the city attracts internal migration from the other regional areas, adding the migrated peoples to the natural population increase. Dhaka has become the most significant economic centre of the country, attracting businesses, factories (e.g., garment factories), real estate developers and labour flows. The city's massive population is enhancing transport demands, and the city's bottlenecking of low infrastructural capacities has made the city people face tremendous traffic congestion problems. The traffic congestion problem has become an enormous burden in the daily urban life of the city people as it destroys a significant amount of working hours by being stuck in Dhaka's streets [1], [5]. This paper attempts to analyze the nature, impacts and practical measures to reduce the traffic congestion problem in the megacity of Dhaka. It will bring two case studies regarding the best practices for traffic management from two world cities: Seoul in South Korea from an Asian context and Copenhagen in Denmark from a European context. Based on the lessons learned from these two case studies, the paper will analyze the vital policy measures adopted for managing traffic congestion in Dhaka and discuss the potential policy measures on the way forward.

This paper consists of seven sections. The first section introduces the megacity Dhaka, the traffic congestion problem, and the scope of this article. The second section discusses the methodology of the paper, revealing the sources of the data and the analytical methods. The third section promotes an analysis based on literature reflecting on the nature, urban impact, and the adopted policy measures for reducing the traffic congestion problem in Dhaka. The fourth and fifth sections introduce two case studies from Seoul in Asia and Copenhagen in Europe regarding the best practices for adopted measures to reduce urban traffic congestion. The sixth section promotes an attentive discussion on contextual practices or policy measures to tackle the traffic congestion problem and reflect on the way forward. Finally, the seventh section develops a conclusion

and indicates the scope of further research on the urban discussions the paper may help delve into.

#### 2. METHODOLOGY

The study relies on analyzing the secondary data from journal papers, books, government and international organization reports, and other relevant policy papers. The article discusses the case studies and relevant insights based on the information collected from the secondary sources cited in the study. The study follows a mixed method of data analysis, focusing on quantitative and qualitative reasoning where appropriate.

This paper adopts the case study-based approach from two different cities of the world (from Asia and Europe) to analyze the problems and the adopted measures and promote a discussion. The case study approach of this study stands on the methodological ground of 'comparative urbanism'. Comparative urbanism is a trend of urban research that promotes urban theorization based on learning from elsewhere in the cities around the world [6]-[9]. This trend develops an openness for ideas from other places while accepting the located-ness of the conceptualizations. It may help build innovative ideologies by thinking of similar problems with different experiences, limits and productive measures [6], [9]. Such an exploration may significantly enhance the realm of pragmatic practices, the revisability of the conceptualizations and the inspiration to learn from the differences [6].

The case study is a research method that accepts the process of maximizing learning to promote a better understanding of the studied problem and finding solutions. This research process accepts "multi-perspectival" methods of analysis for a common problem operating in different contexts [10]. This attribute of the case study method may contribute to concentrating on a problem and learning from different perspectives to find solutions or improve the prevailing measures. Such methodological avenues of the case study may warrant us developing the "multi-perspectival" discussions of the common problem of traffic congestion and finding innovative solutions based on our learning from different world-city's contexts, adopted measures, problems that arose for the measures, and their outcome's scopes. It also promotes a justification for this study to learn from different world contexts, develop discussions for innovative, out-of-the-box measures, and understand their scopes as validated by their positive outcomes. It positions this study's scope to engage in the discussion to learn from world cities to promote innovative responses for a common problem of traffic congestion or understanding 'what has been done' and 'what can be done'. So, the scope of the research is not to discuss the contextual differences of a problem but to promote discussions for innovative solutions by learning from the differences in the adopted measures.

Following its methodological trait, this study first delves into understanding the nature of the traffic congestion problem in Dhaka based on literature analysis of secondary sources. Then, it discusses the case studies of adopting innovative,

practical measures by two other global cities: Seoul and Copenhagen. Based on the insights, it promotes a discussion on the prospective, sustainable policy measures for reducing traffic congestion in Dhaka.

### 3. THE NATURE OF TRAFFIC CONGESTION PROBLEM IN DHAKA

#### 3.1 Causes of Traffic Congestion

It is difficult to explain any core cause or a universal motif of causes of traffic congestion in Dhaka city. Many issues contribute to the traffic congestion problem, and this paper tries to indicate the significant concerns discussed heavily in the available literature in this research field. Dhaka's population density is higher than other parts of the country as it is a megacity. Throughout history, this capital city has emerged as a prime city for economic opportunities. For promoting a sustainable urban transportation system, cities may need to have 25% of their area available for use as road infrastructure in general [11]. Mahmud et al. [11] discuss that Dhaka city has a total road area of 1286 km in length, and considering the city's area, only 9% is the road infrastructure. Among the city's road infrastructure, only 5% comprises the primary roads, and 36% of the total road network has a narrow width of less than 4.75 m.

Moreover, the Bangladesh Road and Transport Authority (BRTA) reports that many new transports are registered annually in Dhaka city [12]. This indicates that there is a heavy demand for transportation in Dhaka. Though a massive volume of new vehicles are registered yearly, the roads have not increased considering those [13]. So, inadequate road infrastructure in the face of high transportation demand may significantly cause traffic congestion problems.

The reluctance to follow the traffic rules also creates traffic congestion problems [14]. Public transport like buses tend to board passengers elsewhere from the road and hardly follow the traffic rules. Mixing non-motorized vehicles with motorized ones on the same street may be another cause of slowing down the speeds of the transports [15]. Drivers are most often reluctant to follow the lanes of the traffic movement on the road, which creates a haphazard movement in the transportation system [13], [14]. There is also a lack of a well-defined plan for pedestrians to follow for crossing the roads and moving along the sides of the streets. Some parts of Dhaka have foot overbridges for pedestrians to cross the vehicular roadways, but they are hardly adequate than necessary. However, pedestrians become unwilling to use those as there is less consideration for the elderly, sick or tired pedestrians to climb up to its significantly high level with its stairs to cross the roads [14], [16]. Some studies have reported that the condition of the pedestrian way or the footpath is not inviting enough for walking as those are occupied mostly by street hawkers, garbage, construction works or materials, and often remain broken, impelling the pedestrians to walk on the main roads [14], [17], [18]. Chowdhury [14] reports that 60% of the city's total 163 km long pedestrian ways are occupied by street hawkers,

roadside shops and construction materials. Parking of vehicles beside the roads, parking rickshaws (a type of non-motorized vehicle) to collect passengers, and grabbing of the road spaces by the street hawkers and petty businesses are also the issues that reduces the usable areas of the roads for free traffic movements [19], [17].

BRAC Institute of Governance and Development (BIGD) conducted a rigorous survey on the public consensus about the causes of traffic congestion in Dhaka city among the city's transport users [20]. The result of the study is presented in Fig. 1.

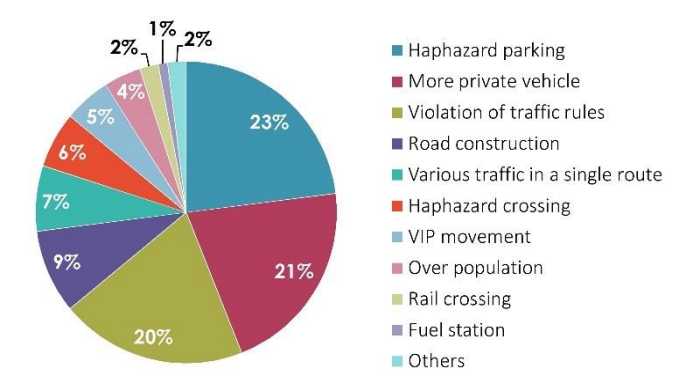


**Fig. 1:** BIGD survey on the public consensus about the causes of the traffic congestion in Dhaka city. Source: Based on [20].

The major trend of the responses in Fig. 1 shows that 'haphazard parking' is reported by 23% of the respondents as being a cause of traffic congestion, while 'violation of the traffic rules' is reported by 20%. The high presence of private vehicles moving on the roads, indicating the lack of public transportation services, is reported by 21% of respondents as a prominent cause of traffic congestion in the city.

#### 3.2 Impacts on Urban Life

Fig. 2 shows that the average travel speed in Dhaka is gradually reducing for traffic congestion. Due to traffic congestion, the average travel speed on the roads of Dhaka was reduced to one-third in 2017 compared to 2007, as the average travel speed plummeted from 21 km per hour to 7 km per hour during this period. Reports show that the average travel speed in 2018 was five km per hour during rush hour in Dhaka, which is close to the human's average walking speed of four km per hour [21], [22].

Traffic congestion causes a significant loss of working hours for city people and creates physical and mental stress for them. Reports show that every day, due to traffic congestion, 3.2 million productive work hours are getting destroyed on the roads in Dhaka. The national loss for traffic congestion in a year is around 370 billion USD, equivalent to 11% of the country's national budget [23].

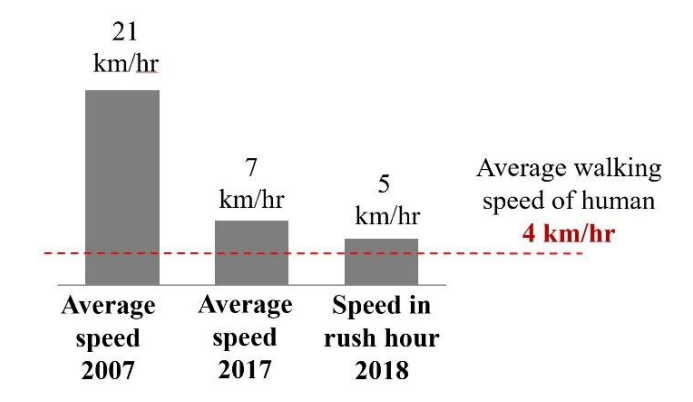


**Fig. 2:** Reduction of the average travel speed in Dhaka due to traffic congestion. Source: Author's composition based on [21], [22].

#### 3.3 Transport Modal Share in Dhaka

Dhaka city's transport modal share and its variation over time are presented in Table I. It may help analyze the preferred modes of transport of the city people and signify the potential of developing a sustainable transport system in Dhaka.

**Table I:** Dhaka City's transport modal share (Percentages of share).

Modes	DITS	DUTP	JBIC	STP	JICA	DSP <sup>1</sup>
	(1994)	(1997)	Study	(2005)	Study	(2016-
			(1999)		(2009)	2035)
Walk	60.1	62.82	62.05	14.0	19.09	19.80
Rickshaw	20.1	20.04	13.28	34.0	38.19	38.30
Bus	12.8*	10.42*	10.22	44.0*	29.83	30.0
Auto- rickshaw			5.83		5.73	6.60
Passenger Car/ Cars	7.0**	6.72**	3.97	8.0**	4.3	5.10
Others			4.65		2.86	0.20***
Total	100	100	100	100	100	100

<sup>\*</sup> Transit

Source: Author's composition based on [24], [3].

The transport modal share of Dhaka city in Table I shows that the share of walking as a mode has reduced significantly from 60.1% to 19.8% from 1994 to 2016. This change may indicate that walking is gradually becoming a less preferred method of transportation in Dhaka. During this period, the share of rickshaws increased from 20.1% to 38.30%, almost doubling. From 1999 to 2016, the share of buses as a mode

<sup>\*\*</sup> Motorized (non-transit)

<sup>\*\*\*</sup> Railway,

<sup>&</sup>lt;sup>1</sup>DSP: Dhaka Structure Plan 2016-2035.

increased almost three times as its share ascended from 10.22% to 30.0% by this period. Such a change may indicate a rapidly growing high demand for public transport in Dhaka. The modal share of passenger cars has an increasing trend from 3.97% in 1999 to 5.10% in 2016. It may imply that the car dependency of the city people is increasing. However, from 2016 data, it is evident that walking, rickshaw, and bus modes cumulatively constitute the paramount share (88.1%) of the total transportation system in the city when compared to the other modes. Such analysis may support an argument that advocating a good walking environment, non-motorized transportation facilities and promoting public transport systems in Dhaka may have prospective scopes for developing efficient urban transportation.

#### 3.4 Measures Adopted

Dhaka city planning authority has adopted 'Strategic Transport Planning' (STP), which contains different policy initiatives to reduce traffic congestion in the city. It promotes a master plan for 20 years, from 2016 to 2035, to develop an efficient transport system in Dhaka. Some of the vital initiatives are discussed in the following sections.

#### 3.4.1 Developing the Ring Roads

Dhaka Structure Plan (DSP) for 2016-2035 proposes constructing three concentric ring roads around Dhaka's central part, allocating a budget of 2 billion USD [3]. The total length of the ring roads will be 273 km, and the inner, middle, and outer ring roads will have a radius of 10 km, 15 km and 20 km respectively [3]. The purpose of these three ring roads is to segregate and divert the cross-traffics toward the outer roads, resulting in the city centre accumulating less traffic. It will prevent vehicles from unnecessarily crossing the city centre to travel to the outer city destination. This policy foresees increasing the average travel speed in Dhaka's city centre, reducing the number of vehicles occupying the roads in that area [3].

#### 3.4.2 Bus Rapid Transit (BRT)

BRT is a mode of low-cost urban transportation that fosters an economically responsive way for mass urban transportation in developing countries with resource constraints. The cost of a BRT project for urban services is one-third of that of the urban Light Rail Transport (LRT) project [24]. Dhaka Structure Plan (DSP) 2016-2035 proposes to develop three separate BRT lines in Dhaka named BRT corridor- 1, 2 and 3. Their routes are as follows as per the planning:

- BRT corridor-1 travels from Uttara to the Saidabad bus terminal by connecting DIT circular and Toyenbee roads.
- BRT corridor-2 travels from Gabtoli to Saidabad bus terminal via Mirpur.
- BRT corridor-3 travels from the city's international airport to Ramna via the airport road [24].

Studies foresee that the BRT corridors will help reduce 48.84% of present travel time [25]. The World Bank and

Asian Development Bank (ADB) are actively supporting the government in implementing the BRT project in Dhaka [24].

#### 3.4.3 Metro-rail: Mass Rapid Transit (MRT)

Dhaka Structure Plan (DSP), in its master plan for up to 2035, has proposed developing five rail-based Mass Rapid Transit routes (MRT-line 1, 2, 4, 5 and 6), allocating a budget of 15 billion USD. DSP foresees that these five lines of MRT may have an urban promotion area of 66.31% when people's catchment belt (walkable area) is considered two km. DSP projects that per year, the trip volume in Dhaka would be composed of 60 million passengers and the MRT system with its fully functional five lines in 2035 may serve the total passengers' 10% [3]. MRT demands the development of an entirely new infrastructure and management system, which may accrue high costs for a developing country. The government has implemented MRT-line 6 (21.26 km) running from Uttara to Kamlapur central railway station; part of it is presently open to the public. Gradually, in different time phases, the other line will be constructed. The government is getting support from the Japan International Cooperation Agency (JICA) for the MRT project [26].

#### 3.4.4 Management of Non-motorized Rickshaws

Following the Land Transportation Policy 2004, a new policy has been adopted in the Dhaka Structure Plan (DSP) 2016-2035 for managing the non-motorized rickshaws in the city. The new policy confines the movement of the non-motorized rickshaws within the city's residential areas, not hampering the movement of the motorized bus routes [3]. This policy focuses on increasing the speeds of motorized vehicles on the streets, avoiding the congestion caused by the slow-moving non-motorized rickshaws. The policy has empowered the Dhaka City Corporation and the Dhaka Metropolitan Police Department to ban non-motorized rickshaws on the city's busy motorized vehicular roads. The policy also directs the law enforcement authorities to actively check the licences of the rickshaws and ban the movement of unauthorized ones on the streets [3].

#### 3.4.5 Foot Over Bridges and Sidewalks

Through the initiatives of the Clean Air & Sustainable Environment (CASE) project sponsored by the World Bank, Dhaka city developed sidewalks and foot-over bridges at different essential locations of the city for pedestrians [3]. However, the proportion of the sidewalks and the foot overbridges is inadequate in this overly populated city.

#### 3.4.6 Policy Outcomes

The government of Bangladesh has taken different long-term steps in its strategic plan (the master plan for 2035) for Dhaka's transport. Implementation of such long-term policies would require some time, and the policy outcomes would be prominent when the city people could access the facilities in full swing.

#### 4. CASE STUDY FROM SEOUL, SOUTH KOREA

Seoul is the capital city of the Asian country South Korea (Republic of Korea), with a population of 9.9 million in 2018 and a projection to increase to 10.1 million by 2030 [2]. Seoul achieved the 'Lee Kuan Yew World City' international prize in July 2018 for developing sustainable solutions enhancing urban liveability, defeating 28 other competitor world cities, including Tokyo (Japan) and Hamburg (Germany) [27]. Some of their adopted measures for managing urban traffic congestion can be studied as the best practices following the scope of this paper.

With the economic development, the city people in Seoul became inclined to use private cars as a predominant mode of transportation. In 2000, the transport modal share of private cars was 77%. Between 1970 and 2002, the number of registered private cars increased 39 times. However, the city's road infrastructure did not increase in the same proportion as the studies show there was an increase of 3.7% in road infrastructure from 1999 to 2003. The high modal share of private cars was causing great suffering, contributing to the city's traffic congestion. To improve the urban transportation system by reducing traffic congestion, the Seoul Metropolitan Government (SMG) has taken some sustainable policy measures that significantly reduce the problem. The following sections will unpack some of those measures.

#### 4.1 Policies to Promote Public Transport

Seoul focused on reducing private car dependency and enhancing public transport use to decrease traffic congestion [28]. A milestone policy was taken in 2004 by the SMG to promote a public-transport-oriented urban system. The policy aimed to increase the modal share of public transport by up to 70% and the average travel speed to 20 km per hour by 2020 [29]. An integrated public transport network was advocated to achieve such targets using metro services, buses, and other public facilities. Fig. 3 shows the city's target plans to achieve the policy goals.

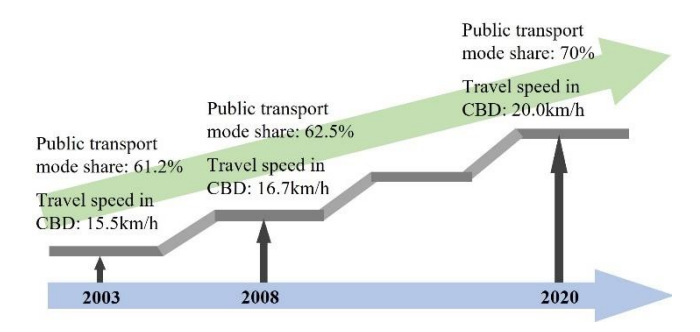


**Fig. 3:** Seoul's plan to achieve the goals of public-transport-oriented policy. Source: Author's illustration based on [29].

#### 4.2 Seoul's Experience with Metropolitan Rail Service

In 1974, Seoul first constructed an eight-kilometre Metrorail line that was developed into a network of 487 kilometres by 2004 with 389 metropolitan rail stations [30]. 8.4 million people travel daily on the metropolitan rail from Seoul's urban and suburban areas. Seoul's number of everyday metropolitan rail passengers is double the number of New York City's subway commuters per day. However, Seoul found that metropolitan rail infrastructure as a mode of urban transportation is costly as it provoked 80% of the city's total debt (6 billion USD). In 2003, the passenger's fare only contributed 75% to the total cost of operating the metropolitan rail service, incurring a 634 million USD deficit in the operating cost of the metropolitan rail [30]. The SMG faced massive pressure to manage the metropolitan rail service's high cost incurred from its construction, operation and management. This phenomenon led the SMG to look for a cost-effective and sustainable way to promote public transportation, such as developing the bus's infrastructure

#### 4.3 Promoting BRT and BMS

The SMG promoted the Bus Rapid Transit (BRT) network with 7,484 buses on 360 bus routes by 2013. Differentiated by colour-coded bus routes, it followed the 'trunk-and-feeder' system connecting different parts of the city such as suburban areas (blue busses), subway stations (green busses), other metropolitan downtowns of the city (yellow busses) and the other satellite towns (red busses) [30], [31]. Fig. 4 illustrates the 'trunk-and-feeder' concept for managing the bus routes serving urban commuters in different regions. By 2012, the SMG had developed 115 km BRT lines and adopted a plan to increase the BRT line to 223km in the future to support the city's public-transport-focused policy [31].

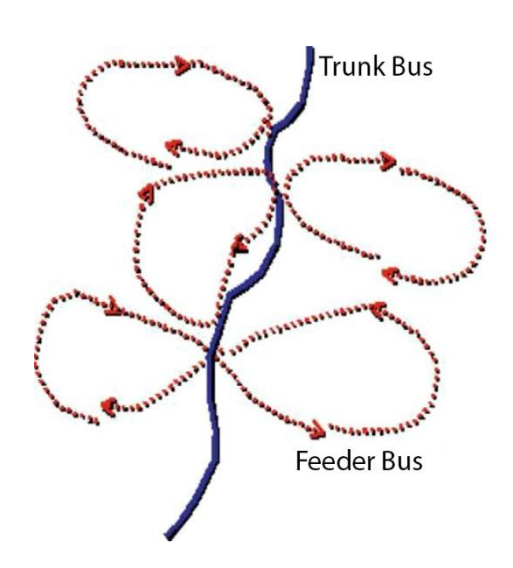


**Fig. 4:** Illustration of bus route's 'trunk-and-feeder system'. Source: Adopted from [28].

The SMG has also developed an integrated Bus Management System (BMS) in Seoul with state-of-the-art technologies. It has introduced median bus stops on the roads and low-floor buses for easy access for uninterrupted transportation. It has also become oriented to electric buses, replacing the previous CNG-driven buses. The SMG follows the quasi-

public revenue management, combining the SMG and the bus companies. It fosters a competitive attitude among the bus companies to provide quality services [31].

#### 4.4 Smart City with Intelligent Traffic Management

Seoul TOPIS (Seoul Transport Operation & Information Service) is a management centre for the integrated, intelligent and effective system of urban transportation networks [31]. Using state-of-the-art technologies, it collects information from different networks of sources and transmits relevant data to different management systems, such as various sorts of urban transport systems, police departments and other types of unmanned enforcing segments. It also enforces an effective CCTV vehicle management system for managing the parking lanes, violation of the traffic rules, median bus tracks, and bus stops. Fig. 5 represents an interior view of the Seoul TOPIS control room [31].



**Fig. 5:** Seoul TOPIS control room, interior view. Source: adopted from [31].

#### 4.5 Congestion Pricing and Parking Policy

Seoul has introduced a 1.5 USD fee for accessing the tunnels connecting CBD with the areas located at the southern part of the Han River (Nasman 1 and 3 tunnels) since 1996. It reduced 24% of traffic (vehicles per day) accessing the CBD, and the traffic speed significantly increased from 21.6 km-per-hour to 33.6 km-per-hour [28].

SMG has reduced the parking requirement in the new building's planning and design from the previous 40% to 20% in the central part of the city (in the CBD) to discourage city people's orientation to private cars [28]. Along with this, SMG has reduced the public parking facilities and the spaces for street parking with the intention that car users need to focus more on private parking spaces, incurring more costs (parking fees), which may help discourage them from using private cars [28].

#### 4.6 Impacts of the Adopted Measures

The SMG's sustainable policies brought a positive impact as they helped to decrease traffic congestion significantly while elevating the movement speed of vehicles and increasing the satisfaction level of city people. Fig. 6 shows that transport speeds in the city centre and the outer city areas increased successively between 2004 and 2013. It also shows that during this period, the movement speed of private cars and public buses increased.

Fig. 7 shows that the total modal share of the city's public transport in 2016 reached 65.1%, composed of the modal shares of the public bus (28%) and the subway system (37.1%). Fig. 8 shows that in 2003, the average satisfaction level was 4.76, which started to increase gradually after the introduction of the new transport policy in 2004, and in 2012, the citizens' satisfaction level was recorded to be 7.5. Seoul's feedback methodology to understand the impact of the policy reform shows a tremendous positive impact of the transport policy on the city.



**Fig. 6:** Gradual increase of vehicular speed in Seoul from 2004 to 2013. Source: Adopted from [28].

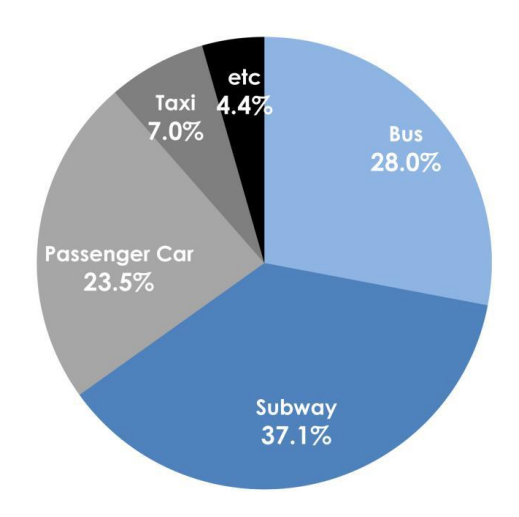


**Fig. 7:** Seoul's transport modal share in the year 2016. Source: Adopted from [31].

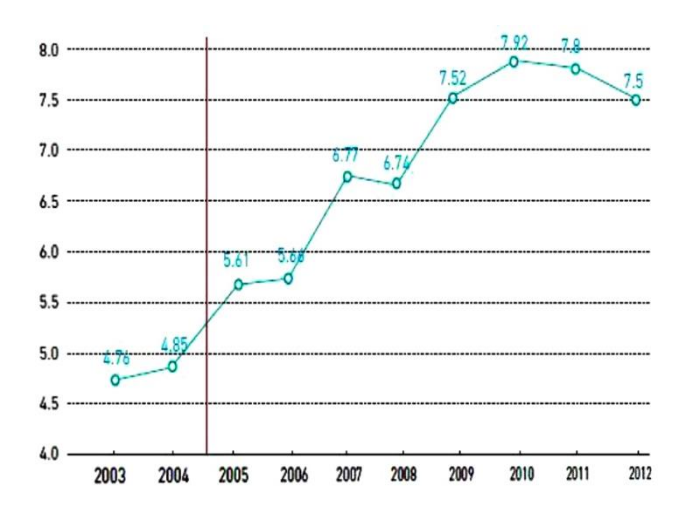


**Fig. 8:** The citizens' satisfaction level in Seoul has increased gradually in different years.

Source: Adopted from [31].

#### 5. CASE STUDY FROM COPENHAGEN, DENMARK

The city of Copenhagen is the capital city of Denmark in northern Europe, having a population of 1.3 million in 2018, with a projection to increase to 1.4 million by 2030 [2]. The city has adopted the transport policy's path dependency to promote walking and biking as the city's primary modes of public transportation. The city promotes biking as a safe, environment-responsive and cheaper mode of urban transportation and focuses on developing well-connected bike networks integrated with other modes of public transport like public buses and urban railway services [32].

The city adopted a 'strategic plan' in 2000 to improve the cycling facilities further by 2012. The city allocated a budget of 9.1 billion USD in 2000 to improve its transportation system, where one-third of this budget was utilized to improve the city's cycling infrastructure [33]. The city aimed to increase the proportion of city people considering cycling as a safe transport mode to 80% by 2012 from 57% in 2000. It also aimed to elevate the proportion of the city's active cyclists from 34% in 2000 to 40% in 2012. The city's strategic plan focused on obtaining the modal share of cycling to be 50% among all the transport modes by 2016 through the enhancement of the urban cycling experience, ameliorating safety, comfort, and services. [33].

Moreover, the city's 'CPH-2025 Climate Plan' stressed cycling as an environmentally responsive transportation mode that reduces carbon emissions [34]. It developed a policy target to attain 75% of the total trips in the city to be covered by walking, biking, and use of different public transport modes by 2025. The plan also aimed to contribute to making Copenhagen a carbon-negative city by reducing 10% emissions from urban vehicles. The 'Copenhagen's cycle-strategy plan' for 2011 to 2025 developed a policy target for the consistent increase in the city's travel speed by 5%, 10% and 15% by 2015, 2020 and 2025 respectively [34]. Some key measures of Copenhagen for attaining such policy goals are discussed in the following sections.

#### 5.1 Developing Bike-networks

The city people have an age-old culture of using bikes as a mode of transportation since the 1960s or 70s. The number of cyclists had increased significantly by 2016, such that one in every three city inhabitants owns a bike [33]. On both sides of the motorways, the city government has built separate infrastructural networks of bike lanes having a total length of more than 3,000 km. Such bike lanes are a separate infrastructure from the motorized and pedestrian circulations and contain a width of 2 meters for bike movements (see Fig. 9).

Along with the bike lanes, the city has focused on developing and managing efficient bike parking facilities. The city has also introduced cargo bikes that bring the facility to carry goods or other heavy baggage using the bike infrastructures. 26% of families in the city containing two or more children possess such a cargo bike [35].

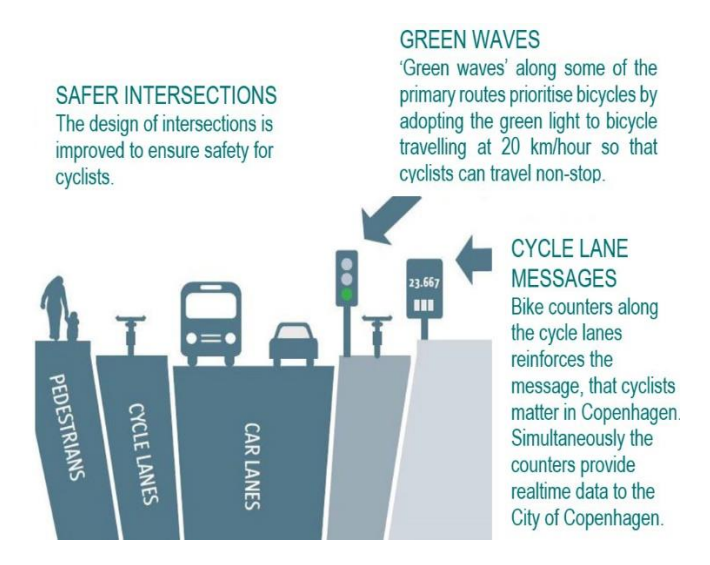


**Fig. 9:** Separate bike lanes in Copenhagen. Source: Adopted from [36].

#### 5.2 Greenways and Bridgeways

The city has developed 43 km of urban greenways and adopted a plan to build another 54 km to help cyclists move away from the motorways and come close to the green nature or the public recreational spaces [35]. The city has also constructed two bridgeways for bicycles over the watery parts of the city to develop a connected bicycle network. Such initiatives may enhance comfort and promote a good biking environment for the city people coming close to nature [36].

#### **5.3 Promoting Public Transport**

The city has developed an efficient public transportation service with the A-bus, S-train and urban metro services that 0.75 million urban people use for travelling each weekday. The city plans to elevate the urban inhabitants' use of public transport by 3.4%. Reports show that 98% of people in

Copenhagen may find access to public transportation facilities within a distance of 350m. All the public transportation systems in the city are managed by the 'intelligent traffic management system' using state-of-the-art technologies to enhance efficiencies [37]. The bike infrastructures and the public transport services are interconnected to promote an efficient network of urban transport systems (see Fig. 10). 27% of the people who use urban rail services for long-distance commutes use bikes for accessing the rail stations [38].



**Fig. 10:** Copenhagen's framework for promoting interconnected bike routes and public transport. Source: adopted from [38].

#### **5.4 Impacts of the Adopted Policies**

The satisfaction level of the urban inhabitants in Copenhagen for the total network of bike lanes developed was boosted from 64% in 2004 to 80% in 2014. Their satisfaction level for the effective maintenance of the bike lanes also increased from 50% in 2004 to 63% in 2014 [35].

Reports show that 88% of Copenhagen's urban inhabitants consider cycling a faster, safer and more convenient mode for city travel [36]. Fig. 11 shows that for all the urban journeys in Copenhagen made in the year 2014 having the purpose of education and work, the city's transport modal share for cycling was 45%, while the modal share of public transport, car, and walking was respectively 27%, 23% and 5% [35]. Here, it is significant to note that the transport modes of cycling, walking and public transport comprise 77% of the total urban modal share, while the car contributes 23%.



**Fig. 11:** Copenhagen's transport modal share in the year 2014 for education and work-related trips. Source: Author's composition based on [35].

Fig. 12 shows that in 24 hours on a weekday, the number of cars travelling in the city centre of Copenhagen decreased from 0.46 million in 1970 to 0.32 million in 2014 [35]. During this period, the number of cycling trips to the city

centre has increased by more than double [35]. A city generally accumulates more cars over the years, but the number of cars in the city centre has reduced significantly due to Copenhagen's sustainable transport policy.

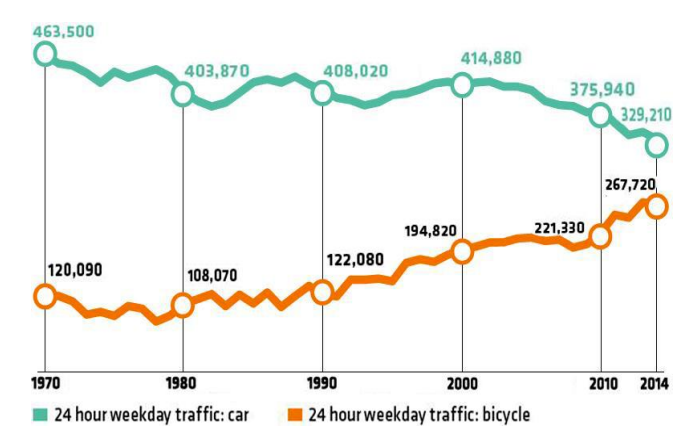


**Fig. 12:** Number of vehicles travelling to and from the city centre in Copenhagen in 24 hours.

Source: Adopted from [35].

#### 6. DISCUSSION: INSIGHTS FROM THE CASE STUDIES AND THE WAY FORWARD

Dhaka city is a densely populated megacity, and the city is accumulating more people due to migration from other regional places in Bangladesh. Though the contexts of the case studies presented in this paper are different from Dhaka city, they may offer different lessons based on the adopted measures, the practicalities of different sorts of transport policies and the positive outcomes of those. As Dhaka contributes highly to the country's economy, it develops the significance for the city's transport planning to consider learning from the world of cities for managing common or similar problems and developing creative, local and sustainable urban solutions. Sustainability is always a locally situated issue that satisfies any practice's environmental, economic, and socially viable aspects. The context of Seoul documents the successful implementation of the action plans for the adopted public-transport-oriented policies in the face of traffic congestion due to the city's high car dependency. The context of Copenhagen from northern Europe presents the city's orientation to a greener arrangement for public transportation, focusing highly on walk-bike urbanism. Both case studies show the public acceptance of the transport policies as the citizens' satisfaction levels have increased.

Dhaka city is rapidly growing with the increased population, which may cause a fast rise in urban transportation demands. There is a lack of workable data regarding the behaviour of the mass people, the traffic loads on different roads, the city's informality, people's levels of responsiveness to the laws, and the projection for future traffic demands. Both case studies show that smart cities adopt high-quality urban data using state-of-the-art technologies that support planning for and managing integrated and efficient urban transport systems. Dhaka city may have the scope to improve the use of state-of-the-art technologies for developing urban

### Traffic Congestion in Megacity Dhaka: Case Studies from Seoul and Copenhagen Analyzing the Potential Measures

transport networks as the city promotes a vital contribution to the county's economic development.

Dhaka city's transport modal share shows that in 2016, the city's major share (88%) of the trips was covered by rickshaws, buses, and walking, which determines that there remains a good scope for promoting public transportation and walk-bike urbanism. The data for the major modal share in Dhaka justifies that improvement of the facilities for public transportation and walk-bike urbanism may also have a profound public acceptance, satisfying the socially viable aspects of sustainability.

The government of Bangladesh has taken a package of strategic plans for the long term to decrease the traffic congestion problem in Dhaka city and has sanctioned an investment budget of over 37 billion USD [3]. Regarding the adopted policy measures, the proposed MRT networks (metro rails) and the BRT lines will help enhance the public transportation facilities in Dhaka. However, from the case study of Seoul, it may be pointed out that the metro rail service may be a costly mode of transportation for promoting public transportation in a developing city. To promote an efficient metro rail network in Dhaka city, new infrastructure, operating and management systems need to be set up. Seoul's case also documents that the urban bus rapid transit (BRT) system may promote a low-cost and relatively easy-executable infrastructure for a city in a developing country with resource limitations compared to the metro rail system. Both the initiatives of developing MRT and BRT in Dhaka are robust measures that may help reduce traffic congestion in Dhaka, and the government must continue to implement such public-transport-oriented policies successfully.

The government's plan to develop separate 'ring roads' around Dhaka city may help decrease traffic congestion, reducing the number of vehicles in the city centre by diverting the vehicles crossing the city redundantly to go elsewhere. As discussed, Dhaka city's total road infrastructure is less than what is required for sustainable urban transportation, which will also be improved with such ring roads. Along with this, congestion pricing may be introduced for the bustling roads in the city centres to discourage car users from using the overloaded routes. Rates of such congestion pricing may vary depending on the travelling time (peak or off-peak rates) on these busy routes. The case study of Seoul shows that congestion pricing has helped reduce the traffic on the busy roads in the city centre and enhance travelling speed.

The case study of Copenhagen points out that walking and non-motorized biking by city people may promote a city's major transport mode, reducing car dependency, traffic congestion and carbon emissions. The study documents that transport modes of walking and non-motorized vehicles can be effectively integrated with the motorized public transport system. Dhaka's transport modal share shows that non-motorized vehicle rickshaws had a 38.3% share in 2016, which has occupied an increasing trend over the past few years. The government's policies for non-motorized vehicles

may help increase the speeds of motorized vehicles, but it demands more robust planning regarding the routes of nonmotorized vehicles. The non-motorized vehicle routes need to be well-organized and well-planned to integrate with the motorized public vehicle routes to promote a sustainable urban transport system. Besides, Dhaka city does not have a separate bike infrastructure at present. Planning for the routes for non-motorized vehicles may help incorporate bicycles and cargo bikes as a mode of mass transportation. Along with the planning and successful implementation, the urban people may need to be encouraged to cycle in the city, and necessary signposting must be provided for the cyclists' ease of integration with the public transport routes. The case of Copenhagen shows that designed bike routes having safety intersections, green waves (speed limits), cycle lane message boards, and the setting of greenways to connect with nature and public places have enhanced the safety and comfort of cyclists.

Dhaka's transport modal share shows that the modal share of walking has a decreasing trend as it plummeted from 60.1% in 1994 to 19.8% in 2016 (decreased 32.9% in 20 years). It documents that walking in Dhaka city is becoming a less popular mode of transportation. The footpaths (pedestrian ways) in Dhaka need to be planned well to enhance the walkability and comfort of the city's people. The footpaths need to be made free from obstacles like construction materials and encroachments of the street hawkers. An integrated design with the vehicular way, separate bike lane, footpath, and a well-designated space for street hawkers alongside the footpath may be developed. Dhaka city's policy measures to develop foot overbridges for pedestrians are good initiatives for safely crossing busy roads, but the foot overbridge's universal accessibility, comfort, and maintenance need to be carefully addressed.

The case study of Seoul shows that reducing publicly available parking facilities and impelling car owners to pay high parking fees may discourage car dependency. Dhaka city may strengthen the traffic laws for unauthorized parking near the roads and promote separate places designed for vehicular parking with parking fees to discourage car dependency.

Both case studies show the importance of the state-of-the-art intelligent traffic management system providing real-time GPS-tracked transport information. Dhaka may need to plan for developing, implementing, and maintaining an intelligent traffic management system. It will help efficiently manage the transport system, promote traffic rules and send relevant information to law enforcement agencies and the users. Both cases have presented the city's innovative methodology to perceive the feedback and public acceptance of the adopted policies (such as citizens' satisfaction levels, speed and number of vehicles on the roads) to plan effectively in the urban areas. Dhaka city may develop a methodology to understand the impacts of the policies and take necessary steps based on that on the way forward. Without a good monitoring and feedback system, no responsive planning and positive outcomes would be possible.

The discussion above regarding the learning from the case studies and the way forward for Dhaka city to reduce traffic congestion demonstrates that some of the measures adopted by the government may positively impact decreasing the traffic congestion problem, and the government must continue to implement the strategic plans successfully. This study builds on the present strategic plans and discusses additional innovative measures justified by their application by the other cities to determine the potential avenues to follow. This study has found that the promotion and successful implementation of the contemporary walk-bike urbanism concept and its effective integration with an efficient urban public transport system may help reduce the traffic congestion problem in the megacity of Dhaka. Such integrated transport planning for Dhaka may have the to advocate an environmentally economically responsive, and socially acceptable system fostering sustainability.

#### 7. CONCLUSIONS

This paper focuses on the traffic congestion problem in the megacity Dhaka and has analyzed its significant causes, impacts on urban life and the adopted policy measures to reduce the congestion problem. It discusses that the government of Bangladesh, through the Strategic Transport Planning in Dhaka, has commissioned a long-term master plan for 20 years (2016-2035). This paper bears significance in suggesting innovative and potential measures to reduce the traffic congestion problem based on the learning from the case studies. This article brings two case studies from Seoul in South Korea and Copenhagen in Denmark to discuss and learn from the best practices of the adopted measures reducing traffic congestion in urban areas. The study suggests that improving Dhaka city's public mass transportation facilities with urban bus and train services may help reduce traffic congestion. Lessons from the case studies document that promoting walking and non-motorized transportation systems in Dhaka city may have tremendous potential to reduce traffic congestion significantly. To promote an efficient urban transportation system, walking and non-motorized biking infrastructure must be integrated with the public transportation routes. The case studies also support the idea that Dhaka needs to adopt an intelligent traffic management system and an effective monitoring and feedback method to learn about the responsiveness of the adopted policies to minimize the congestion problem. The study may promote the scope for further research regarding how the city peoples' responsiveness to different policy measures contributes to reducing the traffic congestion problem in Dhaka.

#### REFERENCES

- [1] S. I. Khan et al., 'Traffic congestion in Dhaka city: suffering for city dwellers and challenges for sustainable development', *European Journal of Social Sciences*, vol. 57, no. 1, pp. 116–127, 2018.
- [2] United Nations, *The World's Cities in 2018—Data Booklet*. Population Division, 2018.
- [3] RAJUK, 'Dhaka Structure Plan Report 2016-2035',Rajdhani Unnayan Kartripakkha, Capital Development

- Authority of the Government of Bangladesh, Dhaka, Bangladesh, 2016.
- [4] BBS, Ed., Bangladesh Population and Housing Census 2011: Urban Area Report, vol. National Report Vloume-3. Dhaka: Bangladesh Bureau of Statistics, Statistics and Informatics Division, Ministry of Planning, Government of Bangladesh, 2014.
- [5] S. Chakraborty, 'Traffic Congestion in Dhaka City and its Economic Impact', *Journal of Business Studies*, vol. 1, no. 1, pp. 45–68, 2016.
- [6] J. Robinson, 'Comparative urbanism: New geographies and cultures of theorizing the urban', *International journal of* urban and regional research, vol. 40, no. 1, pp. 187–199, 2016
- [7] C. McFarlane, 'Studies in comparative urbanism', *The Companion to Development Studies*, p. 296, 2014.
- [8] J. Nijman, 'Introduction—comparative urbanism', *Urban Geography*, vol. 28, no. 1, pp. 1–6, 2007.
- [9] C. McFarlane, 'The comparative city: Knowledge, learning, urbanism', *International journal of urban and regional research*, vol. 34, no. 4, pp. 725–742, 2010.
- [10] W. Tellis, 'Application of a case study methodology', *The qualitative report*, vol. 3, no. 3, pp. 1–19, 1997.
- [11] S. S. Mahmud et al., 'Deficiencies of existing road network in Dhaka metropolitan city', in *Publication in 10th Pacific Regional Science Conference Organization (PRSCO)* Summer Institute, 2008.
- [12] BRTA, 'Number of Registered Motor Vehicles in Dhaka (Yearwise)', Dhaka, Bangladesh, Bangladesh Road and Transport Authority, 2021.
- [13] K. Mahmud et al., 'Possible causes & solutions of traffic jam and their impact on the economy of Dhaka City', J. Mgmt. & Sustainability, vol. 2, p. 112, 2012.
- [14] M. M. Chowdhury, 'Traffic congestion and mismanagement in Dhaka city', Planned Decentralization: Aspired Development, World Town Planning Day, 2013.
- [15] J. Al Mahmud et al., 'Impact of pedal powered vehicles on average traffic speed in Dhaka city: A cross-sectional study based on road class and timestamp', in 2021 IEEE 9th Region 10 Humanitarian Technology Conference (R10-HTC), 2021, pp. 01–06.
- [16] A. K. M. Abir and M. S. Hoque, 'A study on mobility problem of disabled people in Dhaka city', in 4th annual paper meet and 1st civil engineering congress. Dhaka: Bangladesh University of Engineering and Technology, 2011, pp. 152–61.
- [17] S. I. Khan et al., 'Traffic congestion in Dhaka city: suffering for city dwellers and challenges for sustainable development', *European Journal of Social Sciences*, vol. 57, no. 1, pp. 116–127, 2018.
- [18] F. Rahman et al., 'Road users Perception about the Sidewalk Condition of Dhaka City', in *The 2nd International Conference on Innovative Engineering Technologies, Bangkok, Thailand*, 2015.
- [19] K. E. Zannat et al., 'Parking demand and supply analysis of major shopping centers in Dhaka–a case study of New Market Shopping Center along Mirpur Road', *Journal of Bangladesh Institute of Planners ISSN*, vol. 2075, p. 9363, 2013
- [20] BIGD, State of Cities 2016: Traffic Congestion in Dhaka City-governance Perspectives. Dhaka, Bangladesh: BRAC Institute of Governance and Development, BRAC University, 2016.
- [21] The World Bank, (2017, July.19), A Modern Dhaka is Key to Bangladesh's Upper-Middle Income Country Vision.
- [22] R. Ahmed, 'Dhaka on halt!', *Dhaka Courier*, vol. 34, no. 39, p. 40, Apr. 06, 2018.
- [23] bdnews24.com, 'Bangladesh loses Tk 370bn a year to Dhaka

#### Traffic Congestion in Megacity Dhaka: Case Studies from Seoul and Copenhagen Analyzing the Potential Measures

- traffic congestion: Study', Jan. 23, 2019[Online]. Available: https://bdnews24.com/bangladesh/2018/05/19/bangladeshloses-tk-370bn-a-year-to-dhaka-traffic-congestion-study [Accessed: 23 January 2019].
- M. M. Hoque et al., 'BRT in Metro Dhaka: towards achieving a sustainable urban public transport system', in Proceedings of CODATU XV: The Role of Urban Mobility in (re) shaping Cities, 2012.
- [25] S. Anam et al., 'Evaluation of bus rapid transit (BRT) in context of Bangladesh', in 4th 6 Annual Paper Meet and 1st Civil Engineering Congress, 2011.
- DMTCL and DTCL, 'Mass Rapid Transit (MRT Line 1 and Line 5)', Dhaka Mass Transit Company Limited and Dhaka Transport Coordination Authority, Dhaka, Bangladesh, Mar.
- [27] MSN, 'Seoul wins Lee Kuan Yew World City Prize', MSN news, Seoul, South Korea, Jul. 06, 2018[Online]. Available: https://www.msn.com/en-sg/news/newsother/seoul-winslee-kuan-yew-world-city-prize/ar-AAzEkPH.
- [28] S. Lee et al., 'Innovative Public Transport Oriented Policies in Seoul', Transportation, vol. 33, no. 2, pp. 189–204, Mar. 2006 [Online]. Available: 10.1007/s11116-005-3050-6.
- H. Allen, 'Bus reform in Seoul, Republic of Korea', Global Report for human settlement, 2013.
- J. Pucher et al., 'Public Transport Reforms in Seoul: Innovations Motivated by Funding Crisis', Journal of Public *Transportation*, vol. 8, no. 5, pp. 41–62, Dec. 2005 [Online]. Available: 10.5038/2375-0901.8.5.3.

**DUET Journal** 

- 'Seoul Public Metropolitan Government. Transportation', Seoul Metropolitan Government, Jun. 2014.
- [32] N. Jensen, Ed., 'Cycle Policy 2002-2012'. City of Copenhagen, Building and Construction Administration, Roads and Parks Department, Jul. 2002.
- [33] G. Ruggieri, 'The State of Art of Copenhagen's Cycling Infrastructure and Possible Application in Other Urban Contexts', Master Degree Thesis, School of Architecture, Urban planning and construction Engineering, Politecnico Di Milano, 2016.
- City of Copenhagen, 'Better mobility in Copenhagen, ITS Action Plan 2015-2016', Technical and Environmental Administration, Nov. 2014.
- City of Copenhagen, 'Copenhagen City of Cyclists, The bicycle Account-2014', Technical and Environmental Administration, 2014.
- City of Copenhagen, 'Copenhagen: Solutions for Sustainable Cities', Jan. 2014[Online]. Available: https://stateofgreen.com/files/download/1174 [Accessed: 2
- European Commission, 'Local Transport Copenhagen'. 2012[Online]. Available: http://ec.europa.eu/environment/europeangreencapital/wpcontent/uploads/2012/07/Section-2-Localtransport Copenhagen.pdf. [Accessed: 3 March 2019].
- Denmark Ministry of Transport, Denmark on your bike: the national bicycle strategy. Transportministeriet, 2014.

### A Simulation Study of Daylighting Performance for Different Window Configurations in Architectural Design Studio to Enhance Lighting Quality at DUET, Gazipur

#### Farhana Ahsan

Assistant Professor, Department of Architecture, Dhaka University of Engineering and Technology (DUET), Gazipur - 1700,
Bangladesh

#### **ABSTRACT**

Due to a lack of proper knowledge and awareness, the use of some blessings in nature is sometimes overlooked. Daylight is one of the blessings that is received almost free of cost from nature. Students in the design studios of DUET get excess daylight near the window, whereas those farther away do not. To control the glare, they use curtains and again lit the artificial lights to illuminate the entire space. The aim is to study the effectiveness of different window configurations in an architectural design studio to enhance daylighting quality. In the beginning, a 3D model of the studio will be generated in the ECOTECT to study the existing distribution and uniformity of daylight in the case space. Then, to enhance the quality and improve distribution, three alternative options will be generated with different sizes of window, light shelf, and reflector. These models will be exported to a physically-based backward raytracer, RADIANCE Synthetic Imaging software, for generating realistic lighting levels to validate and cross-check the ECOTECT results. Then, existing lighting conditions will be analyzed on some selected grid points. Hourly daylight data for the whole year will be generated at each point using the DAYSIM simulation exercise. It is expected that this paper will generate some ideas that will be beneficial for architects and designers to design windows for architectural design studios through simulation exercises to ensure a better daylighting environment.

#### **Keywords**

Daylighting performance, Architectural design studio, Window configuration, Lightshelf, Simulation exercise

#### 1. INTRODUCTION

In Bangladesh, very few studies have been done on the impact of daylight and student performance. As a result, the consideration of natural lighting quality in the classroom is less concern during designing an educational building. The environment of a classroom has a great impact on students. The lack of a good environment in the classroom can result in physiological and psychological impacts on the student. Each individual student in a classroom often does not get equal daylight on their desk [1]. In the design studio of DUET Gazipur, the quantity of interior daylight is not sufficient for drawing purposes. The students near the windows get much light than the ones sitting far from the windows. On the other hand, those who sit just beside the window most of the time get excess daylight, which creates glare problems [2]. As a result, they shut down the window and use artificial light. Eventually, the electricity bill raises unnecessarily, which gives a negative impact on the national energy consumption. As they work all day long in these studios, they get tired and stressed.

The objective of the study is to use daylight as the main source of light. Again, would try for distributing the illumination evenly to each student on their drifting table. In addition to get rid of glare would be a major concern. Eventually to make an economically beneficial condition by reducing the load of electricity. Overall, to create an enjoyable environment where a pupil can stay for a long period of time without stress and perform better.

This paper consists of three major parts. The importance of daylight, classroom environment, and standards are described in the first part. The second part intricate the steps of the research methodology. Finally, the findings of simulation results with a conclusion, presents the third part. It is expected that the examples of daylight simulation presented in this paper will be helpful to designers for understanding the significance of the simulation process for an effective day-lighted design studio.

#### 2. LITERAURE

Human function depends on light since it enables us to view objects and carry out tasks. But it's also significant since it has an impact on people's physiology and psychology. Numerous studies have shown how important light is for enhancing mood, lowering weariness, increasing alertness, and regulating circadian rhythms [3].

# A Simulation Study of Daylighting Performance for Different Window Configurations in Architectural Design Studio to Enhance Lighting Quality at DUET, Gazipur

#### 2.1 Health and Wellbeing

From the studies of Boyce and colleagues it is clear that various lighting conditions have an impact on people's emotions [4]. Mood changes often affect changes in behaviour and performance at work. One of the characteristics of a high-performance building is the use of daylight or natural light for illumination. Natural light helps building inhabitants greatly on a physical and psychological level, in addition its advantages is the source of light is free [5]. The level of daylight important for the student's vision and it limits the effect of harmful electrical light [6]. The mental health of teachers and students is enhanced by daylight. Lighting influences mood and attitude according to Vetich [7].

#### 2.2 Energy savings

Good daylighting can save electricity as long as electric lights are turned off or dimmed when natural light is adequate. Much of the institutions' energy budget is for lighting. This can be greatly reduced with well-designed natural light. Daylight can be related to economy as it gives some financial benefits [2]. There are various examples of economic advantages for the cost of natural light. A series of schools built in Johnston County, N.C., replaced artificial lights with natural light, which resulted in between 22% and 64% energy savings as compared to typical neighboring schools [8]. According to a report by the National Center for Education Statistics, 72% of the cost of energy in education buildings goes towards electricity, with the majority (56%) going toward lighting. Making a significant cut in electricity costs through daylighting can amount to substantial savings for other school expenses [9].

#### 2.3 Learning space and daylight

The environment of a classroom has a great impact on students. Lack of proper environment of the classroom can result in physiological and psychological impacts on children. The most obvious effect of light on humans is in enabling vision and performance of visual tasks. The nature of the task as well as the amount, spectrum, and distribution of the light determines the level of performance that is achieved [4]. Performance on visual tasks gets better as light levels increase. A study by Santamaria and Bennett shows that, if the amount and distribution of light are controlled, most everyday visual tasks (such as reading and writing) can be performed better under daylight conditions rather than under artificial light sources (such as fluorescent light) [10]. Daylight is superior for tasks involving fine colour discrimination when it is provided at a high level without glare or any reduction in task visibility caused by veiling reflections or shadows [4].

#### 2.4 Window and Glare

During midday, the sun hitting the ground can be more than 10,000 lux in tropical countries. For most people, the tolerable amount of sunlight while reading a book outside is around 40,000 lux. There is a large variation between the

outside tolerable daylight from inside for reading. For a typical classroom, the amount of light tolerable for reading is around 500 lux. In some field studies, desktop illuminances of around 1500 lux to 2000 lux have been found to be too bright not because of the amount of illuminance but because of direct glare and glossy reflections. Care must be taken to avoid a large variation of brightness between surfaces at the far end of the room and those close to windows [11].

#### 2.5 Window, Shading and Lightshelf

Window is the most common phenomena for daylight from the outdoor space. To control the amount of light penetration, window size can act as an important parameter. With a larger window a great extent of natural light can enter into the interior space. To decrease the quantity of illumination window size can be reduced.

Architectural shading solutions are typically part of the exterior facade. Lightshelves, overhangs, fins, shade screens, venetian blinds, vertical blinds, are commonly used shading systems. One drawback of using shading device is the risk of reduced daylight level [12]. The design of effective shading devices will depend on the solar orientation of a particular building facade. For example, in the summer when sun angles are simple fixed overhangs are very effective at shading south-facing windows (Figure 01). However, during the summer's peak heat gain periods, the same horizontal device is unsuccessful at preventing low afternoon light from entering windows facing west. [13].

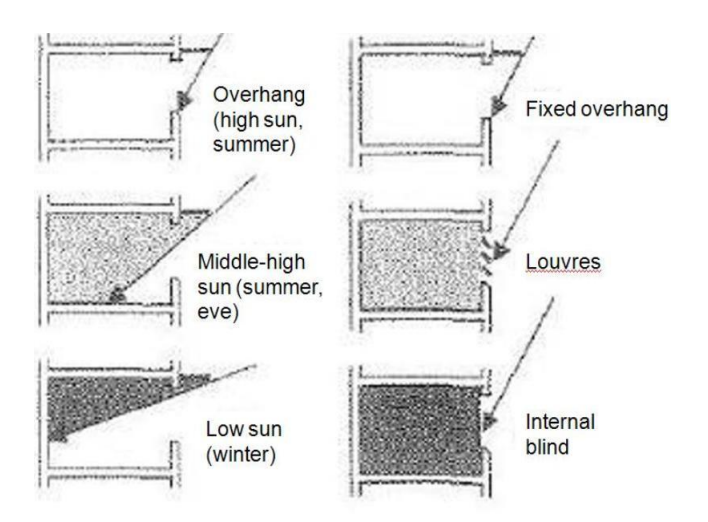


**Fig. 01:** Different types of shading solutions (cited from Don Prowler, 2014)

One of the effective forms of shading device is the lightshelf. A lightshelf is a horizontal surface that reflects daylight deep into a building. Lightshelves with high-reflectance upper surfaces are positioned above eye level to reflect sunshine onto the ceiling and farther into the room [14]. At the same time, the lightshelf shades the lower part of any window, reducing the amount of light near the window, which normally has much higher illumination than the deeper parts of spaces and projects the

light towards the back (Figure 02). The result is balanced luminous environment with less contrast and glare [14].



Fig. 02: Light shelves (cited from A.G.S. 2000)

#### 2.6 Illumination standards

Bangladesh National Building Code 2006 (BNBC) follows a set of minimum recommended illuminance levels for a variety of visual tasks and space functions for educational buildings [15]. The guidelines for consideration of the brightness ratio in classrooms are illustrated in table I.

Table I: Recommended values of illumination for Educational Building (BNBC, 2006).

Area of Activity	Illumination [Lux]
Class and Lecture Rooms	
Desks	300
Black boards	250
Art Rooms	400
Assembly Halls Examination	300
•	

Whereas the International Standard ISO measured the level in Reading area: 500 Lux and in Art rooms: 750 Lux [16]. The European norm provides guidelines for illuminations need for all different types' activities at school buildings are illustrated in table II [17].

Table II: Overview of tasks in a classroom together with the requirements for the luminance by European norm.

The Teacher	The Student	Standard II	luminance
		In the class	In general
Writing on blackboard	Reading on blackboard	500 lux (vertical)	200 lux
Talking to students	Paying attention to the teacher	300 lux	300 lux
Showing presentations (slide, Power Points, television program, etc.)	Looking at the screen	300/10 lux	10 lux
Paying attention to working students	Writing, reading, drawing, etc.	300 lux	300 lux
Coaching computer activities	Looking to the computer screen and the paper	50 lux	300 lux above the computer
Preparing lessons	Not present	300 lux	50 lux

#### 3. METHODOLOGY

The study has been completed in three stages; physical survey, simulation study and analysis. The study building is selected in Gazipur Duet campus (Figure 03, 04), which is an academic building.

In first stage the building (Figure 05) and the study area is surveyed physically. The physical and environmental characteristics like as building type, building heights, orientation and the surrounding condition are observed. Then one room that is a design studio (Figure 06) is selected. Here again the interior space, window type, orientation, glazing characteristics, surface area and materials are inspected.



Fig. 03: Google map view of DUET campus

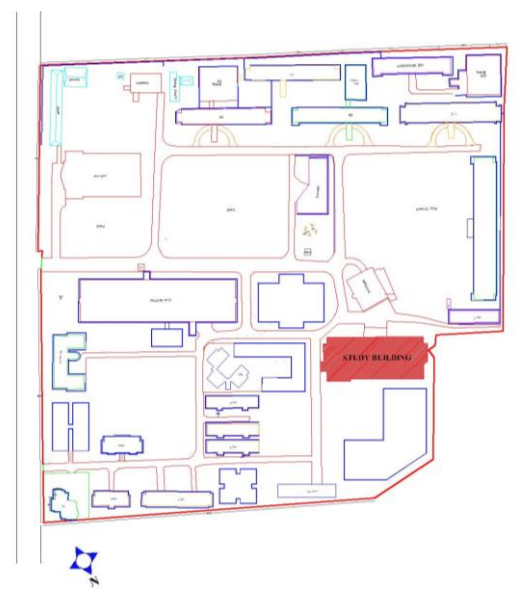


Fig. 04: Master plan of DUET campus

In second stage a 3D model is generated in computer software for simulation. Four types of window configurations are studied in three software's ECOTECT, RADIANCE and DAYSIM.

The analysis is done in the third stage for finding a better design decision.



Fig. 06: Interior of the study design studio

#### 3.1 Simulation Study

The amount of daylight penetration can be calculated by computer simulation study before construction. The parameters can be changed and with different design solution the suitable option can be identified with the help of the computer software. Again, the study can be performed in different climatic condition, date, time etc. Three computer version simulation programs are used in the study for four different window configurations to take the best option. Firstly, the ECOTECT v5.5 is used which a comprehensive building analysis software. It is a highly visual, architectural and analysis tool with lighting thermal,



Fig. 05: South facade of the study building

energy, shading and acoustic performance analysis functions [18], [19]. Then RADIANCE 3p7 is used which is more focused and accurate daylighting simulation tool [20]. Lastly DAYSIM 2.1.p4 simulation program based on the concept of dynamic annual daylight performance metrics is used [21].

#### 3.2 Simulation Parameters

The quantitative and qualitative assessments of the design strategies the following parameters are considered:

Location Dhaka, Bangladesh. (90.4° E.  $23.8^{\circ}$  N) \*

Time 15 April

Calculation Settings Full Daylight Analysis

Precision High
Local Terrain Urban
Window (dirt on glass) Average
Sky Illumination Model
Design Sky Illuminance 16,500 Lux [21].

NB: Though the actual location of the study building is in Gazipur, it is similar and convenient to take the location as Dhaka.

#### 3.3 Study Space

The study building is twelve storey high. The surrounding is mostly open, but there is a six-storey building on the south east corner. As the study space (marked on Figure 05) is on south west side, there is no barrier to entering light into the studio from outdoor area. The study zone is the design studio on the third floor (Fig. 07). The parameters of the study are as follows.

Total floor area17,851 sftThe study area1867 sftClear height of the design studio12 ftWork Plane height3 ft

The parameters (Table I) of the internal finish materials are found by the field survey are used in the modelling.

**Table I:** Parameters of the internal finish materials

Model	Material	Reflectance
Ceiling/Roof	White painted plaster	0.7
Internal wall	white painted brick work	0.7
Floor	White cc finishes	0.5
Glazing	Single pane of glass with aluminium frame	0.92 U value 6W/m <sup>2</sup> K

#### 3.4 Performance Evaluation Process

The total design studio is divided into grids (Figure 08) for the purpose of simulation. Then 275 points in the open studio are found to generate of daylight levels at 3 ft above floor level which represent the table top of drafting tables. Each intersection point of the grid was coded according to the number-letter system shown in Figure 08. Total 275 simulated illumination values are generated by ECOTECT. These values are plotted into tables (Tables III, IV, V and VI), with the codes coinciding with intersection of letters (rows) and numbers (columns) and then compared for the different situations. One axes XX' (Figure 08), were created across the plan, to assess the fluctuation of daylight levels, from the window towards the opposite wall of the space [12].

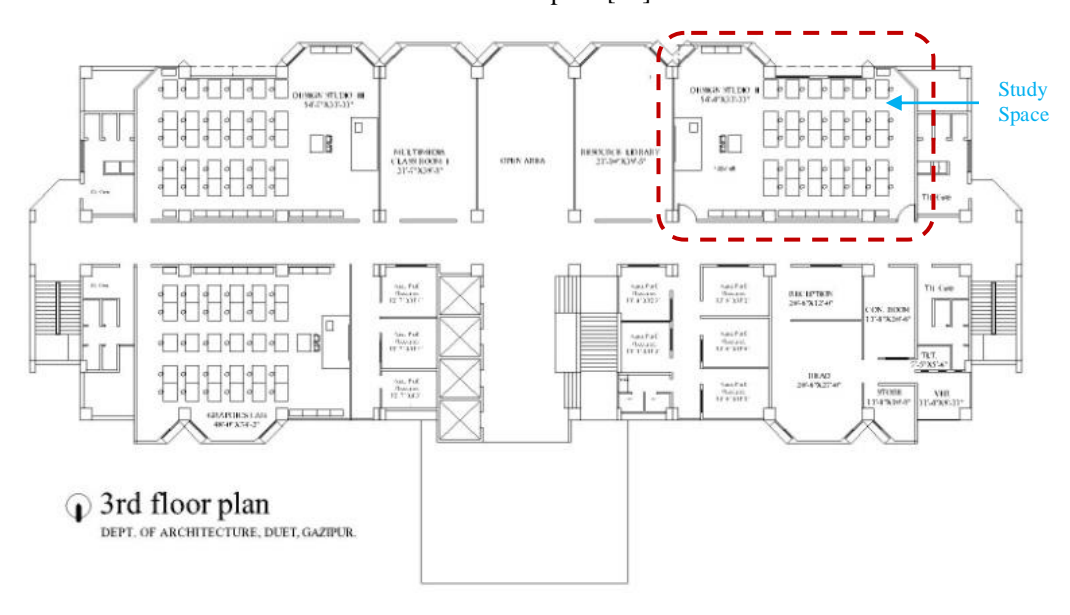


Fig. 7: Study floor plan of NAB building

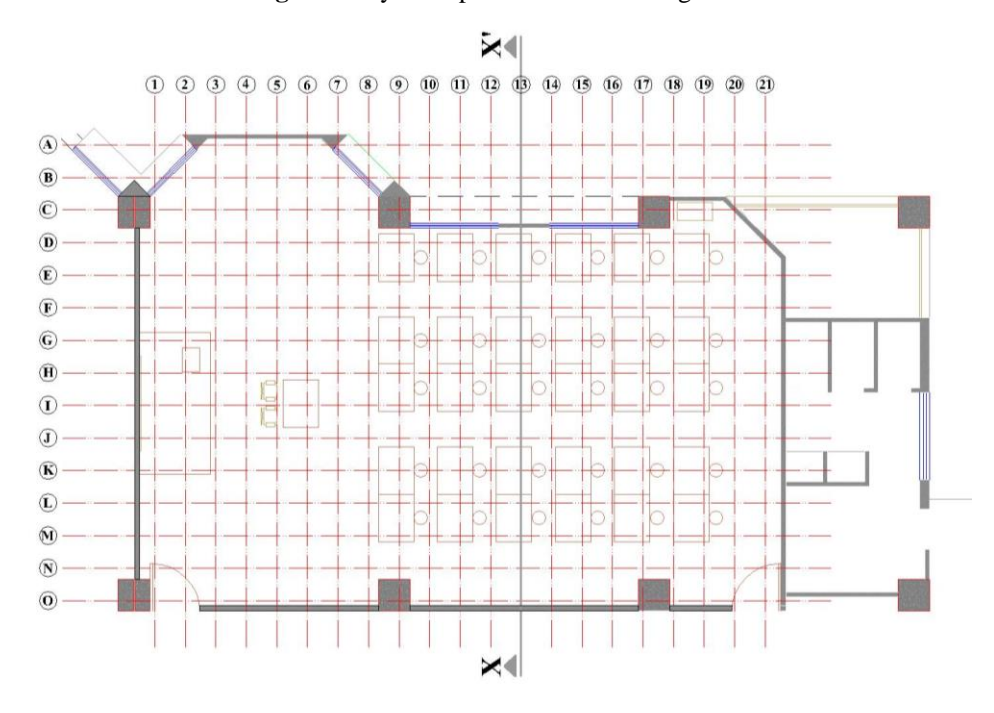


Fig. 08: Plan showing the grid with node references

# A Simulation Study of Daylighting Performance for Different Window Configurations in Architectural Design Studio to Enhance Lighting Quality at DUET, Gazipur

The whole simulation study is done in four types of window configuration one by one with different design parameters (Table II). The types are as follows-

Case A: The simulation study done in the existing situation. There are four windows on the south exterior wall (Figure 05, 08) of the studio.

Case B: In this case the window has been widen through wall and the height is increased to roof level.

Case C: Shading device and light shelve are added on the seal and lintel level outside of the wall in case C.

Case D: Another light shelve is implemented on the lintel level in inner side of the studio.

Table II: Window design parameters for the study

Case	Elevation	Section
A		
В		
С		Outdoor Lightshelf Reflector
D		Indoor Lightshelf Outdoor Lightshelf Reflector

For each cases the 3D model is generated for computer simulation in ECOTECT program to calculate the amount of daylight on each grid point on the work-plane. The models were then exported to Radiance Synthetic Imaging software for generating realistic predictions of lighting

levels. An additional imaginary horizontal plane above 3ft from the floor level is created to show daylight contour map on work plane height, for Dextop RADIANCE. Finally, a performance metrics was done with DAYSIM to get a complete annual picture [12].

#### 4. RESULT AND ANALYSIS

#### 4.1 Evaluation criteria

The findings of the computer simulation were evaluated based on the following criteria [12].

- Average daylight levels and daylight factors on the drafting table height.
- Number of points within acceptable illumination levels.
- c. Fluctuation of daylight levels from the window towards deeper parts of the studio.
- d. Comparison of rendered images of the example studio generated by RADIANCE for luminance levels on specific surface.

e. Different performance metrics with DAYSIM to verify the compliance of the decisions with annual performance.

#### 4.2 Average daylight levels and daylight factors

From the Figure 09 it can be seen that how the daylight factor changes in different cases. In Case A when the window was small the illuminance entered through the window could not cover the whole area but it changed to a great extent while the window size is expanded in Case B. But glare is very high near the window. In next two Cases the glare is reduced by using light shelve without dropping the illuminance.

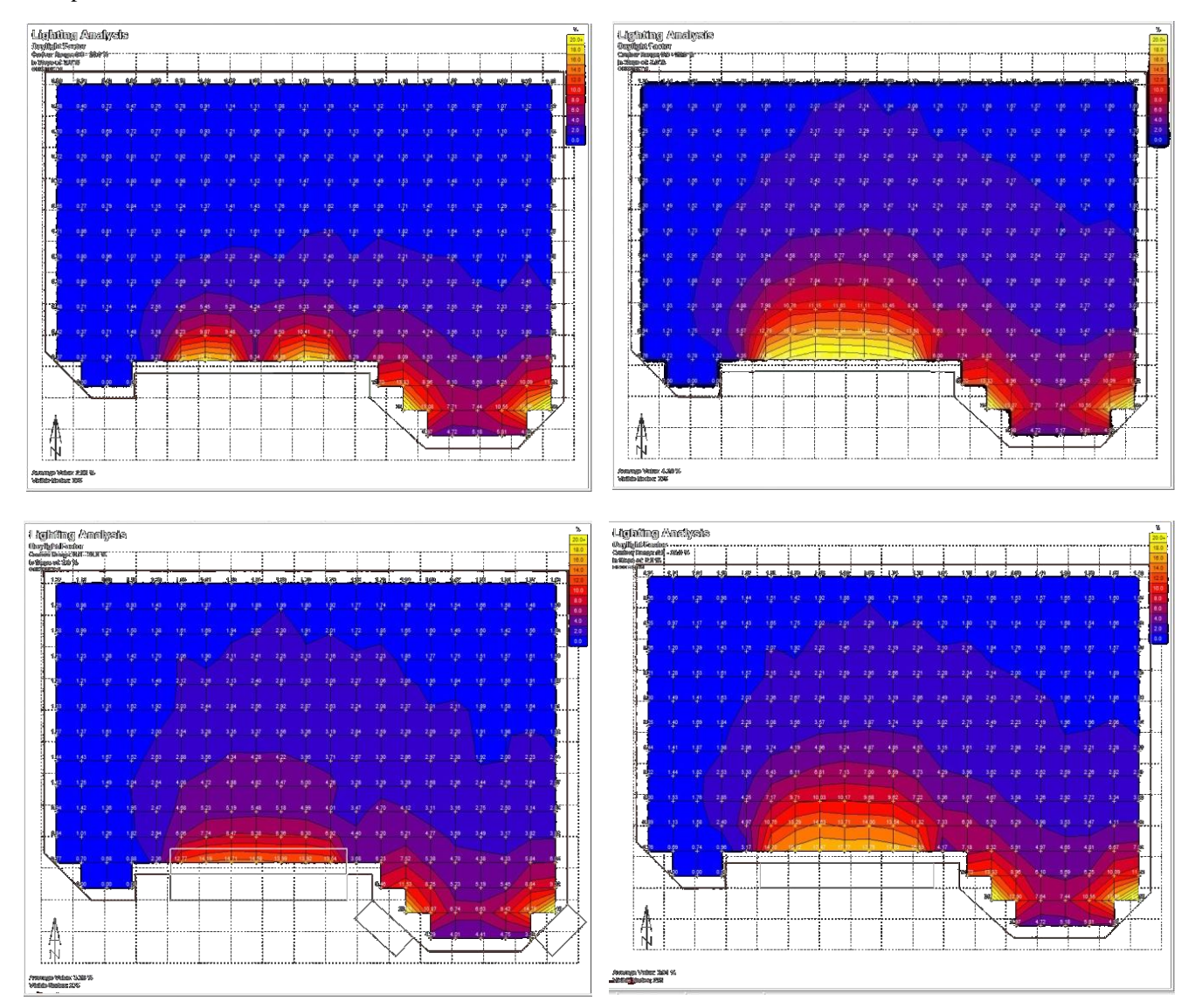
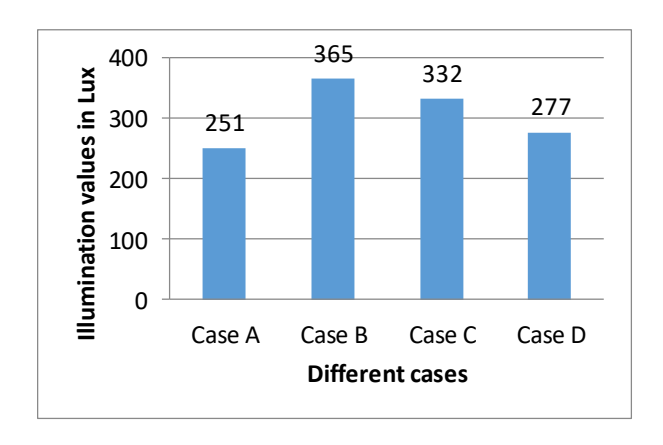


Fig. 09: Daylight factors on node points in different cases A, B, C and D (clockwise)

The following bar diagram (figure 10) explains that average daylight level (250 Lux) is very low in existing situation (Case A). It increased in Case B then again fall down in following two cases but the difference between two points is lessen. Same things happen in daylight factors, first grow

high and then declined. The standard illumination for drawing purpose in BNBC is 400 Lux. In existing situation only, the tables near the window get this amount of daylight. On the last Case though, the average value is not increased very high but the distribution is better. These is found very clearly from the Table III, IV, V and VI.

# A Simulation Study of Daylighting Performance for Different Window Configurations in Architectural Design Studio to Enhance Lighting Quality at DUET, Gazipur



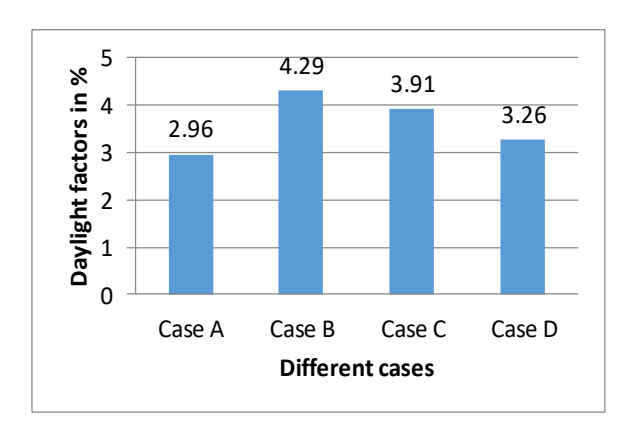


Fig. 10: a) Average daylight levels and b) Average daylight factor

#### 4.3 Comparison of illumination levels

Comparing the four conditions from the Table III, IV, V.VI we found that, in Case A of existing condition only 46 node points get the illumination level higher than 300 lux, which is the recommended level mentioned in Bangladesh National Building Code, 2006 for class room [13]. It is 16.7% of total 275 number nodes. In this case glare is very limited, only 13 points get more than 900 Lux will create glare, as these levels exceed three times the recommended values [22], [23]. In Case B when the window changed to a large one, the number of points over get illumination over

300 Lux increases to 66 points (24%) but glare points increase also high. It increases to 26 points which is 9.4%. Then in Case D the external light shelf added the situation turned better. Glare points (over 900 Lux) decreased to some extent, 21 points (7.6%) and 67 node points (24.3%) get light more than 300 Lux. In last stage, Case D, the glare points decreased very low, only 11 points (4%) and 57 points (20.7%) get more than 300 Lux. So, in Case D the situation is more preferable as the overall distribution of light is even though the average illumination is low. The summery can be seen from the Table VII.

Table III: Daylight distribution on nodes for Case A

	1	2	3	4	5	6	7	8	9	10	11	12	13	14	15	16	17	18	19	20	21
A		424	494	441	401	508															
В	2473	1525	899	632	655	1112	2146														
C	988	857	531	484	519	762	1133	1079													
D	570	540	355	345	385	470	688	586	449	1589	1668	1296	453	1522	1624	1478	278	61	20	31	31
E	328	323	265	265	302	403	439	483	465	741	885	722	484	806	839	699	270	126	60	32	36
F	226	251	198	225	217	251	345	347	296	424	453	393	361	449	464	374	217	122	97	61	41
G	153	209	158	171	172	186	234	248	239	284	272	276	220	265	287	228	163	105	76	68	64
H	151	168	145	142	175	180	188	217	172	204	201	170	204	197	175	171	113	91	81	68	64
I	126	150	122	119	139	131	155	165	154	180	169	139	137	146	144	126	113	91	69	73	61
J	135	124	110	112	137	125	145	135	141	138	157	149	121	120	116	105	98	71	68	65	56
K	120	99	102	96	126	133	130	126	116	128	125	137	95	99	88	83	76	68	61	55	61
L	105	111	99	102	113	114	115	114	118	113	107	109	112	80	87	78	65	69	54	59	61
M	90	104	94	99	88	96	100	107	96	111	108	102	90	103	79	71	66	61	59	37	60
N	86	95	91	82	90	97	95	95	97	101	94	92	94	97	78	66	64	40	61	34	58
0	93	96	92	105	91	99	101	98	105	86	106	95	92	48	68	65	63	70	36	63	59
	Total number of node points = 275																				
	Number of points $300\sim900 \text{ Lux} = 46$																				
							Nu	mber (	of gla	re poii	nts (>9	900 Lu	(x) =	13							

# A Simulation Study of Daylighting Performance for Different Window Configurations in Architectural Design Studio to Enhance Lighting Quality at DUET, Gazipur

Table IV: Daylight distribution on nodes for Case B

	1	2	3	4	5	6	7	8	9	10	11	12	13	14	15	16	17	18	19	20	21
A		424	494	440	401	508															
В	2428	1525	897	632	954	1111	2146														
C	988	857	531	484	519	762	1133	1080													
D	597	567	408	395	423	505	724	658	510	1820	1942	2000	2031	2030	1921	1670	370	112	66	61	65
E	359	352	295	300	344	468	513	587	733	1163	1395	1443	1448	1497	1338	1087	474	247	148	103	80
F	257	289	235	252	281	323	412	509	507	695	888	944	988	948	914	678	415	262	171	130	92
G	197	243	205	238	228	255	323	375	403	545	626	673	655	667	571	497	321	222	160	130	109
H	189	201	188	193	216	262	276	334	303	423	456	461	490	470	390	335	255	175	166	130	122
I	164	189	181	166	202	200	214	256	275	331	346	354	338	333	329	284	211	168	147	135	106
J	157	158	148	173	188	183	221	197	233	267	295	306	259	279	247	217	193	153	129	127	110
K	162	161	139	157	168	185	194	199	211	204	246	273	235	206	202	198	146	137	132	109	106
L	141	144	142	140	164	163	171	183	196	199	204	206	224	189	179	176	149	121	118	113	107
M	149	141	131	142	129	145	151	166	161	188	185	195	171	185	161	141	132	123	109	82	106
N	140	136	130	140	133	142	142	147	149	177	165	182	173	176	130	140	134	91	109	81	107
O	129	139	132	151	131	146	150	156	152	148	160	170	165	125	132	129	126	112	89	97	106
	•	•	•	•	•		•	Total	numb	er of i	node p	oints =	= 275			•			•		
	Number of points $300\sim900 \text{ Lux} = 66$																				
							Nı	umber	of gl	are po	ints (>	900 L	ux) = <mark>2</mark>	6							

Table V: Daylight distribution on nodes for Case C

	1	2	3	4	5	6	7	8	9	10	11	12	13	14	15	16	17	18	19	20	21
A		424	494	441	401	508															
В	2428	1525	897	632	649	1096	2140														
C	988	857	531	484	519	762	1133	1080													
D	597	567	409	395	423	502	708	611	354	1411	1448	1509	1511	1485	1421	1250	269	82	63	59	65
E	359	350	295	300	338	450	484	542	623	962	1151	1190	1165	1244	1130	915	422	204	134	96	75
F	255	284	231	248	277	304	397	482	456	614	818	822	864	852	825	609	361	242	150	130	85
G	197	239	192	220	222	248	308	338	364	487	560	595	606	579	519	461	280	215	155	122	103
H	179	194	188	177	216	253	253	307	268	389	412	414	446	422	356	318	243	169	159	120	122
I	164	175	167	166	186	190	212	234	256	304	318	329	306	304	302	261	194	156	143	119	106
J	156	158	148	158	182	183	206	177	212	243	271	282	238	250	227	200	172	138	120	127	110
K	162	161	139	142	155	170	182	199	194	188	226	250	221	188	185	183	133	137	130	109	103
L	130	133	142	140	164	150	157	183	178	199	186	186	209	189	163	176	149	121	118	102	107
M	149	141	131	142	129	131	151	153	145	174	169	195	171	172	148	141	121	123	100	82	106
N	140	136	130	140	133	130	142	147	149	163	153	169	160	163	120	128	122	84	109	81	107
О	119	139	132	139	120	135	139	145	139	148	148	156	153	117	132	129	116	101	89	97	106
								Total	numb	er of i	node p	oints =	= 275								
	Number of points $300 \sim 900 \text{ Lux} = 67$																				
							N	umber	of gl	are po	ints (>	900 L	ux) = <mark>2</mark>	21							

Table VI: Daylight distribion on nodes for Case D

	1	2	3	4	5	6	7	8	9	10	11	12	13	14	15	16	17	18	19	20	21
A		288	404	375	341	365															
В	2076	1253	800	563	573	924	1776														
C	792	752	463	442	444	701	980	804													
D	514	496	368	373	399	457	640	530	313	1151	1183	1189	1239	1250	1206	1085	200	75	58	60	65
E	325	325	270	297	305	405	442	442	374	588	705	711	712	720	658	515	250	155	107	86	72
F	240	267	212	233	268	264	350	399	295	341	425	440	466	441	444	398	210	165	116	121	80
G	176	224	183	207	201	228	288	288	279	362	425	465	410	415	401	346	216	174	126	106	95
H	174	190	170	163	202	252	243	280	227	316	356	358	363	369	303	245	224	130	142	121	122
Ι	163	176	168	162	187	178	203	220	242	271	286	303	286	285	279	216	170	142	137	116	108
J	154	140	134	161	180	171	202	176	191	224	244	248	218	241	207	173	163	138	112	115	113
K	159	162	132	142	156	165	174	175	193	174	215	239	204	181	184	181	127	129	133	103	106
L	134	137	134	128	149	150	156	189	182	183	181	192	205	179	162	176	145	120	117	105	102
M	153	133	121	136	127	136	140	158	146	171	162	195	172	165	144	137	117	127	103	85	109
N	130	125	134	141	131	131	143	148	150	163	153	169	161	160	117	132	122	79	108	83	106
O	122	142	136	142	121	138	139	145	135	162	144	160	157	113	129	132	116	100	88	96	108
								Total	l num	ber of	node	points	= 275								
							1	Numb	er of	points	300~	900 Lı	1x = 5	7							
							N	umbe	r of g	lare po	oints (	>900 I	_ux) =	11							

Table VII: Summery result of illumination condition for different cases

Different Cases	Average Illumination	No. of Point <300 Lux	No. of Point 300-900 Lux	No. of Glare Point (>900 Lux)
Case A	251	215	46	14
Case B	365	183	66	26
Case C	332	187	67	21
Case D	277	207	57	11

#### 4.4 Fluctuations of daylight levels

The Figure 11 shows how the illuminance levels drop to the end points of the studio. In Case A at D13 point the

illumination was 454 Lux which raised to 1249 Lux in Case D, whereas the last end of the room point O13 was 92 Lux and it increased to 156 Lux in the following case.

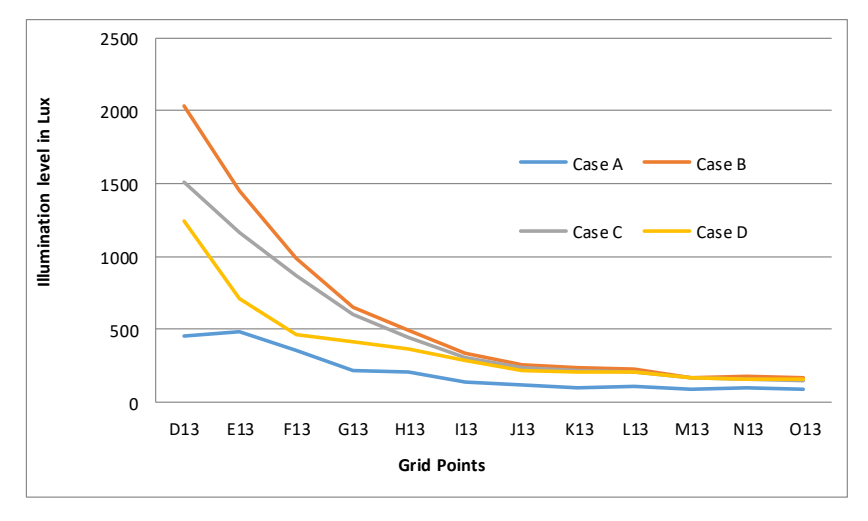


Fig. 11: Drop of light along XX' axis for four different cases

#### 4.5 Comparison of rendered images

A 3d realistic view of four cases (Figure 12) get from the RADIANCE rendered image. Contour lines of daylight

distribution give the notion how the light transmits to the whole study area

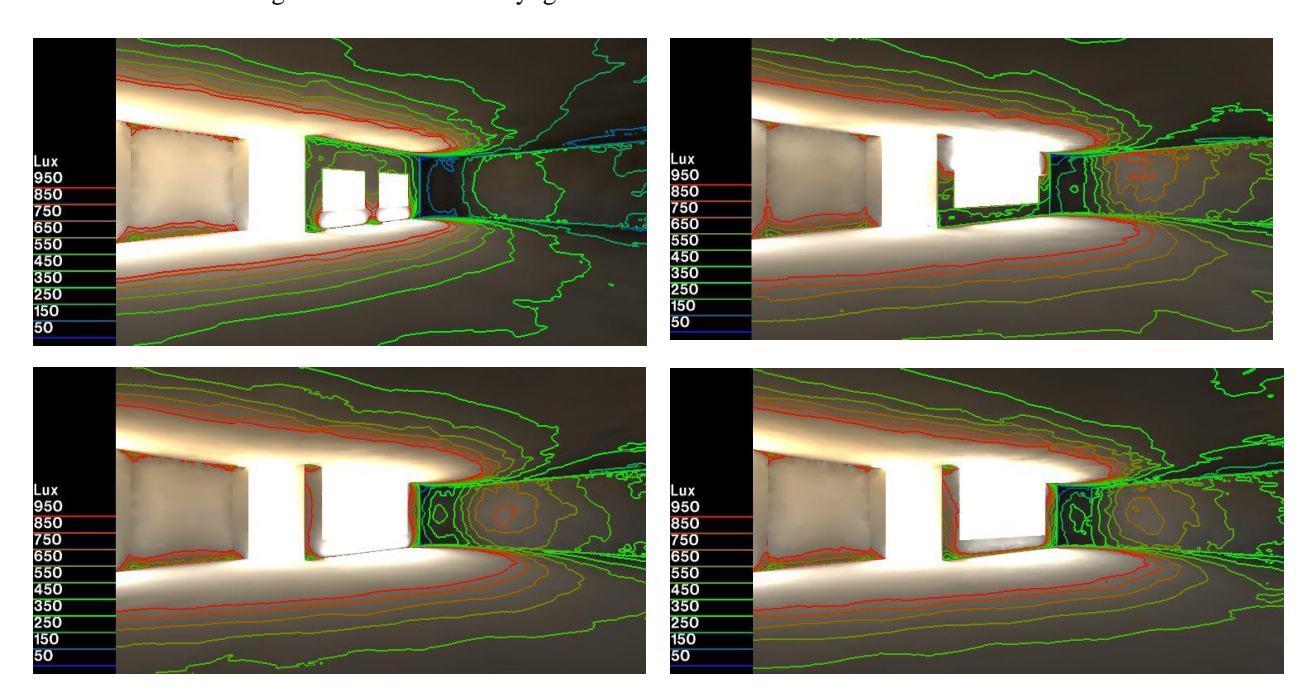


Fig. 12: Daylight contour distributions in different design cases A to D clockwise

#### 4.6 Performance metrics

For four different Cases of window configuration, daylight factor (DF), conventional daylight autonomy (DA), continuous daylight autonomy (DAcon), and useful daylight index (UDI) were calculated. For all performance metrics, the same annual illuminance profiles were used based on DAYSIM calculations. Table VIII shows the different performance metrics in DAYSIM simulation for each Case.

Table VIII: DAYSIM simulation results for different steps

Design steps	DF ≥	DA %	DAcon > 80%	DAmax > 5%	UDI <	UDI 100-	UDI >
_	2%				100	2000	2000
Step A	43%	1%- 99%	93%	29%	53%	0%	47%
Step B	70%	25%- 99%	99%	46%	17%	0%	83%
Step C	65%	20%- 99%	99%	43%	19%	0%	81%
Step D	68%	18%- 99%	99%	40%	19%	0%	81%

Comparing the annual performance metrics for four cases, it is found that the DA, DAcon above 80% and case B, C, D is greater than case A. According to DF Case B is better than other again it will be better if we consider DAmax. But if we analysis UDI levels it is clear that Case C and Case D is best situation.

The simulation results are also shows that the existing situation is not suitable for students because most of the part of the studio does not get light. But only widen the window will increase the glare problem though it brings light to most of the part of studio. Again, if shading and light shelf is used this situation will be better. And the figure 12 shows the step D is the best solution when both inner and outer light shelve has used as the glare is lowest. So, in step D the situation is more preferable as the overall distribution of light is even though the average illumination is low.

#### 5. CONCLUSION

The people of Bangladesh are less aware of daylight use and the benefits of it. Even they have very little knowledge about the negative impact of the absence of natural light. Simultaneously, they are barely informed about the simulation process. Through the study, they can know that any design decision can be taken during the design phase for a better environment of the project. Again, the study opens up different ways to research further aspects related to daylight. By studying more parameters of window configurations and conducting a more critical analysis, a best case can be found and implemented for the studios of DUET.

#### ACKNOWLEDGMENT

We acknowledge Dept. of Architecture, DUET for conducting the physical survey in their studio, the drawings and technical support.

### A Simulation Study of Daylighting Performance for Different Window Configurations in Architectural Design Studio to Enhance Lighting Quality at DUET, Gazipur

### **REFERENCES**

- [1] F. Ahsan, and M. A. R. Joarder, "Effective width of light shelf for daylighting classrooms considering different seasons and sky conditions of Dhaka", Proceedings of the 2017 International Conference on Green Architecture (ICGrA), Dhaka, Bangladesh, pp.163-170, 2 017.
- [2] F. Ahsan, "Investigation Of Adjustable Lightshelf For Daylighting Classrooms Considering Different Sky Conditions Of Dhaka," (Unpublished M. Arch thesis), BUET, Dhaka, Bangladesh, 2019.
- [3] R. S. Ulrich, C. Zimring, A. Joseph, X. Quan, & R. Choudhary, "The role of the physical environment in the hospital of the 21st century: A once-in-a-lifetime opportunity", Concord, CA: The Center for Health Design, 2004.
- [4] P. Boyce, C. Hunter, & O. Howlett, "The benefits of daylight through windows", Troy, NY: Rensselaer Polytechnic Institute, 2003.
- [5] C. J. Kibert, "Sustainable construction; Green building design and delivery," 2nd ed. New Jersey: John Wiley & Sons, Inc., 2008.
- [6] N. Baker and K. Steemers, Daylight design of buildings, Earthscan/James & James, 2002.
- [7] J.A. Veitch, "Principles of Healthy Lighting: A Role for Daylight," National Research Council Canada (NRCC). Report no. NRCC-46758. Canada. P2, 2003.
- [8] U.S. Department of Energy's Office of Building Technology, State and Community Programs Report, "Energy-Smart Building Choices: How School Administrators & Board Members Are Improving Learning and Saving Money," 2002.
- [9] Environmental Monitoring Report, 2016 Local Government Engineering Department, April 2016.
- [10] J. Santamaria, & C. Bennett, "Performance effects of daylight," Lighting Design and Application, 11, 31–34, 1981.
- [11] P. Tregenza, and M. Wilson, "Daylight coefficients and numerical models," Daylighting: architecture and lighting design. New York, NY: Routledge, 2011.
- [12] M.A.R. Joarder, Z.N. Ahmed, A.D.F. Price, and M.M. Mourshed, "A simulation assessment of the height of light shelves to enhance daylighting quality in tropical office buildings under overcast sky conditions in Dhaka," Bangladesh. Eleventh International IBPSA

- Conference, (Building Simulation 2009), 27-30 July, Glasgow, Scotland, pp.920-927, 2009.
- [13] D. Prowler, FAIA, Donald Prowler and Associates Revised and expanded by Joseph Bourg, Millennium Energy LLC Last updated: 12-18-2014
- [14] A. G. S. 2000, Architectural Graphic Standards, John Wiley & Sons, Inc. New York, CD Rom Versions, 2000
- [15] BNBC. 2006. Bangladesh National Building Codes, Housing and Building Research Institute and Bangladesh Standards and Testing Institute, Dhaka, 2006
- [16] Illuminating Engineering Society of North America (2000). The IESNA Lighting Handbook: Reference and Application. Ninth Edition. IESNA Publication Department. USA. pp. 335, 2000
- [17] N. Iqbal, Incorporation of Useful Daylight in Luminous Environment of RMG Factories by Effective use of Skylights in Context of Dhaka. (Unpublished M. Arch thesis), BUET, Dhaka, Bangladesh, 2015.
- [18] D.B. Crawley, J.W. Hand, M. Kummert, and B.T. Griffith, "Contrasting the Capabilities of Building Energy Performance Simulation Programs" Joint Report Version 1.0. International Building Performance Simulation Association, Montreal, August 15 18, 2005.
- [19] E.E. Osaji, and A.D.F. Price, "The Role of Parametric Modelling and Environmental Simulation in Stimulating Innovation in Healthcare Building Design and Performance," HaCIRIC 2nd International Conference, April, pp. 135-44, 2009.
- [20] N. Baker, A. Fanchiotti, K. Steemers, Daylighting in Architecture. James & James Science Publishers Ltd; 1993:2.7, 2. 8, 2.10, 2002.
- [21] C.F. Reinhart, J. Mardaljevic, and Z. Rogers, "Dynamic Daylight Performance Metrics for Sustainable Building Design. Leukos," 3(1). pp. 7–31, 2006.
- [23] P.J. Littlefare, "Designing With Innovative Daylighting. Building Research Establishment report," Herts: Construction research Communications, 1996.
- [24] J.R. Goulding, J. O. Lewis, T. C. Steemers, "Energy Conscious Design: A Primer for Architects," London, Batsford for the European Commission, 1992.

# Development and Quality Assessment of Composite Biscuits Fortified with Potato and Corn Flour

Raju Ahmmed<sup>1\*</sup>, Fatema Ahmed Toma<sup>2</sup>, Kanis Fatema Tuna<sup>2</sup>, Md. Shofiul Azam<sup>1</sup>

<sup>1</sup>Department of Food Engineering, Dhaka University of Engineering & Technology, Gazipur, Bangladesh.

<sup>2</sup>Department of Food Technology and Engineering, Patuakhali Science and Technology University, Dumki, Bangladesh.

\*Correspondence Email: rahmmed@duet.ac.bd

### **ABSTRACT**

Applying composite flour in bread production could provide a healthier alternative to bread made with wheat flour. This study aimed to develop fortified wheat flour bread with improved nutritional properties, thereby enhancing the overall nutritional value of wheat flour bread. This study used potato and corn flour as supplementary components to produce fortified biscuits. Wheat flour contains optimum levels of moisture (13.10%) and protein (9.37%), while potato flour contains the highest levels of ash (1.6%) and total carbohydrates (82.39%). The result shows that corn flour had the maximum fat content at 2.54% and the highest energy content at 360 Kcal/100 g. As the level of supplementation increases, the diameter, thickness, and volume increase significantly while the weight, spread ratio, and density decrease. The control biscuits (F1), composed of 100% wheat flour, exhibited the highest levels of moisture (5.02%) and protein (8.02%) in chemical analysis. In contrast, biscuits containing a blend of 50% potato flour and 50% wheat flour (F2) displayed reduced moisture (4.45%) and protein (7.54) levels, accompanied by the highest ash content of 1.11%. The fat content increased while the protein content decreased as the potato or corn flour percentage increased. Sensory analysis of biscuits revealed that a combination of 50% potato flour and 50% wheat flour (F2) was the most popular among consumers. Based on sensory evaluation and storage studies on the shelf-life of processed biscuits, it is recommended that up to 50% of the wheat flour in fortified biscuits may be replaced with potato flour on an industrial scale.

Keywords: Biscuit, Fortification, Quality, Physical properties, Composite flour, Shelflife.

### 1. INTRODUCTION

Biscuits are a significant processed food item in the human diet commonly consumed across various socio-economic classes. This bakery is made primarily from flour with a low moisture content. It is also commonly found in the form of confectionery [1]. Baked goods in the form of biscuits are widely consumed worldwide [2]. Typically, they are snacks made from dough (which consists of flour, fat, sugar, and water) that are changed into delectable items by applying heat in an oven at a controlled temperature [3]. These products are ready-to-eat, simple to prepare, and relatively cheap, featuring various shapes and sizes predominantly consumed by individuals of both younger and older age groups [4].

Using composite flour in food has been considered beneficial in developing nations as it promotes the utilization of regionally cultivated crops as flour and decreases dependence on imported wheat flour [5, 6]. This approach is being assessed to determine the viability of

substituting wheat flours with alternative locally accessible flours [7]. Potato flour is a great carbohydrate source, has high dietary fiber & vitamins, a good amount of minerals, 6-12% protein and negligible fat content and helps lower the gluten content. Corn is a major source of carbohydrates,

protein, vitamin B, vitamin A (yellow maize) and minerals [8].

In Bangladesh, it is observed that during the production season of potatoes and corn, prices tend to decrease due to inadequate storage and marketing facilities, often resulting in significant losses for the producers. Adding potato and corn flour to wheat flour can improve the sensory attributes of biscuits and may also offer economic benefits in the production of biscuits [1]. This study aimed to determine the proximate composition of wheat, potato and corn flour and establish a uniform procedure for producing fortified biscuits and their subsequent assessment of quality characteristics.

### 2. MATERIALS AND METHODS

The experimental studies were conducted in the Department of Food Technology & Engineering laboratories under the Faculty of Nutrition and Food Science, Patuakhali Science and Technology University, Dumki, Bangladesh.

### 2.1 Materials

Wheat flour (fresh), Corn flour, potato, daldah (Pusti brand), salt (Mollah brand), eggs, sugar (ACI brand), vanilla essence, milk powder (Pran brand) and baking

powder (Noor nobi brand) were bought from the local market. Analytical Research (AR) grade chemicals (high-grade chemicals suitable for different analyses) were used to analyze the raw materials and final products.

### 2.2 Potato flour preparation

Potato flour was prepared using the method described by [9]. Selected potatoes were first cleaned with potable water. Then peel and slice into 2-3 mm thickness and steam blanched for 10 minutes. After overnight drying (80-85°C), the slices were milled and passed through a 30-mesh standard sieve. Subsequently, the flour was enclosed in high-density polyethylene bags for further utilization.

### 2.3 Experimental Plan

In this study, a certain percentage of wheat flour, potato flour, and corn flour were used, as shown in Table 1. Table 2 shows the different combinations of ingredients used to prepare 100g dough.

Table 1. Experimental Plan for the preparation of fortified biscuits

Sample	Wheat flour (%)	Potato flour (%)	Corn flour (%)
F1	100	00	00
F2	50	50	00
F3	50	00	50

Table 2. Ingredients used in the preparation of Biscuits (total 100 g)

Sl.	Inquadiants	\$	Sample		
Ingredients	F1	F2	F3		
1.	Wheat flour (g)	50	25	25	
2.	Potato flour (g)	0	25	0	
3.	Corn flour (g)	0	0	25	
4.	Sugar (g)	15	15	15	
5.	Fat (daldah) (g)	12	12	12	
6.	Milk powder (g)	2	2	2	
7.	Egg (g)	20	20	20	
8.	Baking powder (g)	1	1	1	
9.	Vanilla flavor (drops)	1-2	1-2	1-2	
10.	Salt (g)	0.5	0.5	0.5	

F1= 100% wheat flour; F2= 50% wheat flour + 50% potato flour; F3= 50% wheat flour + 50% corn flour.

### 2.4 Composite biscuits formulation

The method described by [11] was adapted to make biscuits with slight modification. Firstly, finely meshed fat was mixed with sugar powder, egg, salt, milk powder and

vanilla essence. Subsequently, the flour and baking powder were incorporated and thoroughly blended to yield a cohesive dough, flattened into a uniform sheet measuring 3 millimeters in thickness. After cutting a 3 cm round shape, the biscuits were baked at 170°C for 20 minutes using the baking oven.

### 2.5 Quality analysis of flour and fortified biscuits

In this study, the Moisture content [11], Ash content [12], protein content [12], fat content [12], total carbohydrate content and energy content [13], and gluten content [14] of fortified biscuits and flours (wheat, potato and corn) were determined.

### 2.6 Physical properties determination

The weight, thickness, spread ratio, volume, and density of fortified biscuits were determined by the method described by [15].

- **2.6.1 Weight:** The weight of the biscuits was determined by calculating the mean of four individual measurements using a digital weighing balance.
- **2.6.2 Thickness:** It was measured by stacking four biscuits on each other and taking the average thickness (cm).
- **2.6.3 Sread ratio:** The spread ratio was determined by using this formula.

Spread ratio = 
$$\frac{\text{diameter (mm)}}{\text{thickness (mm)}}$$

**2.6.4 Volume:** Volume of biscuit is defined as the area of the biscuit multiplied by thickness.

Volume (cm<sup>3</sup>) = 
$$\frac{\pi D^2}{4} \times T$$

Where, D= average diameter of biscuits (mm) and T= average thickness of biscuits (mm).

**2.6.5 Density:** After calculating volume, density was obtained from the ratio between weight and volume [15].

Density 
$$(g/cm^3) = \frac{Weight(g)}{Volume(cm^3)}$$

### 2.7 Sensory evaluation of developed biscuits

The samples were evaluated based on color, taste, flavor, texture and overall acceptability by a panel of judges (12) using a 9-point hedonic scale according to [16]. A 9-point hedonic rating scale [10] was used for statistical analysis of sensory data to determine the extent of acceptance. The tasters were given a hedonic rating scale from 1 to 9 with the following options: 9 for "extremely like," 8 for "very much like," 7 for "moderately like," 6 for "slightly like," 5 for "neither like nor dislike," 4 for "dislike slightly," 2 for "dislike moderately," 1 for "extremely dislike".

### 3. RESULTS AND DISCUSSION

This section reflects the results and the findings of the studies and their interpretation.

3.1 Proximate composition of wheat, potato and corn **flours:** Table 3 presents the analysis of nutritional quality. The results indicate that wheat flour exhibited the highest moisture content at 13.10%, with corn flour following closely behind at 11.09%. In contrast, potato flour displayed the lowest moisture content at 10.20% among the three types of flour. Potato flour yielded the highest ash content (1.6%) and total carbohydrate content (82.39%), whereas wheat flour exhibited the lowest ash content (0.62%) and fat content (0.85%) but the highest protein content (9.37%). The study results indicate that corn flour exhibited a high-fat content of 2.54% and yielded a maximum energy value of 360 Kcal/100g upon consumption. Conversely, potato flour demonstrated a comparatively lower energy value of 323 Kcal/100g. As per the researcher's findings [17], wheat flour exhibits a moisture content of 12.0%, ash content of 0.60%, protein content of 13.0%, fat content of 1.0%, and total carbohydrate content of 74.7% in wb. On the other hand, corn flour displays a moisture content of 9.3%, protein content of 7.4%, fat content of 2.0%, ash content of 1.2%, crude fiber content of 5.5%, and total carbohydrate content of 80.2%. The compositional dissimilarity observed among authors may be attributed to factors such as varietal diversity, environmental conditions, pre and post-harvest processing, and the degree of drying.

Table 3. Composition of wheat, potato and corn flours

Parameters	Wheat flour	Potato flour	Corn flour
Moisture (%) on dry basis	13.10	10.20	11.09
Ash (%)	0.62	1.60	0.63
Protein (%)	9.37	5.32	6.52
Gluten (%)	15.20	Not detected	Not detected
Fat (%)	0.85	0.49	2.54
Total Carbohydrate (%)	76.06	82.39	79.22
Energy (Kcal/100 g)	332	323	360

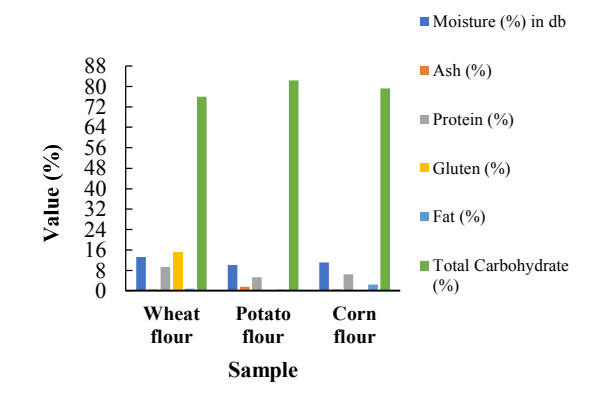


Figure 1. Composition of wheat, potato and corn flour 3.2 Physical properties of biscuits:

Table 4 demonstrates the average findings from the assessment of the biscuits' physical characteristics, including their diameter, thickness, volume, spread ratio, and density. As the level of supplementation increases, there is a noticeable rise in the diameter, thickness, and volume, while a decrease in weight, spread ratio, and density is noted. The F3 sample exhibits the largest values for diameter, thickness, and volume, while the F1 sample displays the highest weight, spread ratio, and density among the three samples. Incorporating potato flour and corn flour impacts a significant impact on the physical characteristics. The thickness of biscuits exhibited a slight increase with the gradual replacement of wheat flour with potato flour by up to 25%. This phenomenon was inversely proportional to the spread ratio, which decreased with the increasing proportion of potato flour. This can be attributed to the higher water-holding capacity of potato flour, as reported in previous studies [18].

Table 4. Effect of potato and corn flour on physical properties of biscuits

Sample	Weight (g)	Diameter D (cm)	Thickness T (cm)	Volume (cm <sup>3)</sup>	Spread Ratio	Density (g/cc)
F1	4.61	3.70	0.68	7.31	5.44	0.63
F2	4.32	3.80	0.72	8.16	5.27	0.53
F3	4.55	3.82	0.82	9.40	4.66	0.43

F1= 100% wheat flour; F2= 50% wheat flour + 50% potato flour; F3= 50% wheat flour + 50% corn flour

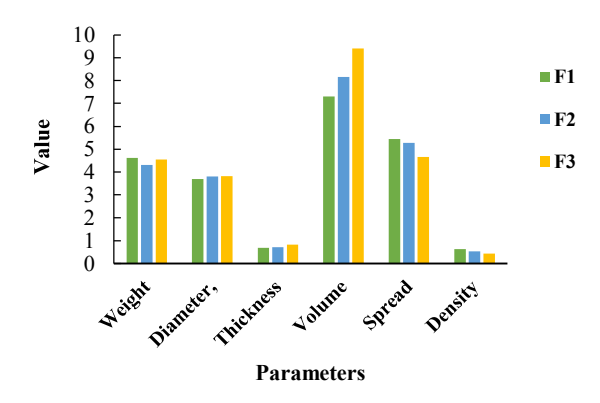


Figure 2. Effect of potato and corn flour on physical properties of biscuits.

**3.3 Nutritional properties of fortified biscuits:** The biscuits samples were analyzed for moisture, ash, protein, fat, and total carbohydrate. The results obtained are presented in Table 5.

Table 5. Nutritional composition of fortified biscuits

Sample	Moisture (%)	Ash (%)	Protein (%)	Lipid (%)	Total Carbohydrate (%)	Energy (Kcal/100g)
F1	5.02	0.72	8.02	16.93	69.31	456.54
F2	4.45	1.11	7.54	17.21	69.69	462.32
F3	4.72	0.78	7.80	17.68	69.02	480.74

F1= 100% wheat flour; F2= 50% wheat flour + 50% potato flour; F3= 50% wheat flour + 50% corn flour.

**3.3.1 Moisture:** According to Table 4, the moisture content of three different types of biscuits ranged from 4.45 to 5.02%. Factors such as the starting moisture content of different types of flour used in baking, storage conditions, and packaging materials may all contribute to the observed difference in biscuits' moisture levels. The F1 sample had a significantly higher moisture content than the rest. Different types of flour, such as wheat flour, potato flour, and corn flour, all have different amounts of solid matter, which may explain this phenomenon. According to [19], research showed that the moisture content of composite biscuits was anything from 5.13 percent to 7.17 percent dry basis. The biscuits used in this study all had moisture levels that were within the acceptable range, as established by earlier researchers.

**3.3.2 Protein:** Due to the larger percentage of gluten in wheat flour, the protein content reduced as the quantity of potato or corn flour increased. Protein content varied greatly between the samples, with F2 having the lowest and F1 having the most. Wheat flour biscuits had a 6.6% (db)

protein content, while potato-enriched biscuits had a 6.1% (db) protein content, as reported in [20]. According to the research by [19], composite biscuits' protein content was between 6.88% and 11.45% (db). The results suggest that potato or corn flour can make low-protein biscuits.

**3.3.3 Lipid:** The lipid composition of the specimens fell within 16.93-17.68%, as presented in Table 4. The potato flour supplementation resulted in a negligible variation in fat content, whereas the corn supplementation increased fat content. This finding is consistent with the study conducted by [20], which revealed that the biscuits supplemented with 20% potato flour contained 25.8% (db) fat, while the control group had 25.9% (db) fat.

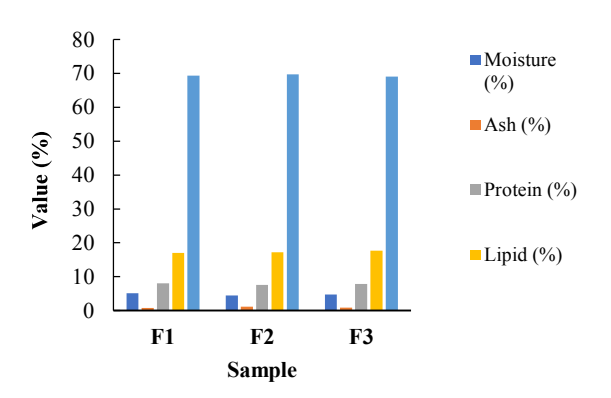


Figure 3. Nutritional properties of fortified biscuits.

**3.3.4 Ash:** The ash percentage ranged from 1.11% in the sample denoted as F2 to 0.72% in the sample denoted as F12. Because potato flour has a higher mineral content than wheat flour, including it in the biscuits caused them to have a higher ash level. According to [21], research showed that the ash content of composite biscuits was between 0.99 and 1.13% (wb). However, biscuits with 20% potato flour were reported to have an ash value of 1.7% by [20], while the control biscuit had an ash value of 1.4% (db).

**3.3.5 Total Carbohydrate:** Carbohydrate content varied from 69.02 to 69.69% throughout the samples (Table 4). Differences in protein, fat, ash, and moisture content may account for the wide range of total carbohydrate values seen in the biscuits we tested.

**3.3.6 Energy:** The total energy, expressed in calories, of the developed biscuits, varied between 456.54 and 480.74 for a 100 g consumption.

The observed variation in the samples is linked to the inclusion of either potato flour, which demonstrated the highest total carbohydrate content (82.39%), or corn flour, which contained the highest amount of fat (2.54%). These findings are presented in Table 3.

**3.4 Shelf-Life analysis for fortified biscuits:** The shelf-life of fortified biscuits was examined over 28 days, as presented in Table 6. The biscuits were packaged in high-

density polyethylene (HDPE) and stored at room temperature. The shelf life was assessed through the periodic evaluation of texture, color, flavor, and overall acceptability at 7-day intervals over a 28-day duration.

Table 6. Shelflife studies of fortified biscuits

riod	ode	Observation				
Storage period (days)	Sample code	Texture	Flavor	Color	Remark	
	F1	Crisp	Good	Good	Good	
0	F2	Crisp	Good	Good	Good	
-	F3	Crisp	Good	Good	Good	
	F1	Crisp	Good	Good	Good	
7	F2	Crisp	Good	Good	Good	
	F3	Crisp	Good	Good	Good	
	F1	Less crisp	Slightly rancid	Slightly faded	Freshness declined	
14	F2	Less crisp	Slightly rancid	Slightly faded	Freshness declined	
-	F3	Less	Slightly	Slightly	Freshness	
		crisp	rancid	faded	declined Not	
	F1	Damp	Rancid	Good	acceptable	
28	F2	Damp	Rancid	Good	Not acceptable	
	F3	Damp	Rancid	Good	Not acceptable	

### 3.5 Sensory evaluation of composite flour biscuits:

The sensory evaluation of biscuit samples was evaluated for color, flavor, texture and overall acceptability by a panel of 25 tasters. Table 7 shows the typical results of a sensory evaluation. The color evaluation for the three samples showed that F2 was the most aesthetically pleasing. Once more, samples F1 and F3 were ranked best and good in terms of aesthetic quality in that order.

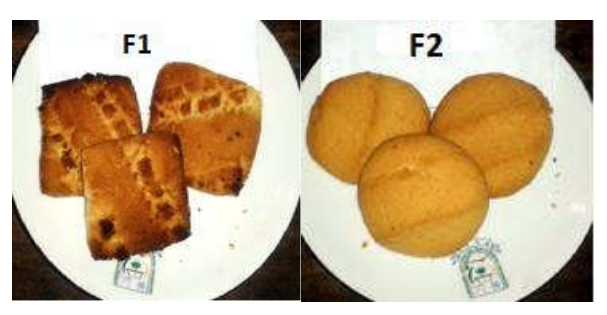
All three samples (F1, F2, and F3) had an appealing smell and the product's distinctive flavor without any unpleasant odors. Sample F2 was deemed to have the highest aesthetic quality, as shown in Table 7. A slight flavor difference was observed in the F3 sample (Figure 4).

Sample F2 scored higher than both F1 and F3 in terms of texture. Sample F2 had the highest rating for overall acceptability; it was also the most dissimilar to the other samples. Fisher's LSD, multiple comparison tests, showed that the F2 sample (biscuits made from 50% potato and 50% wheat flour) was the most popular (Figure 4).

Table 7. Mean score for color, flavor, texture and overall acceptability of fortified biscuits

	Sensory attributes					
Samples	Texture	Flavor	Color	Overall acceptability		
F1	7.7 <sup>b</sup>	7.9 <sup>b</sup>	7.9 <sup>b</sup>	7.6 <sup>b</sup>		
F2	8.5ª	8.6ª	8.3ª	$7.7^{a}$		
F3	7.0°	6.8°	7.8°	6.8°		

a= excellent, b= best, c= good; F1= 100% wheat flour biscuits; F2 = 50% potato + 50% wheat flour biscuits; F3 = 50% corn + 50%wheat flour biscuits.



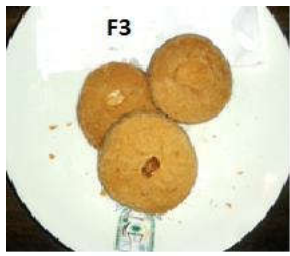


Figure 4: Physical and sensory characteristics of fortified biscuits.

### 4. CONCLUSION

Because of their rapid spoilage, 6.6% of all harvested potatoes in Bangladesh are lost after being wholesaled, 5.3% at the radar level, and 1.1% at the merchant level [22]. Potatoes and corn have the potential to serve as ingredients in the production of biscuits. Biscuits that are both nutritious and signature flavorful can be produced by incorporating potato or corn flour in addition to wheat flour. Wheat flour can be used to supplement potato or corn flour up to a maximum of 50% to produce biscuits that appeal to a wider range of consumers. The enhancement of the formulation can be achieved through the incorporation of food coloring agents, flavoring compounds, and vitamin supplements. Additional research can be conducted pertaining to vitamins and mineral contents, anti-oxidant activity, particle size distribution, hydration properties, etc.

#### 5. REFERENCES

- [1] Das, P. C., Rana, M. S., Saifullah, M., & Islam, M. N. (2018). Development of composite biscuits supplementing with potato or corn flour. *Fundamental and Applied Agriculture*, *3*(2), 453-459. doi:10.5455/faa.292438.
- [2] Woldegebreal, D., Luo, H., Vosti, S., & Engle-Stone, R. (2019). Modeling the Potential of Fortified Biscuits Too Address Micronutrient Deficiencies Among Preschool Children and Women in Cameroon (P10-116-19). Current Developments in Nutrition, 3, 3013450. doi:10.1093/cdn/nzz034.P10-116-19
- [3] Adeyeye, S. A. O., Adebayo-Oyetoro, A. O., Fayemi, O. E., Tiamiyu, H. K., Oke, E. K., & Soretire, A. A. (2019). Effect of co-fermentation on nutritional composition, anti-nutritional factors and acceptability of cookies from fermented sorghum (Sorghum bicolor) and soybeans (Glycine max) flour blends. Journal of Culinary Science & Technology, 17(1),59-74. doi:10.1080/15428052.2017. 1404536.
- [4] Sharma, V., & Bhardwaj, A. (2019). Scanning electron microscopy (SEM) in food quality evaluation. In Evaluation technologies for food quality (pp. 743-761). Woodhead Publishing. Elsevier. doi: 10.1016/B978-0-12-814217-2.00029-9.
- [5] Hugo, L. F., Rooney, L. W., & Taylor, J. R. N. (2000). Malted sorghum as a functional ingredient in composite bread. *Cereal chemistry*, 77(4), 428-432. doi: 10.1094/cchem.2000.77.4.428.
- [6] Mamat, H., Matanjun, P., Ibrahim, S., Md. Amin, S. F., Abdul Hamid, M., & Rameli, A. S. (2014). The effect of seaweed composite flour on the textural properties of dough and bread. *Journal of applied phycology*, 26, 1057-1062. doi: 10.1007/s10811-013-0082-8.]
- [7] Abdelghafor, R. F., Mustafa, A. I., Ibrahim, A. M. H., & Krishnan, P. G. (2011). Quality of bread from composite flour of sorghum and hard white winter wheat. Advance Journal of Food Science and Technology, 3(1), 9-15. doi: 10.19026/ajfst.5.3357.
- [8] Misra, A., & Kulshrestha, K. (2003). Potato flour incorporation in biscuit manufacture. *Plant Foods* for Human Nutrition, 58, 1-9. doi: 10.1023/B:QUAL.0000040337.69812.cb.
- [9] Srivastava, S., Genitha, T. R., & Yadav, V. (2012). Preparation and quality evaluation of flour and biscuit from sweet potato. J Food Process

- *Technol*, *3*(12), 1-5. doi: 10.4172/2157-7110.1000192.
- [10] Sarker, A., Islam, M. N., & Shaheb, M. R. (2012). Kinetics of dehydration of potato and development of baked product based on dehydrated potato. *Journal of the Bangladesh Agricultural University*, *10*(2), 303-312. doi: 10.3329/jbau.v10i2.14923.
- [11] Thiex, N. (2009). Evaluation of analytical methods for the determination of moisture, crude protein, crude fat, and crude fiber in distillers dried grains with solubles. *Journal of AOAC international*, 92(1), 61-73. doi: 10.1093/jaoac/92.1.61.
- [12] Thiex, N., Novotny, L., & Crawford, A. (2012). Determination of ash in animal feed: AOAC official method 942.05 revisited. *Journal of AOAC International*, 95(5), 1392-1397. doi: 10.5740/jaoacint.12-129.
- [13] Maclean, W., Harnly, J., Chen, J., Chevassus-Agnes, S., Gilani, G., Livesey, G., & Warwick, P. (2003, February). Food energy—Methods of analysis and conversion factors. In Food and agriculture organization of the united nations technical workshop report (Vol. 77, pp. 8-9). Agricultural Research Service, US Department of Agriculture, Beltsville, MD, USA.
- [14] Barbhai, M. D., Hymavathi, T. V., Kuna, A., Mulinti, S., & Voliveru, S. R. (2022). Quality assessment of nutri-cereal bran rich fraction enriched buns and muffins. *Journal of Food Science* and *Technology*, 59(6), 2231-2242. doi: 10.1007/s13197-021-05236-9.
- [15] Srivastava, S., Genitha, T. R., & Yadav, V. (2012). Preparation and quality evaluation of flour and biscuit from sweet potato. *J Food Process Technol*, 3(12), 1-5. doi: 10.4172/2157-7110.1000192.
- [16] Ranganna S. (2005). Hand Book of Analysis of Quality Control for Fruit and Vegetable Products, Second edition. Tata McGraw Hill Publications Company Limited, New Delhi, India.
- [17] Chung, S. Y., Han, S. H., Lee, S. W., & Rhee, C. (2010). Physicochemical and bread-making properties of air flow pulverized wheat and corn flours. Food Science and Biotechnology, 19, 1529-1535. doi: 10.1007/s10068-010-0217-5.
- [18] Khaliduzzaman, M., Shams-Ud-Din, M., & Islam, M. N. (2010). Studies on the preparation of chapatti and biscuit supplemented with potato flour. *Journal of the Bangladesh Agricultural University*, 8(1), 153-160. doi: 10.3329/jbau.v8i1.6413.

### DEVELOPMENT AND QUALITY ASSESSMENT OF COMPOSITE BISCUITS FORTIFIED WITH POTATO AND CORN FLOUR

- [19] Grah, A. B., Beda, M. Y., Aubin, P. D., Niaba, K. P. V., & Gnakri, D. (2014). Manufacture of biscuit from the flour of wheat and lentil seeds as a food supplement. European Journal of Food Science and Technology, 2(2), 23-32.
- [20] Seevaratnam, V., Banumathi, P., Premalatha, M. R., Sundaram, S. P., & Arumugam, T. (2012). Studies on the preparation of biscuits incorporated with potato flour. *World Journal of Dairy & Food Sciences*, 7(1), 79-84. doi: 10.5829/idosi.wjdfs.2012.7.1.6148.
- [21] Agu, H. O., Ayo, J. A., Paul, A. M., & Folorunsho, F. (2007). Quality characteristics of biscuits made from wheat and African breadfruit (Treculia africana). doi: 10.4314/ni-foj.v25i2.50827.
- [22] Uddin, M. A., Yasmin, S., Rahman, M. L., Hossain, S. M. B., & Chowdhury, R. U. (2010). Challenges of potato cultivation in Bangladesh and developing digital databases of potato. *Bangladesh Journal of Agricultural Research*, 35(3), 453-463. doi: 10.24018/ejfood.2022.4.2.45.

M. Abdeen<sup>1</sup>, K. Rayhan<sup>2</sup>, S. Hasan<sup>3</sup>, N. Zishan<sup>4</sup>, and S. Anwar<sup>5</sup>

<sup>1, 2, 3</sup>Graduate, Department of Civil Engineering, Dhaka University of Engineering and Technology, Gazipur
 <sup>4</sup>Post Graduate, Department of Civil Engineering, Dhaka University of Engineering and Technology, Gazipur
 <sup>5</sup>Associate Professor, Department of Civil Engineering, Dhaka University of Engineering and Technology, Gazipur

E-mail: minhazulabdeen260@gmail.com, kawsarrayhanshihab@gmail.com, sajib.hasan133046@gmail.com, nazmul.zishan@gmail.com, shibly@duet.ac.bd

### ABSTRACT

The Jamuna River exhibits significant erosion along its banks, resulting in changes to its course and posing challenges for local communities. This study aimed to detect the changes of Jamuna River flow path and to estimate the rate of change of flow area, erosion, and accretion along the Jamuna River for the period of 1990 to 2020. Landsat satellite images of 30 m resolution from 1990 to 2020 at five years interval were collected from USGS website. River flow area and bank lines were detected from raster calculation of MNDWI. The rate of bankline shifting and bankline movement were computed in LRR (m/year) and NSM (m) method respectively. The Jamuna River had consistently lost its water body at an average rate of 4.6 km² per year from 1990 to 2000. However, the river's flow area remained relatively stable, with an average annual decrease of 0.35 km² during 2000-2020. The upstream areas of Kazipur and downstream areas of Nagarpur and Shahajadpur were identified as the most vulnerable regions. Conversely, the middle segments of Sirajganj Sadar and Bhuapur were relatively stable. The area downstream of Jamuna Bridge has experienced significant land gain, with a maximum width of 4.2 km. On average, the right bank of the river experienced an erosion rate of -11.97 m/year, while the left bank eroded at an average rate of -52.44 m/year. This study advocates for policymakers to mitigate the risk of Jamuna riverbank erosion and implement sustainable management strategies.

### 1. INTRODUCTION

Bangladesh is known as the land of rivers due to its extensive river network. The rivers in Bangladesh play a vital role in the country's geography, economy and culture. The river system directly or indirectly influences many aspects of the environment and plays a vital role in the livelihood pattern of millions of inhabitants. Bangladesh owns three mighty rivers, the Ganga (Padma), Brahmaputra (Jamuna) and Meghna. The Brahmaputra-Jamuna is a classic example of a braided river and is highly susceptible to channel migration and avulsion, making the river very dynamic and unstable, which is prone to erosion and accretion. The Jamuna is provided to have exquisite bank erosion and highest rate of bank line movement (N. I. Khan & Islam, 2003). It has been evidently observed that changes in the proportion of erosion and accretion differ in different points of Jamuna River. The highest eroded area, spanning over 3.82 km<sup>2</sup>, occurred between 1995 and 2005, while the highest accreted area, covering 6.15 km<sup>2</sup>, was observed between 1995 and 2015 (M. A. Hassan et al., 2017). During the period of 1973 to 2015, the net erosion along the 220 km long Jamuna River was about 88,462 ha. (Klaassen et al., 1988).

The erosion and accretion of the Jamuna River is a serious problem that is having a significant impact on the people who live along the river. These processes can have far-reaching impacts including the loss of valuable agricultural land damage to infrastructure and settlements

changes in river flow patterns and alterations to the ecological balance. The erosion is causing the river to widen and deepen, which is displacing millions of people along river bank. The accretion is causing the river to narrow and become shallower, making it difficult for boats to navigate and leading to huge floods due to water overflow. This case study focused on the erosion and accretion dynamics of the Jamuna River, aiming to understand the patterns, rate of bank line changes, and extents of these processes. By utilizing GIS and remote sensing technology, we can obtain detailed and accurate spatial information, enabling comprehensive analysis of the river's changes over time. It also helps to identify areas at risk of rapid erosion and accretion. This information can be used to develop plans to mitigate the effects of erosion and accretion along the bankline of Jamuna River.

However, the main objectives of this study are as follow:

- 1. To detect the change of Jamuna River flow path using Landsat Satellite images.
- 2. To estimate the rate of change of flow area, erosion and accretion along the Jamuna River for the period of 1990 to 2020.

### 2. DATA COLLECTION AND STUDY AREA

### 2.1 Study Area

The Brahmaputra originates in the Chemayung-Dung glacier, approximately at 31'30'N and 82'0'E. The total length

of the Tsangpo-Brahmaputra-Jamuna River up to its confluence with the Ganges is about 2,700 km. Within Bangladesh territory, Brahmaputra-Jamuna is 276 km long, of which Jamuna is 205 km. The Jamuna River is braided in nature. Within the braided belt of the Jamuna, there are lots of chars of different sizes. An assessment of the 1992 dry season Landsat image showed that the Jamuna contained a total of 56 large island chars, each longer than 3.5 km. The study area for this study is Jamuna River passes through Sirajganj and Tangail District, which is 85 km long started from Kazipur to Shahjadpur. The study area which lies between latitude 24°00'N -24°48'N and longitude 89°38'E-89°52'E.

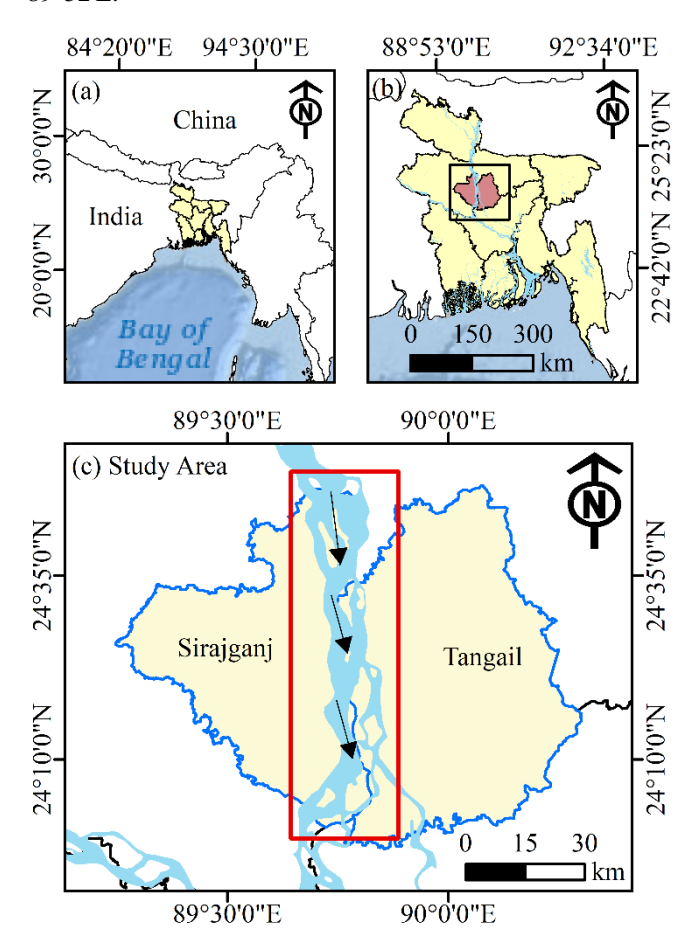


**Fig. 1:** Map showing (a) World view, (b) Bangladesh, (c) Zoomed view of 85 km long study area of Jamuna River passes through Tangail and Sirajganj district.

The left bank (Sirajganj side) is vulnerable in case of bank erosion than right bank (Tangail side) erosion of the river. Sirajganj and Tangail district were connected through 5 km long Jamuna Bridge which was constructed over the Jamuna River in 1998 (R. Islam et al., 2017). River training structures have been built more than 30 places along the Sirajganj and Tangail Bankline since 1996 (Sarker et al., 2011). Fig. 1 shows the study area in between Tangail and Sirajganj district. Many important places i.e., Kazipur, Sirajganj Sadar, Shahjadpur, and Bhuapur are located along the Bankline of Jamuna River. The density of the population in Sirajganj district along the riverbank is higher than that of the population density in Tangail district. Nagarpur, located in Tangail side, has the highest population density.

### 2.2 Data Collection

Identification of the river morphology from satellite imagery of different years using GIS and Remote Sensing technology is found to be useful for studying the fluvial geomorphology of a river. The Landsat Program is the longest running exercise in the collection of multispectral, digital data of the earth's surface from space since 1972. In this study, dry season Landsat imagery from 1990 to 2020 was collected from the USGS website archives. The details information of the imagery are listed in Table I.

**Table I:** Acquisition date of Landsat images and their resolution.

S.L	Image Acquisition Date mm/dd/yyyy	Sensor Type (Landsat)	Image Resolution (m)	Source
1.	11/14/1990	5 TM	30	
2.	01/28/1995	5 TM	30	
3.	01/26/2000	5 TM	30	
4.	01/07/2005	5 TM	30	USGS
5.	01/21/2010	5 TM	30	
6.	02/04/2015	8 OLI	30	
7.	01/17/2020	8 OLI	30	

We primarily collected Landsat dry season cloud-free images available during the January to February months. This choice was made to facilitate the clear detection of the river's main flow path and bar land, as rainwater on the surface of bar land could potentially interfere with the results. All the Images were collected from path 138 and row 43 of Landsat USGS archive. We used three Band images i.e., green, near infrared (NIR), and short-wave infrared (SWIR). The data obtained were in a GeoTIFF format for each individual band. Short-wave infrared is mostly absorbed by water which helped us to detect the river and the land area.

### 3. METHODOLOGY

### 3.1 Flow Path Changes of Jamuna River

Remote Sensing (RS), Geographic Information System (GIS) methods, and other statistical data techniques have been employed to assess river erosion and accretion, as well as to identify shifting patterns of Jamuna River. Various methods for extracting the river body from Landsat imagery have been developed using ArcGIS software. The river body was extracted from the image using the MNDWI method, which stands for Modified Normalized Difference Water Index developed by (Xu, 2007). The reflectance of water is higher in the green band and lower in NIR band. Xu (2007) proposed that the MNDWI is suitable for extracting the waterbody from a landmass. The modification of the NDWI using a MIR band instead of a NIR band can considerably improve the enhancement of open water features. The MNDWI is more suitable for enhancement of water with many built-up land areas in the background than the NDWI because it can efficiently reduce and even remove built-up land noise (Xu, 2007).

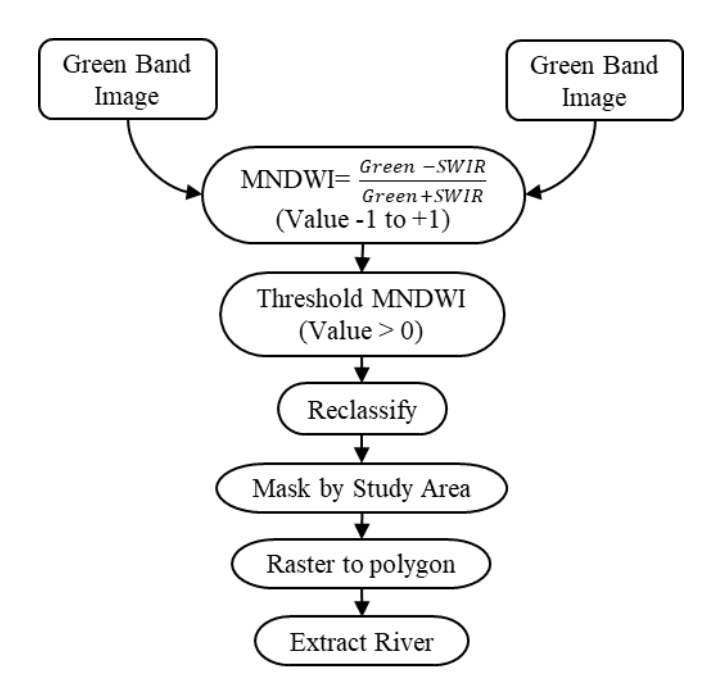


**Fig. 2:** Methodology flowchart to extract waterbody from satellite images.

Fig. 2 shows the methodology of extracting the river polygon from satellite imagery. The threshold values for the MNDWI to achieve best water extraction result are usually much less than those of the NDWI, suggesting using zero as a default threshold value can produce better water extraction accuracy for the MNDWI than for the NDWI (Xu, 2007).

 $\underline{Green-SWIR}$ MNDWI =(1) 89°40'0"E 89°50'0"E 89°40'0"E 89°50'0"E 24°35'0"N 24°35'0"N C C 24°10'0"N 24°10'0"N 24°10'0"N 24°10'0"N D 2000 2005 89°40'0"E 89°40'0"E 89°50'0"E 89°50'0"E

**Fig. 3:** Extracted River flow area in 2000 (green) and 2005(blue).

The value of MNDWI Ranges from -1 to +1. The higher reflectance of built-up and lower reflectance of water in SWIR band result in negative values of built-up and positive values of water features in the MNDWI-derived image.

Each extracted river polygon from 1990 to 2020 at 5-year interval was divided into 4 rectangular segments i.e., Segment A (22.4km×24.8km), Segment B (20.8km ×24.8km), Segment C (20.6km ×24.8km) and Segment D (22.6km ×24.8km). Fig. 3 represents the detected waterbody from Landsat images of 2000 and 2005. Extracted rivers indicated the waterbody of the river. We measured the total area of each individual segment, and then subtracted the river area to estimate net land area. Thus, we quantified only the land area of each segment throughout the year 1990 to 2020. Comparing consecutive two years images, we estimated net erosion and accretion area of each segment throughout the years 1990-1995.

Net land area of each segment = (Segment Area - River flow area) (2)

Net Area of erosion or accretion in the segment = (land area in 90 – land area in 95) (3)

(Positive value indicates accretion and negative vale indicates erosion)

### 3.2 Bankline Detection

Bankline is defined as the feature that separates the outer margin of a river channel from the floodplain (Hassan et al., 1997)

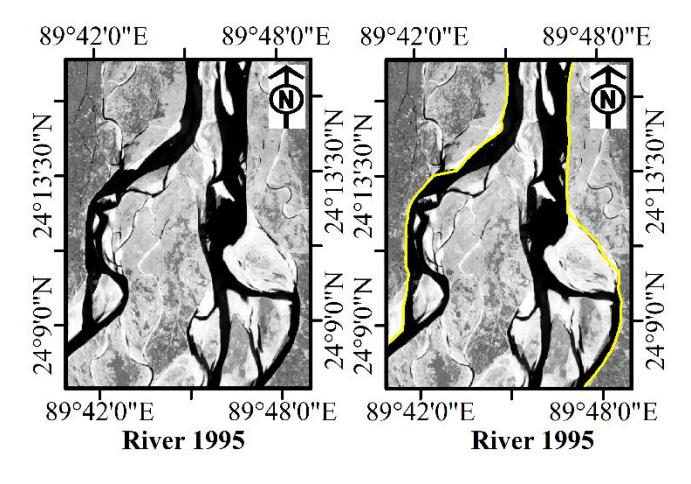


**Fig. 4:** Landsat SWIR image of 1995, black portion indicate as waterbody and yellow as river Bankline.

The analysis of historical Bankline changes helped us understanding the erosion rate and vulnerable areas near the river Bankline. This study relied on Remote Sensing satellite image for Bankline detection. Water exhibits a high degree of infrared energy absorption, while it is strongly reflected by vegetation and land. The short wavelength band shows significant difference between land and water interface. Hence, we used a single SWIR band for Bankline detection. The water appears black and land surface or vegetation appears grey in Landsat SWIR band. Fig. 4 shows the detection of the Bankline of Jamuna River in the year 1995.

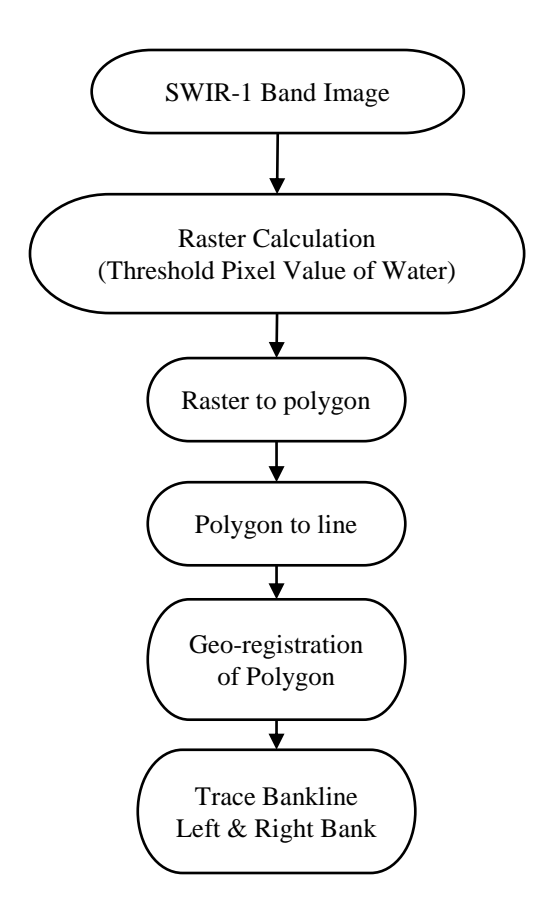


**Fig. 5:** Methodology flowchart to extract river bankline from satellite images.

In this study, Automatic Bankline detection techniques were employed to detect the Bankline of the Jamuna River for the period 1990 to 2020. First, we performed georegistration based on the World Geodetic System WGS-84 with projected coordinate system UTM zone 45N to adjust the geographic positions of all images. Raster calculation was then performed from the threshold values of water exhibited pixels. The threshold value for water pixel was selected by trial-and-error method. Then, the riverbank line was traced for both left and right bank from 1990 to 2020 at 5-year interval. Fig. 5 represents the sequential process of river Bankline detection from SWIR image.

### 3.3 Bankline Change Analysis in DSAS

In this study, we used the Digital Shoreline Analysis System (DSAS) version 5.1, an extension tools of ArcGIS, to compute the rate of Bankline changes. The processes were carried out in four steps i.e., bankline preparation, creating baseline, transects generation and computing the rate of Bankline changes (Raj et al., 2020). DSAS used baseline measurements of a time series of banklines to estimate the rate of Bankline change and it required another shapefile in the same personal geodatabase (Leatherman, 1983). We positioned approximately 15000 m long baseline parallel to the riverbank and cast transects along this baseline at 100 m intervals perpendicular to that baseline. These transects were generated using the cast transects tool in DSAS, with a smoothing distance set at 0.00 m. Overall, 645 transects were created and the data from the transect feature class were used to compute the changes.

### 3.3.1 Linear Regression Rate (LRR)

Linear Regression Rate (LRR) estimates the rate of variation by fitting the least squares regression line to all the Bankline points of a transect (Himmelstoss et al., 2021).

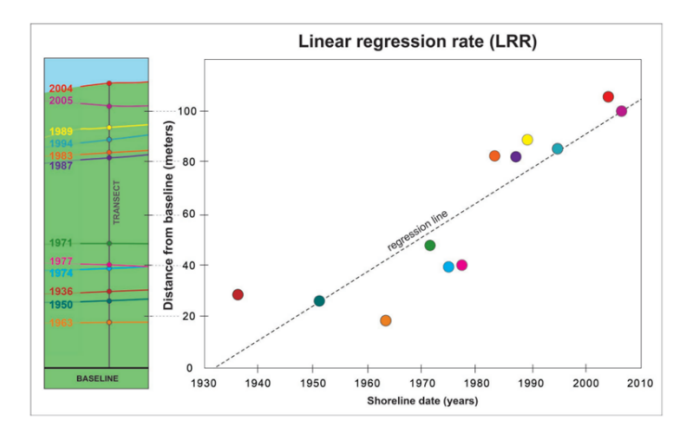


**Fig. 6:** Shoreline distance vs shoreline date graph represents Linear Regression Rate of a single transect. The slope of the equation describing the line is the rate (Himmelstoss et al., 2021)

The regression line is placed (Fig. 6) so that the sum of the squared residuals (determined by squaring the offset distance of each data point from the regression line and adding the squared residuals together) is minimized. The linear regression is the slope of the line. This method includes all the data regardless of modifications in trend or accuracy. The entire computation was carried out on the accepted and widely demonstrated statistical concepts of LRR (Dolan et al., 1991; Crowell et al., 1997).

### 3.3.2 Net Bankline Movement (NBM)

Net Bankline Movement (NBM) is another statistical parameter that enumerates the actual distance between the oldest and the youngest shoreline for each transect laid perpendicular to the shorelines (Himmelstoss et al., 2021). In this study, we quantified the net Bankline movement of the study area.

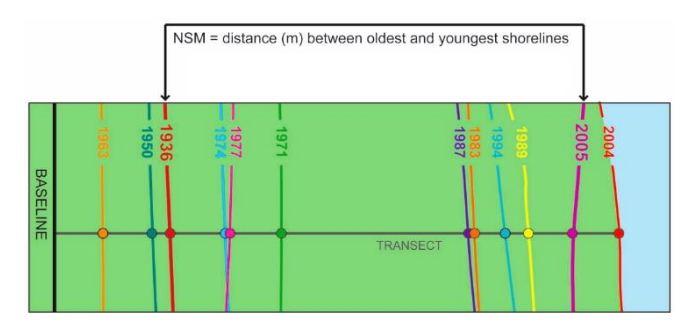


**Fig. 7:** A Bankline dataset including baseline (black), transect (gray), and shoreline and intersect data (multicolor) to illustrate the relationship between net Bankline movement

However, it was calculated using the following formula:

Net Bankline Movement = 
$$\{d_{\text{newest bank}} - d_{\text{oldest bank}}\}\ m$$
 (4)

44

### 4. RESULT AND DISCUSSION

### 4.1 Variation of River Flow Area

The net area of extracted river water body was calculated by ArcGIS software.

Change of River Flow Area From 1990-2020

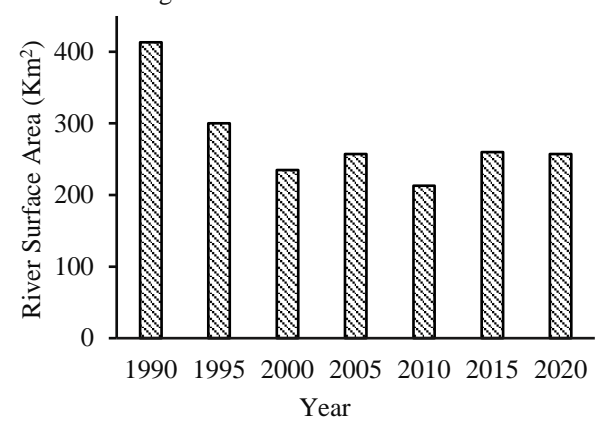


Fig. 8: Area of river net waterbody from 1990-2020.

The area includes all the area of major and minor channel of Jamuna River in this study. As the most of the images were collected in the dry season, the result was not affected by precipitation water. Fig. 8 shows net flow area of Jamuna River for different periods from 1990 to 2020. The flow path was maximum in the year 1990. The river net area decreased in the period from 1990 to 2000, which is because of char land accretion. After the year 2000 change of flow path area was mostly stabilized.

**Table II:** Jamuna River flow path area from 1990 to 2020.

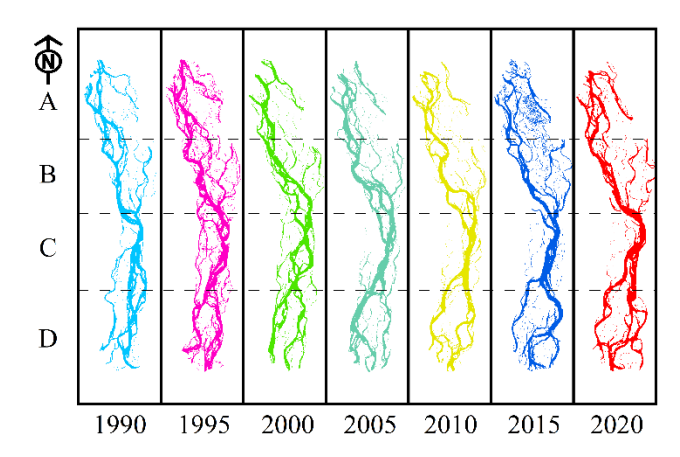
Year	River Net Flow Area (Km <sup>2</sup> )
1990	413
1995	300
2000	235
2005	257
2010	213
2015	260
2020	257

Table II reveals that the maximum river flow area of the Jamuna River was detected in 1990, while the minimum flow area was observed in 2010. Subsequently, after the year 2000, the river's flow area remained predominantly stable. The flow area for the years 2005, 2015, and 2020 is almost the same. Increase in flow area occurred in the period of 2000-2005 and 2010-2015 respectively. An increase in flow area corresponds to a decrease in the land area of the riverbank and instability in the bar land. As the Jamuna River is of the alluvial type, its flow path is inherently unstable and subjected to change over time. Reduced river velocity and a higher sediment settling within the river influence a decrease in flow during the dry season. The sediment load of the

Jamuna was 555 Mt/year during the early-1960s (Coleman, 1969).

### 4.2 Segment Wise Flow Area Changes

We divided study area into four different rectangular segments i.e., A, B, C, and D to understand the change pattern of Jamuna River flow area throughout the entire study period. After measuring the area of each segment, we compared the flow area of each segment in different periods.



**Fig. 9:** Rate of change of net river flow area from 1990-2020.

Fig. 9 shows the segmented river of different year. It can be perceptible from the figure that the upstream river sifted slightly towards west and main channel became narrow in the middle, which was because of the construction of Jamuna Bridge in 1998.

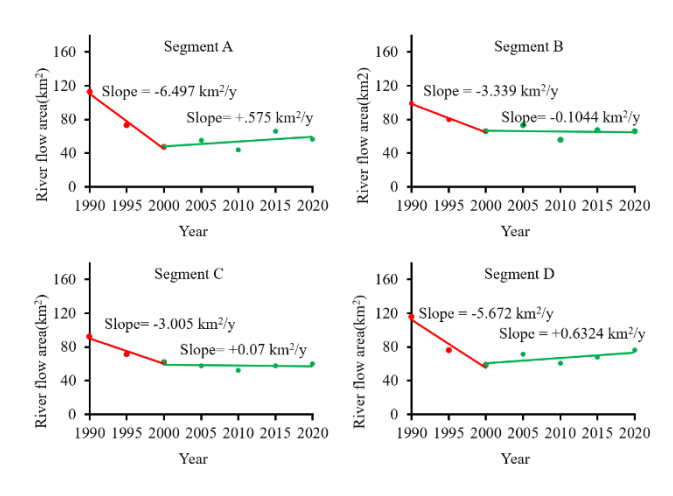


**Fig. 10**: Distribution of segment-wise changes of river flow path from 1990 to 2020.

Fig. 10 illustrates that segment A experienced a reduction in its flow area from 1990 to 2000. The rate of waterbody loss in the upstream segment was the highest of all segments, standing at -6.497 km²/year. After 2000, the river started gaining flow area, signifying an increase in land area upstream, amounting to +0.577 km²/year. Several river protection works were undertaken between 1998 and 2000 on the right bank of this segment, including Meghna spur-1, 2 & 3, Shingrabari spur- 1 & 2, and Subagacha spur-1 & 2

(Sarker et al., 2011). These efforts contributed to the stabilization of the river's flow area after 2000.

**Table III:** Segment-wise change of flow area in five years interval from 1990 to 2020.

	Net Changes of Jamuna River Flow Area (km²)					
Time	A 554.3 (km <sup>2</sup> )	B 515.02 (km <sup>2</sup> )	C 511.09 (km <sup>2</sup> )	D 566.13 (km <sup>2</sup> )		
1990-1995	39.52	19.43	20.54	39.67		
1995-2000	25.45	13.96	9.51	17.05		
2000-2005	-7.59	-7.36	4.1	-12.28		
2005-2010	11.18	17.13	5.57	10.31		
2010-2015	-22.11	-11.11	-5.44	-7.25		
2015-2020	9.61	0.94	-2.45	-8.12		

In segment B, the river's waterbody declined at a rate of  $-3.339 \text{ km}^2/\text{year}$  from 1990 to 2000. Subsequently, from 2000 to 2020, the rate of change in waterbody was  $+0.1044 \text{ km}^2/\text{year}$ , indicating a relatively stable condition in that area. This stability can be attributed to riverbank protection measures upstream of the Jamuna Bridge and surrounding river training works.

In segment C the rate of change of waterbody was +0.07 km²/year from the year 2000 to 2020. In this segment Jamuna bridge was constructed in 1998, before that the area was eroded at -3.337 km²/y from the year 1990-2000. The construction of guide banks at the Jamuna Bridge in segment C has led to a reduction in the rate of flow area change in this particular segment, resulting in a minimal rate of change.

Segment D, located downstream of the Jamuna River where it converges with the Ganges-Padma River, experiences sediment deposition due to suspended sediment in the water. The rate of change in flow area from 1990 to 2000 was computed at -5.672 km<sup>2</sup>/year, which is equivalent to the changes observed upstream during that period. In this segment, river training works, including PIRDP bank protection, Betil Spur-1, and Enayetpur spur-2, were constructed between 2001 and 2006 (Sarker et al., 2011). In recent years, this segment continues to be susceptible to erosion, with an erosion rate of +0.63 km<sup>2</sup>/year. However, a detailed segment-wise analysis of flow area changes over five-year intervals from 1990 to 2020 is presented in Table III. A prior study indicated that in the years 2004, 2006, and 2007, there were instances of significantly higher water discharge, exceeding 12,000 m<sup>3</sup>/s, during a span of 34 years. Conversely, the lowest discharge was recorded in the years 2012 and 2013, spanning the period from 1982 to 2016 (Khan et al., 2020). This recent decline in discharge has had a considerable impact on the river's flow area. Additionally, this study observes a reduction in the river's flow path after the year 2000.

### 4.3 Bankline Changes

Fig. 11 shows rate of Bankline changes Jamuna River for the Periods of 1990–2000 (brown), and 2000-2020 (blue) along different vertical transects.

**Table IV:** Rates of Bankline changes of Sirajganj side for the different segments of Jamuna River in the study period of 1990-2020.

<b>X</b> 7	Rate of Bankline change right bank in each segment (m/y)				
Years	P	Q	R	S	T
	15Km	10km	9Km	16Km	5Km
1990-2000	-69	-152	+177	-90	-37
2000-2020	-43	+3.4	-5	+170	-48
Average	-11.	.965 m/y	ear (Sira	ajganj Sid	le)

The rates of changes in Bankline position were calculated for the different designated segments P, Q, R, S and T located at right bank (Sirajganj side) and I, J, K and L for left bank (Tangail side) of the river.

**Table V:** Rates of Bankline changes of Tangail side for the different segments of Jamuna River in the study period of 1990-2020.

	Rate of Bankline change left bank in			
Years				
rears	I	J	K	${f L}$
	15Km	10km	9Km	16Km
1990-2000	+47	-185	-118	-107
2000-2020	+13	-31	+99	-101
Average	-52.44 m/year (Tangail Side)			

At the right bank erosion was maximum at Q (152 m/year) section (Table IV) and at the left bank was at J (185 m/year) section (Table V) for the period of 1990-2000. For the period of 2000-2020 erosion was dominating along the bank line of segment P and T at Sirajganj side and in Tangail side segment L is the most eroded (101 m/year) area. In that period at right bank S segment is the area of accretion at a rate of 170 m/year.

**Table VI:** Shifting of Jamuna riverbank line of Sirajganj and Tangail side for the different segments in the study period of 1990-2020.

Bank Position	Segment	Net Bankline Movement (m)	
		1990-2000	2000-2020
Left Bank (Sirajganj Side)	P (15 Km)	-674	-870
	Q (10 Km)	-1525	-121
	R (9 Km)	1773	-359
	S (16 Km)	-902	4200
	T (15 Km)	-366	-704
Right Bank (Tangail Side)	I (15 Km)	475	346
	J (25 Km)	-1860	-446
	K (15 Km)	-1186	1612
	L (10 Km)	-1068	-1813

Erosion was reduced in period of 2000-2020 at 10 km of Q and 9 Km of R segment (Table VI) because of construction of various river training works along the river. In segment I, Bankline moves towards west direction at a rate of +13

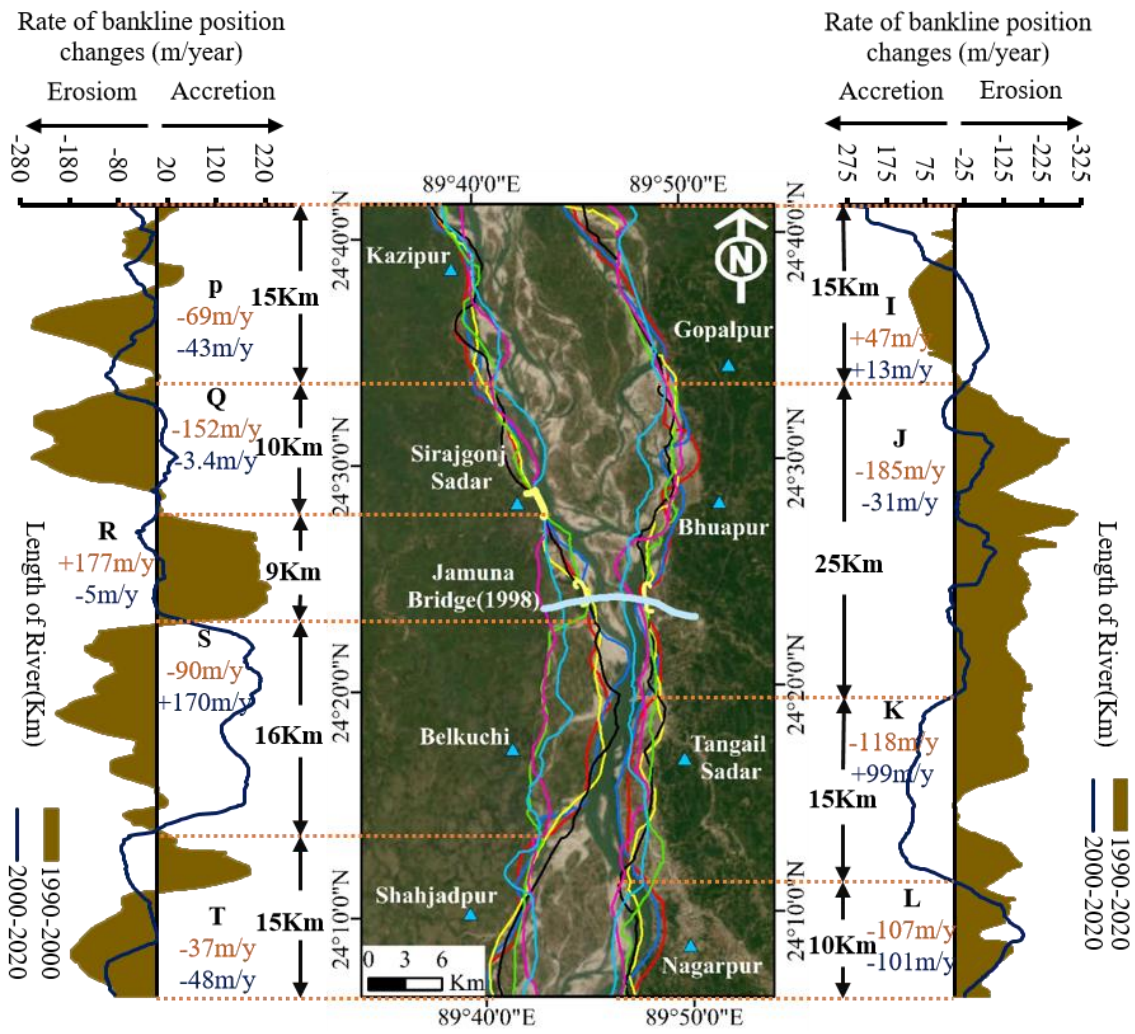


**Fig. 11:** Bankline change rates along Jamuna River for the periods of 1990–2000 (brown) and 2000-2020(blue), negative values indicate erosion (landward movement of bank line).

m/year, which indicates shifting of upstream river towards west side. The Tangail side was maximum eroded from 1990-2000 and Nagarpur was very vulnerable zone prone to erosion. We observed that the river shifted towards west side (Right bank) from 1990 to 2020. From this study we find westward migration of right bank at a rate of 63.4 m/year, and left bank at a rate of 53 m/year. Westward shifting of the centerline resulted from westward migration of the west (right) bank at an average rate of 90 m/year, combined with westward migration of the east (left) bank at average rates of 48 m/year for westward migration between 1953 and 1989 (Sarker et al., 2014).

A study conducted on the Kazipur riverbank revealed that the mean eastward shift of the riverbank from 1972 to 1988 was 0.55 km, while the west bank exhibited a shift of approximately 0.77 km (Islam et al., 2019). In this study, we observed a riverbank shift of 0.797 km on the right bank of Kazipur and a shift of 0.410 km on the east bank. This is consistent with the previous movement observed in that segment. Average rate of Bankline movement in Sirajganj side was -11.965 m/year, while average rate of Bankline movement in Tangail side is -52.44 m/year. Which means both banks were still prone to erosion.

### 5. CONCLUSION

The study of the Jamuna River reveals diverse morphological characteristics, including changes in flow patterns, shifts in riverbanks, sandbar formation, channel migration, erosion, and sediment deposition. However, this paper sincerely focuses on erosion, sedimentation, and bank shifting between Kazipur and Shahjadpur during 1990-2000 using the Landsat images collected from United States Geological Survey (USGS). The research indicates that during the year 1990, the river's maximum flow area was 413 km<sup>2</sup>, gradually decreasing until 2000. During the year 2000 to 2020, the flow area remained relatively stable, with a minimum of 213 km<sup>2</sup> observed in the year 2010. In contrast, Segments Q (Sirajganj), J (Bhuapur), K (Tangail Sadar), and L (Nagarpur) experienced the highest erosion rates, averaging -184 m/year in between the year 1990-2000. However, in the recent years between 2000 and 2020, the areas around Kazipur (15 km) upstream, Nagarpur (10 km), and Shahajadpur (15 km) downstream faced the most severe bank erosion. Furthermore, the downstream of the Jamuna Bridge, a significant land gain of 4.2 km on the right bank and 1.6 km on the left bank was witnessed due to sediment settlement resulting from Jamuna bridge construction.

#### REFERENCES

- Coleman, J. M. (1969). Brahmaputra river: Channel processes and sedimentation. *Sedimentary Geology*, 3(2–3), 129–239. https://doi.org/10.1016/0037-0738(69)90010-4
- Crowell, M., Douglas, B. C., & Leatherman, S. P. (1997). On Forecasting Future U.S. Shoreline Positions: A Test of Algorithms. *Source: Journal of Coastal Research Journal of Coastal Research*, 13(4), 1245–1255. http://www.jstor.org/stable/4298734%5Cnhttp://about.jstor.org/terms
- Dolan, R., Fenster, M. S., & Holme, S. J. (1991). Temporal Analysis of Shoreline Recession and Accretion. *Journal of Coastal Research*, 7(3), 723–744. https://doi.org/10.2112/SI63-011.1
- Hassan, A., Huque, I., Huq, P. A. K., Martin, T. C., Nishat, A., & Thorne, C. R. (1997). Defining the Banklines of Brahmaputra-Jamuna River using Satellite Imagery. 3rd International Conference on River Flood Hydraulics, 35(January 1997), 349–358.
- Hassan, M. A., Ratna, S. J., Hassan, M., & Tamanna, S. (2017). Remote Sensing and GIS for the Spatio-Temporal Change Analysis of the East and the West River Bank Erosion and Accretion of Jamuna River (1995-2015), Bangladesh. *Journal of Geoscience and Environment Protection*, 05(09), 79–92. https://doi.org/10.4236/gep.2017.59006
- Himmelstoss, E. A., Henderson, R. E., Kratzmann, M. G., & Farris, A. S. (2021). Digital Shoreline Analysis System (DSAS) Version 5.1 User Guide: U.S. Geological Survey Open-File Report 2021–1091. *U.S. Geological Survey*, 2021–1091, 104. https://doi.org/10.3133/ofr20211091
- Islam, M. N., Biswas, R. N., Shanta, S. R., Islam, R., & Jakariya, M. (2019). Morphological Dynamics of the Jamuna River in Kazipur Subdistrict. *Earth Systems and Environment*, 3(1), 73–81. https://doi.org/10.1007/s41748-018-0078-2
- Islam, R., Islam, M. N., & Islam, M. N. (2017). Impacts of Bangabandhu Jamuna Multi-purpose Bridge on the dynamics of bar morphology at the Jamuna River in Bangladesh. *Modeling Earth Systems and Environment*, 3(3), 903–925. https://doi.org/10.1007/s40808-017-0342-8
- Khan, N. I., & Islam, A. (2003). Quantification of erosion patterns in the Brahmaputra-Jamuna River using geographical information system and remote sensing techniques. *Hydrological Processes*, *17*(5), 959–966. https://doi.org/10.1002/hyp.1173
- Khan, T. I., Mehrun, C. M., Opu, R. K., & Islam, M. N. (2020). MODELING ON PROBABILITY ANALYSIS OF FLOOD FREQUENCIES AT. International Journal of Contemporary Applied Researches, 7(April 2020), 2308–1365.

- Klaassen, G., Engineer, S. C., & Vermeer, K. (1988). Confluence scour in large braided rivers with fine bed material. *International Conference on Fluvial Hydraulics, January*.
- Leatherman, S. P. (1983). 1983 UMD Shoreline Mapping Project. *IEE Geoscience Remote Sensing Society Newsletter*, 22(December), 5–8.
- Raj, N., Rejin Nishkalank, R. A., & Chrisben Sam, S. (2020). Coastal Shoreline Changes in Chennai: Environment Impacts and Control Strategies of Southeast Coast, Tamil Nadu. *Handbook of Environmental Materials Management*, 1–14. https://doi.org/10.1007/978-3-319-58538-3\_223-1
- Sarker, M. H., Sarker, M. H., & Ferdaous, M. R. (2011). River bank protection measures in the Brahmaputra-Jamuna River: Bangladesh Experience Living with floods in Bangladesh View project Levee effect View project River bank protection measures in the Brahmaputra-Jamuna River: Bangladesh Experience. Center for Environmental and Geographic Information Services (CEGIS), Dhaka, Bangladesh, 5, 1–17.
  - https://www.researchgate.net/publication/263125674
- Sarker, M. H., Thorne, C. R., Aktar, M. N., & Ferdous, M. R. (2014). Morpho-dynamics of the Brahmaputra-Jamuna River, Bangladesh. *Geomorphology*, 215(6), 45–59. https://doi.org/10.1016/j.geomorph.2013.07.025
- Xu, H. (2007). Extraction of urban built-up land features from landsat imagery using a thematic-oriented index combination technique. *Photogrammetric Engineering and Remote Sensing*, 73(12), 1381–1391. https://doi.org/10.14358/PERS.73.12.1381

